Universidade Nova de Lisboa

Instituto de Higiene e Medicina Tropical

Domain dynamics and control of electron flux of NADPH cytochrome P450 oxidoreductase

Diana Isabel Viana da Fonseca Campelo Delgado

DISSERTAÇÃO PARA A OBTENÇÃO DO GRAU DE DOUTOR
NO RAMO DE CIÊNCIAS BIOMÉDICAS, ESPECIALIDADE DE GENÉTICA

MAIO 2019

Universidade Nova de Lisboa

Instituto de Higiene e Medicina Tropical

Domain dynamics and control of electron flux of NADPH cytochrome P450 oxidoreductase

Autor: Diana Isabel Viana da Fonseca Campelo Delgado

Orientador: Michel Kranendonk

Co-orientador: Celso Cunha

Dissertação apresentada para cumprimento dos requisitos necessários à obtenção do grau de Doutor no Ramo de Ciências Biomédicas, especialidade de Genética

Apoio financeiro da Fundação para a Ciência e a Tecnologia (projecto FCT-ANR/BEX-BCM/0002/2013).

Dedico este trabalho aos que me são mais queridos,
Ao meu marido, aos meus pais, aos meus irmãos e sobrinhos.

AGRADECIMENTOS

Gostaria de expressar o meu agradecimento e gratidão a todos os que apoiaram e contribuíram para a realização deste longo trabalho.

Ao Doutor Michel Kranendonk, agradeço a oportunidade de realizar este estudo sob a sua orientação e todos os ensinamentos ao longo destes anos.
Ao Professor Celso Cunha, por ter aceite orientar este trabalho a partir do Instituto de Higiene e Medicina Tropical.

Quero agradecer a todos os meus colegas de laboratório que me acompanharam ao longo do doutoramento. Francisco Esteves, Susana Silva, Bruno Gomes, Bernardo Palma, Célia Martins, Cláudio Pinheiro, Rita Jerónimo, Rita Lourenço, Marisa Cardoso, D. Lucrécia. Agradeço o apoio e convívio amigo, que tornaram todas as horas de trabalho mais fáceis.

A todos os colegas e colaboradores do ToxOmics. Prof. Sebastião Rodrigues, Prof. Joaquim Calado, Prof. Aldina Brás, Dr. Helena Borba, Isabel Borba. Agradeço todos os contributos e colaboração para este trabalho. Em especial, ao Professor José Rueff, pelos conselhos sábios e discussões científicas profícuas.

Aos nossos colaboradores de Toulouse. Gilles Truan, Philippe Urban, Thomas Lautier, Robert Quast. Obrigada pelas discussões científicas e por confiarem no meu trabalho.

Aos colegas de doutoramento, Ana Armada, Luísa Ganço e Tiago Vaz. Obrigada pela amizade e companheirismo. Tornaram aquele duro ano lectivo mais fácil de suportar.

Aos meus amigos de sempre, que acompanharam este processo à distância, sempre motivantes, alegres e confiantes. Em especial às amigas de longa data Filipa e Sara, já vão vinte anos a crescer juntas!

Aos colegas de faculdade que se tornaram amigos de uma década Joana Pereira, Inês Figueira, Inês Nunes, André, Joaquim, Andreia.

À malta dos Olivais, os amigos em Jesus, sempre barulhentos e alegres, a minha alegria! Sou muito grata pela vossa presença na minha vida.

À malta dos escuteiros da Portela. Em especial à fantástica patrulha Tigre. Seremos amigos para a vida toda. Cresci muito convosco, dentro e fora do escutismo. Obrigada pelo vosso testemunho, são exemplos para mim!

Um agradecimento especial à minha família. Em particular à minha mãe, por todo o amor, apoio, paciência, esforço e dedicação. Aos meus irmãos pelos anos de convivência e aprendizagem juntos e pelo apoio incondicional e incentivo alegre. E aos meus sobrinhos. Como é bom ver-vos crescer! Espero ser sempre um bom exemplo para vocês!

Ao meu marido João. Pelo amor, genuíno, discreto, sem floreados. Não sei pôr em palavras o quanto significas para mim e o quão essencial te tornaste. Foste e serás sempre a minha âncora. Acreditaste mais em mim, neste meu trabalho e no que sou capaz do que eu própria. No meio de todo este trabalho, concretizámos um sonho belo juntos. Somos uma família! Obrigada, meu amor.

TABLE OF CONTENTS

LIST OF PUBLICATIONS AND COMMUNICATIONS

This thesis contains data and/or methodologies published in international peer-reviewed articles or book chapters:

D. Campelo, F. Esteves, B. P. Palma, B. C. Gomes, J. Rueff, T. Lautier, P. Urban, G. Truan, M. Kranendonk. (2018) "Probing the role of the hinge segment of cytochrome P450 oxidoreductase in the interaction with cytochrome P450". Int J Mol Sci. 19 (12). doi: 10.3390/ijms19123914.

D. Campelo, T. Lautier, P. Urban, F. Esteves, S. Bozonnet, G. Truan, M. Kranendonk (2018). "The Hinge Segment of Human NADPH-Cytochrome P450 Reductase in Conformational Switching: The Critical Role of Ionic Strength" *In* Pandey, A. V., Henderson, C. J., Ishii, Y., Kranendonk, M., Backes, W. L., Zanger, U. M., eds. Role of Protein-Protein Interactions in Metabolism: Genetics, Structure, Function. (pp-125-137). Lausanne: Frontiers Media. doi: 10.3389/978-2-88945-385-6. ISBN 978-2-88945-385-6.

F. Esteves, **D. Campelo**, P. Urban, S. Bozonnet, T. Lautier, J. Rueff, G. Truan, M. Kranendonk (2018). "Human cytochrome P450 expression in bacteria: Whole-cell high-throughput activity assay for CYP1A2, 2A6 and 3A4". Biochem. Pharmacol. 158: 134-140.

D. Campelo, T. Lautier, P. Urban, F. Esteves, S. Bozonnet, G. Truan, M. Kranendonk (2017). "The hinge segment of human NADPH cytochrome P450 reductase in conformational switching: the critical role of ionic strength". Front Pharmacol. 8:755. doi: 10.3389/fphar.2017.00755.

The results obtained in this thesis were presented in scientific meetings in the following oral communications:

D. Campelo, F. Esteves, B. P. Palma, B. C. Gomes, J. Rueff, T. Lautier, P. Urban, G. Truan, M. Kranendonk. (2018) "Probing the Role of the Hinge Segment of Cytochrome P450 Oxidoreductase in the Interaction with Cytochrome P450". 2nd NMS Symposium on Chronic Diseases and Translational Science 2018. CEDOC Chronic Diseases. Lisboa, Portugal.

D. Campelo, F. Esteves, B. P. Palma, B. C. Gomes, J. Rueff, T. Lautier, P. Urban, G. Truan, M. Kranendonk. (2018) "Ionic interactions in the protein dynamics of Cytochrome P450 oxidoreductase". National Science Summit – Ciência 2018. Lisbon, Portugal.

D. Campelo, T. Lautier, P. Urban, F. Esteves, S. Bozonnet, J. Rueff, G. Truan, M. Kranendonk. (2017) "The hinge region of human NADPH-cytochrome P450 reductase in conformational switching: the critical role of ionic strength". 20th International Conference on Cytochrome P450: Biochemistry, Biophysics and Biotechnology. Dusseldorf, Germany.

D. Campelo, T. Lautier, P. Urban, F. Esteves, S. Bozonnet, J. Rueff, G. Truan, M. Kranendonk. (2017) "A região "hinge" da NADPH-citocromo P450 reductase na troca conformacional e o papel crítico da força iónica". 8as Jornadas Científicas do IHMT, Instituto de Higiene e Medicina Tropical - Universidade NOVA de Lisboa. Lisbon, Portugal.

D. Campelo, T. Lautier, P. Urban, F. Esteves, S. Bozonnet, J. Rueff, G. Truan, M. Kranendonk. (2017) "The hinge region of human NADPH-cytochrome P450 reductase in conformational switching: the critical role of ionic strength". National Science Summit – Ciência 2017. Lisbon, Portugal.

T. Lautier, **D. Campelo**, P. Urban, F. Esteves, S. Bozonnet, G. Truan, M. Kranendonk. (2017) "Cytochrome P450 reductase chimera: turn around the hinge". 19th International Symposium on Flavins and Flavoproteins. University of Groningen, The Netherlands.

The results obtained in this thesis were presented in scientific meetings in the following poster communications:

D. Campelo, F. Esteves, B. P. Palma, B. C. Gomes, J. Rueff, T. Lautier, P. Urban, G. Truan, M. Kranendonk. "Probing the Role of the Hinge Segment of Cytochrome P450 Oxidoreductase in the Interaction with Cytochrome P450". 2nd NMS Symposium on Chronic Diseases and Translational Science 2018. CEDOC Chronic Diseases. Lisboa, Portugal, 2018.

D. Campelo, T. Lautier, P. Urban, F. Esteves, S. Bozonnet, J. Rueff, G. Truan, M. Kranendonk. "The hinge region of human NADPH-cytochrome P450 reductase in conformational switching: the critical role of ionic strength". NOVA Food for thoughts - NOVA Doctoral School, Universidade NOVA de Lisboa Rectorate, Lisboa, Portugal, 2017.

D. Campelo, T. Lautier, P. Urban, F. Esteves, S. Bozonnet, J. Rueff, G. Truan, M. Kranendonk. "The hinge region of human NADPH-cytochrome P450 reductase in conformational switching: the critical role of ionic strength". 3rd NOVA Health Genetics Workshop, Universidade NOVA de Lisboa Rectorate, Lisboa, Portugal, 2017.

F. Esteves, **D. Campelo**, P. Urban, S. Bozonnet, T. Lautier, J. Rueff, G. Truan, M. Kranendonk. "Bacterial Whole-cell Human Cytochrome P450 Activity Assay". 3rd NOVA Health Genetics Workshop, Universidade NOVA de Lisboa Rectorate, Lisboa, Portugal, 2017.

F. Esteves, **D. Campelo**, P. Urban, S. Bozonnet, T. Lautier, J. Rueff, G. Truan, M. Kranendonk. "Bacterial Whole-cell Human Cytochrome P450 Activity Assay". 20th International Conference on Cytochrome P450: Biochemistry, Biophysics and Biotechnology. Dusseldorf, Germany, 2017.

D. Campelo, T. Lautier, P. Urban, F. Esteves, S. Bozonnet, J. Rueff, G. Truan, M. Kranendonk. "The hinge region of human NADPH-cytochrome P450 reductase in conformational switching: the critical role of ionic strength". National Science Summit '17 – Ciencia 2017. Lisboa, Portugal, 2017.

D. Campelo, F. Esteves, M. Kranendonk, "Dynamics in NADPH Cytochrome P450 oxidoreductase: Identification of critical protein residues". 7as Jornadas Científicas do IHMT, Instituto de Higiene e Medicina Tropical - Universidade NOVA de Lisboa, Portugal, 2016.

D. Campelo, F. Esteves, M. Kranendonk, "The importance of hinge and FMN genetic variants of NADPH cytochrome p450 oxidoreductase". 2nd Workshop of Genetics – NOVASaúde, Universidade NOVA de Lisboa (UNL), Reitoria da UNL (Campus de Campolide), Lisboa, Portugal, 2016. [Prize: Most Votation Poster Presentation]

F. Esteves, **D. Campelo**, M. Kranendonk, "Structural features controlling the protein dynamics of NADPH cytochrome P450 oxidoreductase in gated electron transfer". 1st Workshop of Genetics – NOVASaúde, Universidade NOVA de Lisboa (UNL), Reitoria da UNL (Campus de Campolide), Lisboa, Portugal, 2015.

D. Campelo, F. Esteves, M. Kranendonk, "Domain dynamics and control of electron flux of NADPH cytochrome P450 oxidoreductase: Identification of critical residues in the hinge region". 1st Workshop of Genetics – NOVASaúde, Universidade NOVA de Lisboa (UNL), Reitoria da UNL (Campus de Campolide), Lisboa, Portugal, 2015.

F. Esteves, **D. Campelo**, M. Kranendonk, "Structural features controlling the protein dynamics of NADPH cytochrome P450 oxidoreductase in gated electron transfer". Centre for Toxicogenomics and Human Health (ToxOmics) Scientific Meeting – Instituto Nacional de Saúde Dr. Ricardo Jorge (INSA), Lisbon, Portugal, 2015.

D. Campelo, F. Esteves, M. Kranendonk, "Domain dynamics and control of electron flux of NADPH cytochrome P450 oxidoreductase: Identification of critical residues in the hinge region". Centre for Toxicogenomics and Human Health (ToxOmics) Scientific Meeting – Instituto Nacional de Saúde Dr. Ricardo Jorge (INSA), Lisbon, Portugal, 2015.

RESUMO

A NADPH citocromo P450 oxidoredutase (CPR) é o fornecedor electrónico obrigatório para os citocromos P450 (CYPs) microssomais. Estes desempenham um papel central no metabolismo de hormonas esteróides, vitaminas, fármacos e outros xenobióticos. Demonstrou-se que a CPR existe num equilíbrio conformacional dinâmico, altamente dependente da força iónica, determinante para a sua função de transferência eletrónica (TE). A CPR transita entre uma conformação compacta (estado fechado) e conformações abertas (estado aberto). Admite-se que uma secção específica de um domínio funcional da CPR, conhecida como segmento *hinge* ("dobradiça"), desempenhe um papel importante na dinâmica e TE da CPR.

O principal objetivo deste trabalho de Doutoramento foi estudar o papel de resíduos específicos da *hinge* no equilíbrio conformacional da CPR, o seu papel no efeito da força iónica na dinâmica aberto-fechado e na interacção com diversos parceiros redox estruturalmente diversos. Para tal, foram construídos oito mutantes, visando os resíduos da *hinge* G240, S243, I245 e R246, com o objetivo de modificar a flexibilidade e potenciais interações iónicas. Verificou-se o efeito destas mutações na CPR na forma solúvel ou membranar, medindo a redução da proteína solúvel citocromo *c* a várias concentrações de sal. Todos os mutantes foram capazes de reduzir o citocromo *c* ainda que com diferentes eficiências, no entanto, as taxas de redução máxima foram deslocadas para concentrações de sal menores. Os resultados levam-nos a admitir a hipótese de uma rede de pontes de hidrogénio em torno do resíduo R246, envolvido na dinâmica aberto-fechado. Curiosamente, os efeitos das mutações, embora semelhantes, demonstraram diferenças entre formas solúveis e membranares da CPR. Os resultados demonstraram o aspecto crítico das propriedades eletrostáticas e de flexibilidade da *hinge* para a função de TE da CPR.

Embora a utilização de um parceiro redox substituto, citocromo *c*, tenha sido informativo, a CPR pode funcionar de maneira diferente com os seus aceitadores naturais. Por conseguinte, foram selecionados três mutantes da CPR (S243P, I245P, R246A), e combinados com três CYPs representativos do metabolismo de fármacos, nomeadamente as isoformas 1A2, 2A6 ou 3A4. Diferentes abordagens experimentais foram empregues

para verificar o efeito dessas mutações na funcionalidade dos CYPs: capacidade de bioactivação de pré-carcinogénios, cinética enzimática, efeito da força iónica e competição do citocromo *b*5 (CYB5). As mutações na *hinge* influenciaram a bioactivação de pré-carcinógénios de um modo dependente da isoforma do CYP e até do substrato. Os desvios nos parâmetros cinéticos dos três CYPs quando combinado com cada enzima mutante, tendem a confirmar essa discrepância. Isto foi ainda confirmado pelos perfis de sal/actividade, específicos para cada CYP e mutante *hinge*. As experiências de competição CPR:CYB5 indicaram um papel menos importante da afinidade na dinâmica aberto-fechado. Juntos, os dados sugerem que a *hinge* é responsável pela existência de um agregado de diferentes conformações abertas, permitindo a interacção e TE com parceiros redox estruturalmente variados.

Globalmente, este trabalho de doutoramento identificou resíduos-chave da *hinge* importantes na dinâmica e na função da CPR. Os dados obtidos suportam a existência de um mecanismo molecular subjacente que permite à CPR a TE para parceiros redox estruturalmente diversos, uma questão intrigante que estava pouco clara até agora.

Palavras-chave: NADPH citocromo P450 oxidoredutase (CPR); citocromos P450 (CYP); dinâmica proteica; transferência eletrónica (TE); interação proteína-proteína.

ABSTRACT

NADPH cytochrome P450 oxidoreductase (CPR) is the obligatory electron supplier for all microsomal cytochrome P450s (CYPs). These play a central role in the metabolism of steroid hormones, vitamins, therapeutic drugs and other xenobiotics. CPR has been shown to exist in a dynamic conformational equilibrium, highly dependent on ionic strength conditions, determinant for its electron-transfer (ET) function. CPR transitions between a compact conformation (locked state) and open conformations (unlocked state). A specific section of one of CPR's functional domains known as the hinge segment has been postulated to play a major role in CPR's dynamics and ET.

The main goal of this PhD-research was to study the role of specific residues of the hinge in the conformational equilibrium of CPR, their role in the ionic strength effect of the open-closed dynamics and in the interaction of CPR with structural diverse redox partners. For this purpose, eight mutants were constructed, targeting hinge residues G240, S243, I245 and R246, with the aim of modifying flexibility and potential ionic interactions. The effect of these CPR mutations were verified either in a soluble or in its membrane bound form, measuring the reduction of the soluble protein cytochrome *c* at various salt concentrations. All mutants were found capable of reducing cytochrome *c* yet with different efficiencies, however maximal reduction rates were shifted to lower salt concentration. Results lead us to hypothesize a hydrogen bond network around residue R246, involved in the open/closed dynamics. Interestingly, the effects of mutations, although similar, demonstrated specific differences between soluble and membrane-bound CPR forms. Results demonstrated the critical aspect of electrostatic and flexibility properties of the hinge for CPR's ET function.

Although the use of the surrogate redox partner cytochrome *c* was informative, CPR may function differently with its natural acceptors. Therefore, three CPR hinge mutants were selected (S243P, I245P and R246A) and combined with three representative drug-metabolizing CYPs, namely isoforms 1A2, 2A6 or 3A4. Different experimental approaches were employed, to verify the effect of these hinge mutations on CYP functionality: bioactivation capacity of pre-carcinogens, enzyme kinetic analysis, effect of ionic strength and cytochrome b_5 (CYB5) competition. The hinge mutations influenced

the bioactivation of pre-carcinogens, which seemed CYP-isoform and even substrate dependent. The deviations of enzyme kinetic parameters of the three CYPs when combined with each of the mutants, tend to confirm this discrepancy. This was further confirmed by the CYP-isoform and hinge mutant specific salt/activity profiles. The CPR/CYB5 competition experiments indicated a less important role of affinity in the open/closed dynamics. Together data suggest that the hinge is responsible for the existence of a conformational aggregate of different open CPR conformers, enabling ET-interaction with structurally varied redox partners.

Overall, this PhD research has uncovered several key residues of the hinge in CPR's protein dynamics and function. The obtained data seem to support an underlying molecular mechanism, permitting CPR's ET to structurally diverse redox partners, an intriguing issue which has been unclear so far.

Keywords: NADPH-cytochrome P450 reductase (CPR); microsomal cytochrome P450 (CYP); protein dynamics; electron-transfer (ET); protein–protein interaction.

LIST OF FIGURES

LIST OF TABLES

LIST OF ABBREVIATIONS AND ACRONYMS

2AA	2-aminoanthracene
4NQO	4-nitroquinoline-1-oxide
7-OH C	7-hydroxy coumarin
ABS1	*POR* deficiency or Antley-Bixler Syndrome
ACN	Acetonitrile
ADR	Adverse drug reaction
AfB1	Aflatoxin B1
CPR	NADPH-cytochrome P450 oxidoreductase
CYB5	Cytochrome b5
CYP	Cytochrome P450
DBF	Dibenzylfluorescein
DCPIP	Dichlorophenolindophenol
DHCR7	7-dehydrocholesterol reductase
DME	Drug metabolizing enzymes
DMSO	Dimethyl sulfoxide
EDTA	Ethylenediamine tetraacetic acid
ER	Endoplasmic reticulum
EROD	Ethoxyresorufin O-deethylation
ET	Electron transfer
EthR	Ethoxyresorufin
F	Flourescein
FAD	Flavin adenine dinucleotide
FMN	Flavin mononucleotide
Fw	Forward primer
HIV	Human immunodeficiency virus
HO/HMOX	Heme oxygenase
IPTG	Isopropyl β-D-thiogalactoside
IQ	2-amino-3-methylimidazo(4,5-f)quinoline
k_{cat}	Turn-over rate
K_M	Affinity constant

k_{obs}	Observed rate constant
LD	Linker domain
LPS^{d}	Deficient lipopolysaccharide core
$NADP^{+}$/NADPH	Nicotinamide adenine dinucleotide phosphate
NMR	Nuclear Magnetic Resonance
NNdEA	N-nitrosodiethylamine
NNK	4-(methylnitrosamino)-1-(3-pyridyl)-1-butanone
NOS	Nitric oxide synthase
PMSF	Phenylmethanesulfonyl fluoride
POR	CPR encoding gene
R	Resorufin
Rev	Reverse primer
SAXS	Small Angle X-ray Scattering
SDS-PAGE	Sodium dodecyl sulfate–polyacrylamide gel electrophoresis
SQLE	Squalene monooxygenase
TM	N-terminal transmembrane domain
UDP	Uridine diphosphate
V_{max}	Enzyme's maximum rate
WT	Wild-type
δ-Ala	δ-aminolevulinic acid

1. INTRODUCTION

CONTENT

1.1 Biotransformation

Humans are daily exposed to a wealth of chemicals, such as pharmaceuticals, cosmetics, dietary, environmental or occupational chemicals, designated as xenobiotics. This exposure, although often involuntary, may be chronic. These compounds may come into contact with the human body through a variety of routes, namely respiratory, cutaneous or oral. Once absorbed, the chemicals may exert a local effect and can then enter the systemic or portal circulation, being distributed to other tissues (Guengerich and MacDonald, 2007).

Some of these compounds are lipophilic which facilitates absorption through the skin, lungs and gastrointestinal tract and makes elimination more difficult as they can more easily cross membranes, being reabsorbed and accumulating in the body. After absorption and distribution, the elimination of compounds usually depends on their conversion to hydrophilic molecules, with higher polarity and greater aqueous solubility, in a process called biotransformation or drug metabolism to facilitate its excretion in the urine, bile or feces, either by the action of the kidneys or liver (Parkinson and Ogilvie, 2008).

Xenobiotics can exert a variety of effects on biological systems, which may be beneficial as most therapeutic drugs or may result in harmful effects. These effects are dependent on the physicochemical properties of the parent compounds and respective metabolites, determinant for their potential interaction with cellular targets. Biotransformation may result in the formation of chemically reactive metabolites (metabolic activation or bioactivation), capable of interacting with cellular molecules, which may lead to toxicity and genotoxicity (Parkinson and Ogilvie, 2008; Claesson *et al*., 2013; Pelkonen *et al*., 2015).

Biotransformation occurs in almost all tissues, but its main site of action is the liver and is mediated by several types of drug metabolizing enzymes (DMEs). These enzymes may be classified by the different types of chemical modifications they mediate (Zanger *et al*., 2008). Phase I reactions involve the introduction or modification of a functional chemical group of the compound by oxidation, hydrolysis or reduction, typically resulting in an increase of hydrophilicity of the compounds. Phase II type reactions involve the conjugation with endogenous polar cofactors, normally resulting in greater increase in

hydrophilicity. These conjugation reactions include glucoronidation and formation of Acyl-CoA thioesters, sulfonation, acetylation, methylation, phosphorylation, glutathione and amino acid conjugation (Xu *et al*., 2005*;* Parkinson *et al*., 2013).

In Phase I metabolism, the CYP family is the major enzymatic system involved (Guengerich and Isin, 2008; Rendic and Guengerich, 2015). The remaining of Phase I metabolism is carried out by a variety of other contributing enzymes including flavin-containing monooxygenases, NADPH:quinone oxidoreductase and several other, such as dehydrogenases, esterases and oxidases (Guengerich and Isin, 2008). Phase II metabolism is carried out by UDP-glucuronosyl transferases, epoxide hydrolases, sulfotransferases, N-acetyl transferases, gluthathione S-transferases and various methyltransferases (Jancova *et al*., 2010).

Drug metabolism plays a major role in adverse drug reactions (ADRs). These concern harmful and undesired response to drugs in therapeutic doses and are in majority the result of bioactivation (Park *et al*., 2011). Individual susceptibility to chemical toxicity is largely dependent on genetic polymorphism of phase I and II enzymes, altering expression, structure or function of the enzymes. Many drugs known to cause ADRs are metabolized in processes catalyzed by polymorphic CYP (Johansson and Ingelman-Sundberg, 2011; Zhou *et al*., 2017; Ingelman-Sundberg *et al*., 2018; Lauschke and Ingelman-Sundberg, 2018). The understanding of the role of genetic polymorphism and variation in CYP mediated biotransformation is therefore fundamental for the comprehension of inter-individual differences in chemical exposure, adverse drug effects and toxicity in general. For example, individuals carrying the variant CYP2C9 alleles *2 and *3 have a significant reduction of warfarin clearance and are more susceptible to adverse bleeding events. Genotyping of CYP2C9 can predict warfarin dose and patients predisposed to unstable anticoagulation during initiation of therapy (Zanger *et al*., 2008; Johansson and Ingelman-Sundberg, 2011; Zanger and Schwab, 2013). A detailed knowledge on the molecular mechanism of function of the CYP enzyme complex is desired to gather fundamental insights, to explain how genetic variation of protein factors of this enzyme complex may cause altered activities, and to rationalize their role in toxic responses in chemical exposure.

1.2 Cytochrome P450

Mammalian CYP are a superfamily of monooxygenases heme-proteins (Guengerich *et al*., 2005 *in Montellano*). Of the 57 human CYPs identified, all are integral membrane-bound proteins, with fifty located on the cytosolic side of the endoplasmic reticulum (ER) and the remaining seven on mitochondrial membranes (Table 1.1, Rendic and Guengerich, 2015). CYP or P450 was designated due to its rather unique spectral properties: an absorption band at approximately 450 nm in its reduced state and when complexed with CO (Omura and Sato, 1964a, 1964b). CYP are classified based on their amino acid sequence homology. With <40% of homology, CYPs belong to a different family and are identified by a number. With 40-55% homology, CYP are grouped in the same sub-family, which is identified by a letter. Within a sub-family of CYPs, individual isoforms are distinguished by a number (Nelson *et al*., 2004; Nelson *et al*., 2006).

CYP enzymes are involved in the metabolism of drugs, carcinogens, pesticides but also of endogenous compounds such as steroids, fat-soluble vitamins, and many other types of chemicals (Guengerich *et al*., 2016). CYPs are versatile enzymes and capable of catalyzing a wealth of detoxification and biotransformation reactions with a multitude of different classes of substrates (Table 1.1). The broad substrate specificity of this enzyme superfamily is due to its active site that can bind a wide variety of structurally different compounds, often in multiple orientations. Moreover, the multiplicity of CYP enzymes, each with its own characteristics, have in many cases overlapping substrate selectivity (Anzenbacher *et al*., 2001).

CYPs are the major catalysts in phase I metabolism in humans, being responsible for approximately 75% of the metabolism of prescribed drugs (Rendic *et al*., 2012; Rendic and Guengerich, 2015). The majority of human CYP reactions is mediated by a set of five CYPs (1A2, 2C9, 2C19, 2D6, and 3A4) with a major role for the CYP3A4 isoform. Minor contributions are ascribed to CYP2C8, 2A6 and 2E1 (Figure 1.1). Interestingly, the isoforms know to be responsible for bioactivation of chemicals to toxic products (see below), such as CYP1B1, 2A6, and 2E1, contribute only in a minor extent to the metabolism of xenobiotics in general (Rendic and Guengerich, 2015) (Figure 1.1).

Table 1.1. Classification of Human CYPs Based on Major Substrate Class.

Steroids	Xenobiotics	Fatty acids	Eicosanoids	Vitamins	Unknown
1B1	1A1*	2J2	4F2	2R1**	2A7
7A1*	1A2*	2U1	4F3	**24A1****	2S1
7B1	2A6*	4A11	4F8	26A1	4A22
8B1	2A13*	4B1**	5A1	26B1	20A1
11A1*	2B6*	4F11	8A1*	26C1	
11B1	2C8*	4F12	(2W1)	**27B1**	
11B2	2C9*	4V2		**27C1**	
17A1*	2C18	4F22			
19A1*	2C19*	4X1			
21A2*	2D6*	4Z1			
27A1	2E1*				
39A1	2F1				
46A1*	3A4*				
51A1*	3A5*				
	3A7				
	3A43				

* X-ray crystal structure(s) reported (for human enzyme). **Animal orthologue (Rat or rabbit X-ray crystal structure). Mitochondrial CYPs are highlighted. Adapted from Guengerich FP, personal communication, 2017.

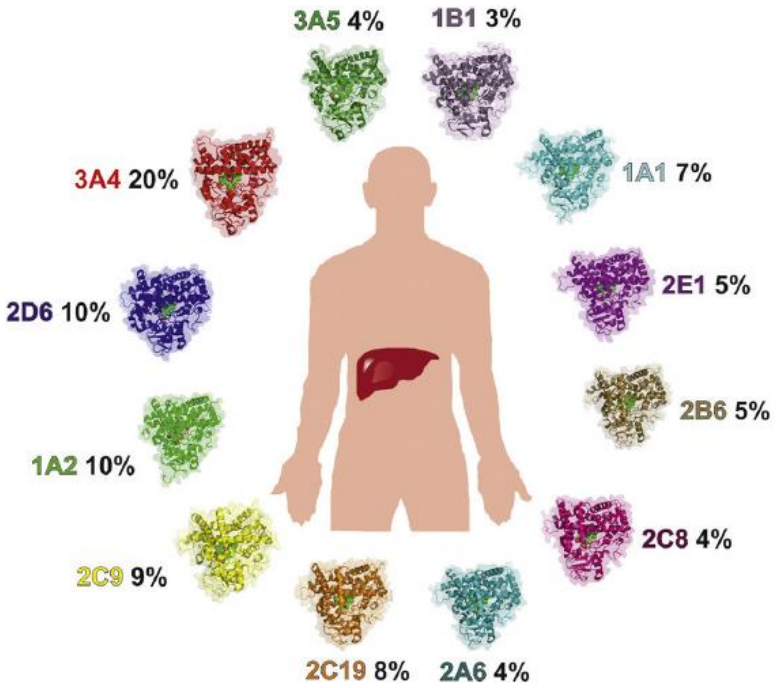

Figure 1.1. CYP isoforms involved in metabolism of all chemicals, according to Rendic and Guengerich (2015). The percentages represent the participation of individual CYP isoforms in metabolism of xenobiotics. CYP isoforms are represented as individual X-ray structures (from Šrejber *et al.*, 2018).

Although the majority of CYP reactions involves the introduction of polar groups to parent compounds, enabling their detoxification and excretion, this may cause reversibly bioactivation, e.g. of chemical carcinogens. Many carcinogens are pro-carcinogens (i.e. are relatively non-reactive) but require metabolic activation to exert their genotoxic effects (Guengerich and Isin, 2008; Reed *et al*., 2018). Oxidative activation of carcinogens by CYP enzymes leads to the formation of highly reactive electrophilic intermediates which may react with nucleophilic centers of cellular constituents, such as proteins, RNA and DNA. This latter may give rise to DNA adducts and lesions which potentially may cause mutations (Nebert and Dalton, 2006). For example, aflatoxin B_1 (AfB1), a very potent hepato-carcinogen, is by itself relatively inert, but is metabolized in the liver, by CYP1A2 and 3A4, leading to the formation of highly reactive genotoxic and carcinogenic metabolites (Kamdem *et al.*, 2006).

1.2.1 Catalytic Cycle of CYPs

CYP enzymes catalyze a variety of oxidation and some reduction reactions, collectively involving thousands of substrates (Guengerich *et al*., 2007, Table 1.1). Although CYPs are named cytochromes (electron-transferring proteins) they are in fact oxygenases, in the sense that they transfer electrons to oxygen and catalyze the oxidation of organic chemicals. CYP catalyze oxidations of many different types of substrates. Specifically, they are generally known as ‘monooxygenases’ or ‘mixed-function oxidases’ (Guengerich *et al.*, 2016).

For catalytic activity, CYPs require a source of electrons which are provided by reduced pyridine nucleotides. However, CYPs do not receive electrons directly from these cofactors, requiring auxiliary redox protein partners to shuttle the electron to the heme moiety in the active site. Depending on the cellular location and their redox partners, CYPs are generally divided into two major classes, class I and class II. Class I includes mitochondrial and some bacterial CYPs, which in their activity depend on two separate redox partners, consisting of an iron–sulfur protein (ferredoxin/adrenodoxin) and a flavin-containing reductase (ferredoxin/adrenodoxin reductase). The class II CYPs are microsomal (i.e. located on the endoplasmic membrane) monooxygenases that receive

electrons from CPR, the founding member of the diflavin reductase family (Paine *et al*., 2005; Lamb and Waterman, 2013).

Microsomal CYP receives two electrons, donated by CPR one at a time at two distinct steps of the reaction cycle (Figure 1.2). By this sequential ET, CYP activates molecular oxygen (O_2) and mediates the transfer of one atom of the activated O_2 into the substrate and reduce the other atom into water (see scheme in Figure 1.2). Substrate RH is hydroxylated by the CYP to form the oxidized product ROH, and a water molecule is released as a byproduct of this reaction. In each monooxygenation reaction cycle, the two electrons are supplied by CPR functioning as an electron donor by accepting two electrons from NADPH, in the form of hydride (H^-) and transferring them to CYP during catalysis. The CYP reaction can be summarized as: $RH + O_2 + NADPH + H^+ \rightarrow ROH + H_20 + NADP^+$ (Denisov *et al*., 2005; Barnaba *et al*., 2017).

Alternatively, the second electron can be donated by CYB5 (see Figure 1.2) (Paine *et al*., 2005; Scott *et al*., 2016). CYB5 is a small heme protein (15 kDa), involved in lipid and sterol biosynthesis, and is found together with CPR anchor on the cytoplasmic side of the ER of eukaryotic cells through a hydrophobic transmembrane binding domain (Vergeres and Waskel, 1995, Wang *et al*., 1997). CYB5 is thought to promote catalysis not only via ET of the second electron, but also through allosteric regulation (Porter *et al*., 2002). Depending on the CYP isoform involved, substrate and experimental conditions, CYB5 has been shown to stimulate, inhibit, or not to interfere with CYP reactions but its mode of action is still not fully understood (Bart and Scott, 2017).

The efficiency of CYP catalysis is measured in terms of "coupling", i.e. the amount of transferred electron that is committed to the monooxygenase activity *versus* the extent of the "uncoupled" (or unproductive) pathways. Three unproductive pathways exist (see Figure 1.2): (a) release of superoxide from the ferrous dioxygen (the autoxidation shunt), (b) release of hydrogen peroxide (the peroxide shunt), and (c) the 4e− reduction of heme to produce water (the oxidase shunt) (Denisov *et al*., 2005; Barnaba *et al*., 2017).

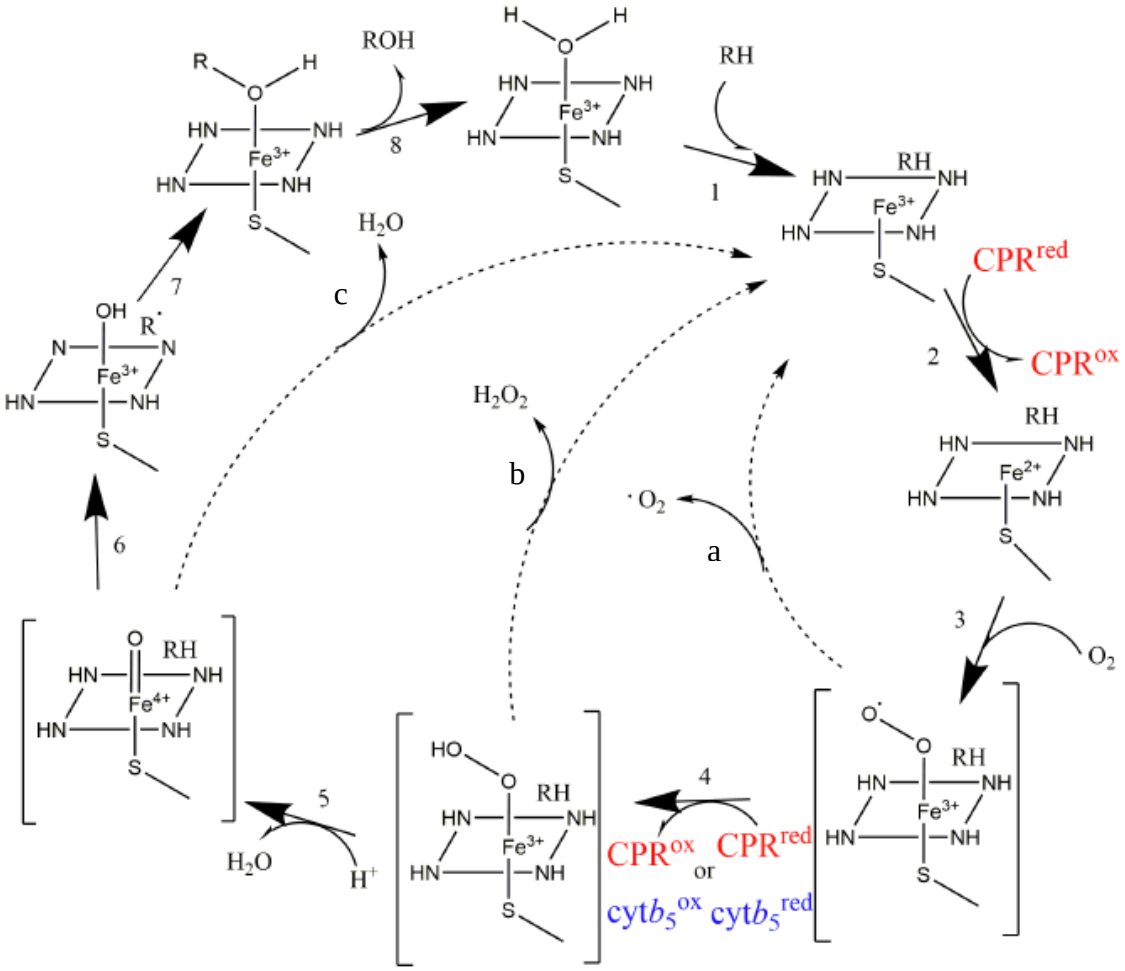

Figure 1.2. The catalytic cycle of CYP. The binding of substrate RH (1) causes a decrease of the redox potential, which allows the first ET from CPR (2). The reduction of Fe^{3+} to Fe^{2+} makes O_2 binding suitable (3), which now can accept a second electron from either CPR or CYB5 (4), to form a hydroperoxyl intermediate known as compound 0. The O_{2-2} complex reacts with surrounding protons to form the highly reactive oxyferryl intermediate, also known as compound I (5). The Fe-ligated O atom (6) is transferred to the substrate forming a hydroxylated form of the substrate (7). The product is finally released (8), replaced by a molecule of water. Three uncoupling reactions are shown as dashed lines, with the respective products: (a) the autoxidation shunt (O_2), (b) the peroxide shunt (H_2O_2), and (c) the oxidase shunt (H_2O) (from Barnaba *et al.*, 2017).

1.2.2 CYP Isoforms used in the studies of this thesis: CYP1A2, 2A6 and 3A4

Studies of this thesis involved three human CYPs, namely CYP1A2, 2A6 and 3A4, which are major isoforms in drug metabolism. In this section these three CYPs will be discussed more in detail.

CYP1A2 belongs to the CYP1 family which comprises three functional genes in two subfamilies (see Table 1.1). The highly conserved CYP1A1 and CYP1A2 genes consist of seven exons and six introns and are located on chromosome 15q24.1 (Jiang *et al*., 2005). Catalytic activities of the CYP1 enzymes are overlapping and include hydroxylations and other oxidative transformations of many polycyclic aromatic hydrocarbons and other aromatic substances. Whereas CYP1A1 prefers planar aromatic hydrocarbons, CYP1A2 shows a preference for aromatic amines (e.g. 2-aminoanthracene (2AA)) and heterocyclic compounds (e.g. 2-amino-3-methylimidazo(4,5-f)quinoline (IQ) and 4-(methylnitrosamino)-1-(3-pyridyl)-1-butanone (NNK)) (Duarte *et al*., 2005a/b, Guengerich and Isin, 2008). CYP1 enzymes play a prominent role in the bioactivation of procarcinogens, such as benzo[a]pyrene, arylarenes, nitroarenes, and arylamines present in charbroiled food and industrial combustion products to reactive and carcinogenic intermediates able to cause DNA damage (Zanger and Schwab, 2013).

CYP1A2 is the main enzyme of CYP family 1, corresponding to approximately 10% of total CYP-content of the human liver (Parkinson and Ogilvie, 2008). The crystal structure of CYP1A2 revealed a rather compact active site with a cavity larger than that of CYP2A6 but much smaller compared to CYPs 3A4 and 2C8 (Sansen *et al.*, 2007a). Prototypical biotransformations catalyzed by CYP1A2 include 7-ethoxyresorufin O-deethylation, phenacetin O-deethylation, and caffeine N3-demethylation to paraxanthine, which are commonly used as probe-substrates for *in vitro* or *in vivo* phenotype determination (Zhou *et al.*, 2004).

In humans, CYP1A2 is constitutively expressed in the liver at high levels. In this organ, CYP1A2 plays a significant role in the metabolism of several clinically important drugs, including analgesics and antipyretics (acetaminophen, phenacetin, lidocaine), antipsychotics (olanzapine, clozapine), antidepressants (duloxetine), anti-inflammatory

drugs (nabumetone), cardiovascular drugs (propranolol, guanabenz, triamterene), among others (Zanger and Schwab, 2013).

The CYP-allele website (https://www.pharmvar.org/) lists to date 41 defined alleles variants, some of which are associated with altered expression levels or code for proteins with altered enzyme activity. Because of the role of CYP1A enzymes in the metabolism of procarcinogens and cellular signaling molecules, their polymorphisms have been extensively studied as susceptibility factors in the context of various cancers (Zanger and Schwab, 2013).

CYP2A6 is a member of the CYP2 family, which comprises 16 full-length genes, each containing 9 exons and 8 introns. The genes are located on different chromosomes and organized in multi-gene clusters containing one or several subfamilies. The human CYP2A genes are found in a 370 kb gene cluster on chromosome 19q13.2, containing genes and pseudogenes of the CYP2A, 2B, 2F, 2G, 2S and 2T subfamilies (Nelson *et al.*, 2004). The CYP-allele website lists currently 89 defined alleles and haplotype variants for CYP2A6.

Human CYP2A6 is mainly expressed in the liver and corresponds to 7% of its CYP content (Parkinson and Ogilvie, 2008). CYP2A6 has been recognized as the major isoform involved in the oxidative metabolism of the psychoactive tobacco ingredient nicotine to the inactive cotinine (Raunio and Rahnasto-Rilla, 2012). The crystal structure of CYP2A6 revealed an active site cavity suitable for nonplanar low molecular weight molecules (Sansen *et al.*, 2007b). The 7-hydroxylation of coumarin is a selective marker activity for CYP2A6 used *in vitro* experimentations (Fuhr *et al.*, 2007).

CYP2A6 was identified as the main isoenzyme responsible for bioactivation of the cancer prodrug tegafur (Komatsu *et al.*, 2000), the 7-hydroxylation of the anti-HIV drug efavirenz and the biotransformation of the aromatase (CYP19A1) inhibitor letrozole (Murai *et al.*, 2009). Furthermore, CYP2A6 contributes to the metabolism of a number of clinically used drugs (Di *et al.*, 2009). CYP2A6 is involved in the bioactivation of carcinogens, including nitrosamines such as NNK, a major tobacco procarcinogen (Su *et al.*, 2000); aromatic amines present in smoke, and AfB1 (Nakajima *et al.*, 2006; Rossini *et al.*, 2008). Most pharmacogenetic studies involving CYP2A6 were to delineate the

effect of genotype either on nicotine metabolism, smoking behavior, nicotine withdrawal symptoms or lung cancer risk (Benowitz *et al.*, 2006; Nakajima *et al.*, 2006; Mwenifumbo and Tyndale, 2007; Rossini *et al.*, 2008).

CYP3A4 belongs to the CYP3 family, which consists only of one subfamily, CYP3A, located on chromosome 7q22.1 and has a size of 231 kb. It comprises four CYP genes 3A4, 3A5, 3A7, and 3A43 (Nelson *et al.*, 2004). The CYP3A subfamily enzymes play a major role in drug metabolism (Zanger *et al.*, 2008; Zanger and Schwab, 2013). The CYP-allele website lists currently 53 defined alleles and haplotype variants for CYP3A4.

The active site of CYP3A4 is large and flexible and can accommodate and metabolize many, preferentially lipophilic compounds with comparatively large structures (Scott and Halpert, 2005; Hendrychová *et al.*, 2011). Typical large substrates are immunosuppressants, such as cyclosporine A and tacrolimus, macrolide antibiotics e.g. erythromycin, and anticancer drugs including taxol. Still smaller compounds are also accepted including ifosfamide, tamoxifen, benzodiazepines, several statins, antidepressants, opioids and many others (Zanger and Schwab, 2013).

Although several probe drugs that measure general CYP3A activity are available, e.g. midazolam, erythromycin, alprazolam, and dextromethorphan (Fuhr *et al.*, 2007; Liu *et al.*, 2007), phenotyping data obtained with different CYP3A substrates are not generally well correlated to each other. This is a CYP3A4-typical feature that may be related to the occurrence of several overlapping substrate binding regions and the well-known allosteric regulation of CYP3A4 enzyme activity (Niwa *et al.*, 2008; Foti *et al.*, 2010; Roberts *et al.*, 2011). Nevertheless, some limited substrate and regioselectivity differences were observed. Several probe-substrates are being used for CYP3A4, for *in vitro* activity evaluations (Ghosal *et al*., 2003), e.g. the fluorogenic substrate dibenzyl fluorescein (DBF).

1.3 NADPH dependent P450 oxidoreductase

The human multi-domain CPR, is encoded by the *POR* gene located on chromosome 7q11.2. This protein is a multidomain diflavin reductase, approximately 80 kDa, containing 680 amino acids (RefSeq protein: NP_000932, UniProt P16435). Evidence for the requirement of CPR in microsomal hydroxylation reactions was first obtained by La Du *et al.* (1955) and Gillette *et al.* (1957) in experiments in which cytochrome *c* was shown to inhibit the NADPH-mediated oxidative demethylation of monomethyl-4-aminoantipyrine by liver microsomes. When Williams and Kamin (1962) and Phillips and Langdon (1962) published their characterization studies of CPR, they showed that this enzyme was localized in the ER of hepatocytes and, therefore, it was unlikely that cytochrome *c* was its natural electron acceptor. In fact, the inhibition of drug demethylation by cytochrome *c* predated the discovery of CYP by Omura and Sato (1962) and the demonstration by Estabrook *et al.* (1963) that the photochemical action spectrum of the reversal of carbon monoxide inhibition of steroid or drug hydroxylation corresponded to the reduced CO-bound CYP difference spectrum, indicating its role as the terminal oxygenase (Masters and Marohnic, 2006).

Currently, it is known that CPR is the sole obligatory electron donor for all mammalian microsomal CYP proteins, but also of other redox-partner dependent enzymes such as heme oxygenase (HO), squalene monooxygenase (SQLE) and CYB5 (Guengerich, *et al*., 2005; Pandey *et al*., 2010) (see Figure 1.5). CPR plays therefore a key role in multiple physiological pathways involving redox metabolic processes such as the metabolism of steroid hormones, vitamins, drugs and xenobiotics (Pandey *et al*., 2010; Miller *et al*., 2011).

1.3.1 Electron-transfer function

Multidomain enzymes belonging to ET systems, such as CPR are generally comprised of transporter and reductase domains, assembled with connecting and hinge domains. CPR is a microsomal membrane-bound diflavin-protein attached to the cytoplasmic side of the ER via an N-terminal transmembrane hydrophobic anchor, approximately 55 amino acids

long (Figure 1.3 A). The domains that bear the two cofactors are a flavodoxin-like FMN-binding domain (transporter) and a ferredoxin-NADPH reductase like FAD-binding domain (reductase) (Porter *et al*., 1990; Murataliev *et al*., 2004). A third highly flexible stretch, called the hinge segment, links the FMN and the connecting/FAD domain (Wang *et al*., 1997; Grunau *et al*., 2006; Grunau *et al*., 2007; Ellis *et al*., 2009) (Figure 1.3). In mammalians, CPR shares highly conserved amino acid sequences which form the binding domains for FMN, FAD and NADPH. Additionally, both the FAD- and NADPH-binding domains are similar to the FAD and NADPH binding domains of ferredoxin reductases and nitric oxide synthases (Waskell and Kim, 2015).

CPR transfers electrons between cofactors in a precise and timely controlled manner, from NADPH through the FAD and FMN coenzymes to the final acceptor such as CYP (NADPH → FAD → FMN → CYP) (Murataliev *et al*., 2004; Aigrain *et al*., 2012; Iyanagi *et al*., 2012; Paine *et al*., 2005). Reduced FMN transfers the electrons one at a time to the redox partners of CPR (Masters *et al*., 2005).

1.3.2 CPR protein conformation

The first X-ray diffraction studies on soluble (N-terminal deleted) rat CPR showed a tightly packed and compact structure in which the two isoalloxazine rings of FMN and FAD are juxtaposed for ET between the two flavins (Wang *et al*., 1997). Subsequently, several other crystallography studies (Lamb *et al*., 2006; Xia *et al*., 2011b; McCammon *et al*., 2016) as well as Nuclear Magnetic Resonance (NMR) analysis of soluble human CPR (Vincent *et al*., 2012) showed similar closed structures. Another study, using a CPR mutant in which the FMN domain was linked to the FAD domain via a disulfide bridge, demonstrated a compact structure with the two flavins in a clear competent state for ET from FAD to FMN with a short inter-flavin distance (Xia *et al*., 2011a). In this closed structure, CPR was fit for internal flavin ET but unable to reduce external acceptors unless the disulfide bridge was reduced, allowing the re-opening of the protein structure. Since the closed conformation of CPR is incompatible for ET to redox partners, the occurrence of inter-domain motions was suggested to render the FMN domain accessible for ET to external cytochrome acceptors such as CYPs (Pudney *et al*., 2011).

In 2009, three separate studies reported on the existence of "open" or extended conformations of CPR (Hamdane *et al*., 2009; Aigrain *et al*., 2009; Ellis *et al*., 2009). The conformational study using X-ray crystallography of a CPR variant with a 4-amino acid deletion (ΔTGEE) in the hinge region, which connects the FMN domain to the remaining of the protein demonstrated three remarkably extended conformations (Hamdane *et al*., 2009). The protein was defective in its intramolecular ET between the two flavins. However, it was able to successfully reduce CYP, by external chemical reduction of the FMN group. In this deletion mutant, the FMN domain was structurally rearranged, separated from FAD and exposed for interaction with its redox partners.

In a second study of that year, an active CPR chimera, in which the FMN domain was replaced with its yeast counterpart was produced (Aigrain *et al*., 2009). Crystal structures of this fusion protein demonstrated different extended conformations from those of previously solved structures. The enzyme has a complete disrupted interface between the FAD and the FMN domain but remains functional for cytochrome *c* or CYP reduction, although with a strong decrease in efficiency. Both the distance between the flavins and the differences in flavin redox potentials indicated that CPR can undergo large conformational changes. Disturbing either the hinge region (ΔTGEE) (Hamdane *et al*., 2009) or the interface FMN (yeast)-FAD (human) of CPR (Aigrain *et al*., 2009) leads to an open conformation, nonetheless still active with CYP.

A third study by Ellis *et al.* of the same year, provided evidence for the existence of a second conformation in which the FMN domain is involved in a different inter-domain interface (Ellis *et al*., 2009). Small Angle X-ray Scattering (SAXS) analysis showed that oxidized and NADPH-reduced human CPR had different overall shapes. Additional NMR studies showed a mixture of approximately equal amounts of two forms of CPR. These newly found open CPR conformations were compatible with ET to redox-partners.

The data of these three studies of 2009 taken together implied the presence of a control mechanism, devoted to opening and closing of the domains, in the course of the catalytic cycle (Pudney *et al*., 2011).

Subsequent studies which were reported until the start of this PhD research, clearly established that human CPR co-exists in these two different types of conformations

(closed and open) which exist in a conformational equilibrium (Ellis *et al*., 2009; Huang *et al*., 2013; Jenner *et al*., 2011; Frances *et al*., 2015) (Figure 1.3 B). Molecular dynamic (*in silico*) studies suggested the transition between states to occur through a swinging and rotational movement (Sündermann and Oostenbrink, 2013), which was experimentally shown to be a rapid switch (600 s^{-1}) (Frances *et al*., 2015). Dynamics of CPR requires substantial spatial reorganization in the protein (Sugishima *et al*., 2014) leading to the accessibility of the FMN to external electron acceptors (Grunau *et al*., 2007) such as cytochrome *c*, being reduced with a turnover rate of approximately 3000 min^{-1} (Guengerich *et al*., 2009), i.e. more than 10 times slower than the open-closed frequency mentioned above. Conformational equilibrium has been shown to be dependent on the redox state of CPR and the binding of NADPH (Huang *et al*., 2005; Ellis *et al*., 2009) as well as pH and ionic strength (Frances *et al*., 2015). Notwithstanding, the structural determinants of the CPR protein that control the conformational changes, particularly in relevant physiological conditions, were poorly known. To elucidate this point is the main objective of this thesis (see section 1.5).

1.3.3 The hinge segment of CPR

Linker regions in proteins are important components of the dynamic identity of structures, providing flexibility and contributing to allostery and conformational changes of the protein, induced by the binding of substrate, or regulator molecules (Papaleo *et al*., 2016). The linker domain (LD) of human CPR connects the FAD and FMN domains through a highly flexible hinge (Wang *et al*., 1997; Grunau *et al*., 2006; Grunau *et al*., 2007; Ellis *et al*., 2009). The hinge is a specific section of the CPR protein that forms a loop, encompassing Gly235 to Tyr248, which has no particularly defined secondary structure (Wang *et al*., 1997; Xia *et al*., 2011a). The hinge segment has been postulated to play a major role in CPR's protein dynamics, allowing the FMN-binding domain to "swing" into and out of position to allow ET from the reduced FAD, through the FMN, to the heme moiety of its redox partners (Hamdane *et al*., 2009; Laursen *et al*., 2011) (Figure 1.3).

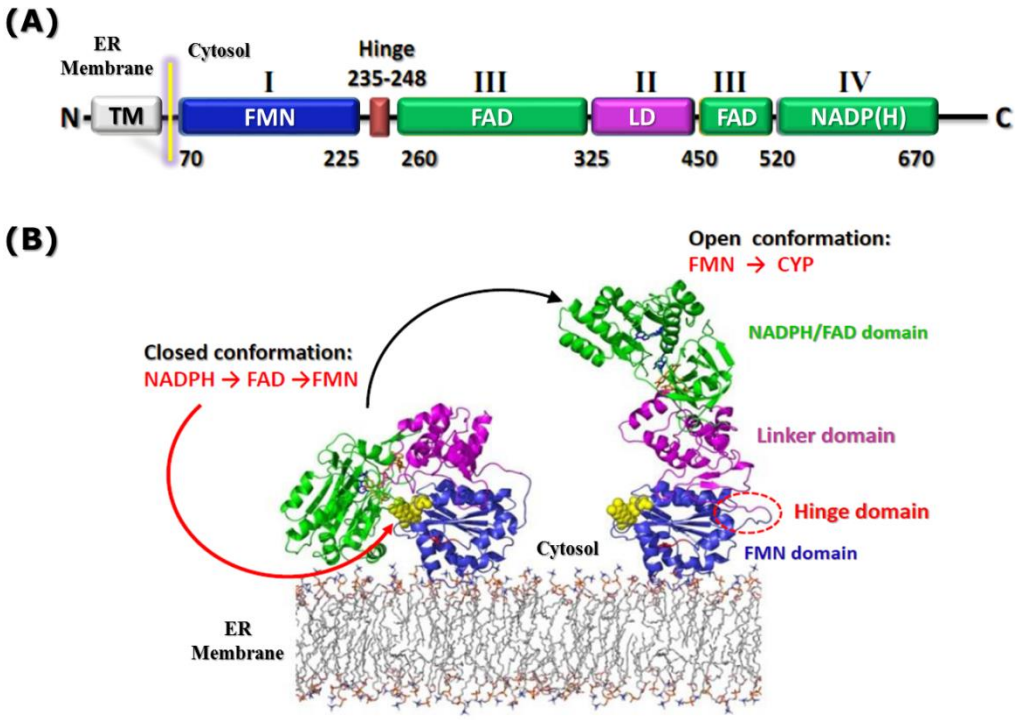

Figure 1.3. Structure of human CPR. (A) Domain organization in *POR* gene: Hydrophobic N-terminal transmembrane (TM) domain; Co-factors binding domains FAD/FMN; Linker domain (LD) inserted in the FAD domain; connecting domain containing a flexible loop (hinge) (numbers indicate estimated amino acid positions) (by M. Kranendonk). (B) Model of the protein dynamics of CPR in its ET function and conformational equilibrium. CPR is represented on the membrane as it would be when attached by its N-terminal hydrophobic anchor. Left, the compact form, represented by the crystal structure, appropriate for interflavin ET. Right, the extended form, with the FMN exposed, appropriate for ET to CYP (adapted from Ellis *et al*. 2009, by M. Kranendonk).

Certain residues in the hinge segment of CPR have been suggested to be important for the transition between closed and open conformations. In the study with the human-yeast chimera described above, Aigrain and colleagues suggested residues G240 and S243 to be of importance for large conformational changes in the protein (Aigrain *et al*., 2009). Subsequently, the *in silico* molecular dynamics study mentioned above, seem to reveal residues I245 and R246 as part of the conformational axis on which the opening and rotational movement of CPR occurs (Sündermann and Oostenbrink, 2013). These residues seem to be pivotal in the movement of the FMN domain relative to the remainder of the protein.

1.3.4 CPR genetic variations

Genetic variations of the *POR* gene, encoding human CPR, have been found both in healthy individuals (genetic polymorphisms) and in patients with *POR* deficiency, know as the Antley-Bixler Syndrome or ABS1 (OMIM # 201750), caused by rare genetic mutations. The syndrome ranges from mild clinical manifestations to severe forms of congenital adrenal hyperplasia, severe skeletal malformation and genital ambiguity, thought to be caused by perturbed steroidogenesis, visceral anomalies (particularly of the genitourinary system), among other clinical manifestations (Huang *et al*., 2005; Dhir *et al*., 2007; Miller *et al*., 2011; Pandey *et al*., 2013).

The structural *POR* mutations are scattered over the multi-domain CPR protein (Figure 1.4) and several have been found to be difficult for structural interpretation (Pandey *et al*., 2013). Some of these mutations are located at structural areas supposedly important for ET control from CPR to CYP. Others were found to interfere directly with the binding of CPR's cofactors (NADPH, FMN and FAD), which in some cases lead to severe losses of function (Kranendonk *et al*., 2008; Marohnic, *et al*., 2010). However, a number of these mutations did not seem to interfere directly with cofactor binding, demonstrating only partial loss of function (Nicolo *et al*., 2010; Agrawal *et al*., 2010; Fluck *et al*., 2010; Chen *et al*., 2012; Moutinho *et al*., 2012; Pandey and Sproll, 2014; McCammon *et al*., 2016).

Several of these mutations might be expected to interfere with CPR protein dynamics, altering structural requirements necessary for the optimal transition between conformations, perturbing the interaction of CPR with its redox acceptors. Some of these mutations seem to have a differential effect depending on the CYP isoform interacting with CPR (Dhir *et al*., 2007; Moutinho *et al*., 2012). Studies on the impact of genetic variations in *POR* affecting drug metabolism in healthy human population are at an early stage, and more information is needed to clarify the differences in metabolism due to variations in *POR* (Pandey *et al*., 2013).

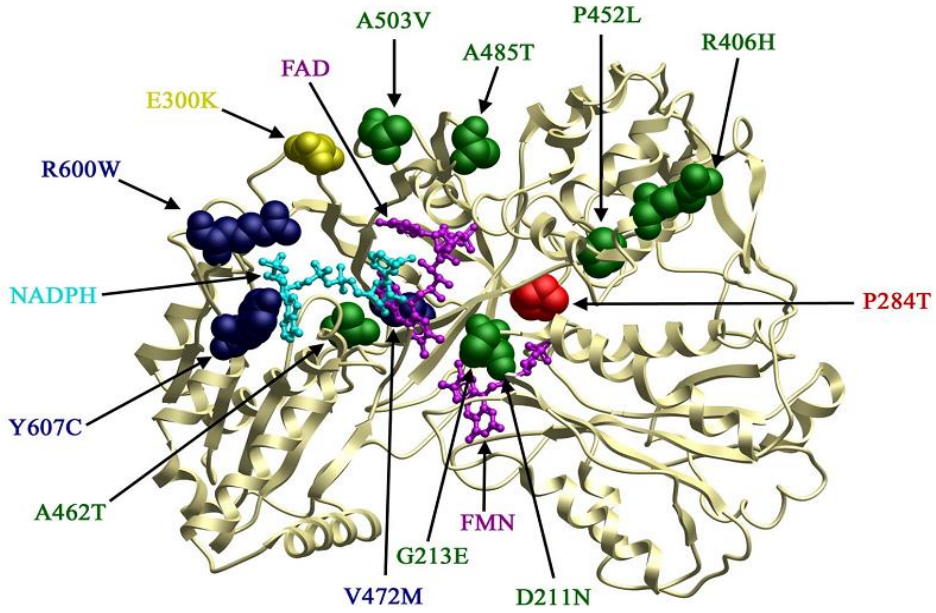

Figure 1.4 Model of human CPR showing the locations of the sequence variants identified. The model described by Huang *et al*., (2005) based on the crystal structure of rat CPR lacking 65 N-terminal residues (Wang *et al*., 1997). The α-carbon backbone is depicted as a narrow ribbon, the FAD and FMN moieties (magenta) and NADPH (cyan) are depicted as ball-and-stick models, and the variant amino acids are depicted by packed sphere images of different colors (from Huang *et al*., 2008).

1.3.5 Multiple Redox partners

CPR is attached to the cytoplasmic side of the ER via a transmembrane segment at its N-terminus, together with its redox partners. CPR is the obligatory electron supplier of all microsomal CYP, thereby controlling the function of major metabolic systems involving microsomal CYP enzymes: steroid synthesis in adrenal glands and gonads, cholesterol synthesis (e.g. in developing bone), retinoic acid metabolism and metabolism of sterols, drugs and other xenobiotics, mainly in the liver.

Drug-metabolizing microsomal CYP enzymes include major isoforms CYP1A2, 2C9, 2C19, 2D6 and 3A4; steroidogenic microsomal CYP enzymes are CYP17A1 (17α-hydroxylase/17,20 lyase), 21A2 (21-hydroxylase) and 19A1 (aromatase); while CYP51A1 (14α-lanosterol demethylase) is involved in sterol synthesis and metabolism (Tomalik-Scharte *et al.*, 2010).

CPR also donates electrons to other non-CYP key enzymes such as HO, the unique enzyme responsible for the initial as well as rate limiting reaction for heme degradation (Schacter *et al.*, 1972); SQLE, rate limiting enzyme for ergosterol and cholesterol biosynthetic pathways, catalyzing the epoxidation of squalene across a C–C double bond to yield 2,3-oxidosqualene in a reaction more typical of CYP-type oxidations (Ono and Bloch, 1975) and although not uniquely may reduce CYB5 (Oshino *et al.*, 1971; Waskell and Kim, 2015) (Figure 1.5).

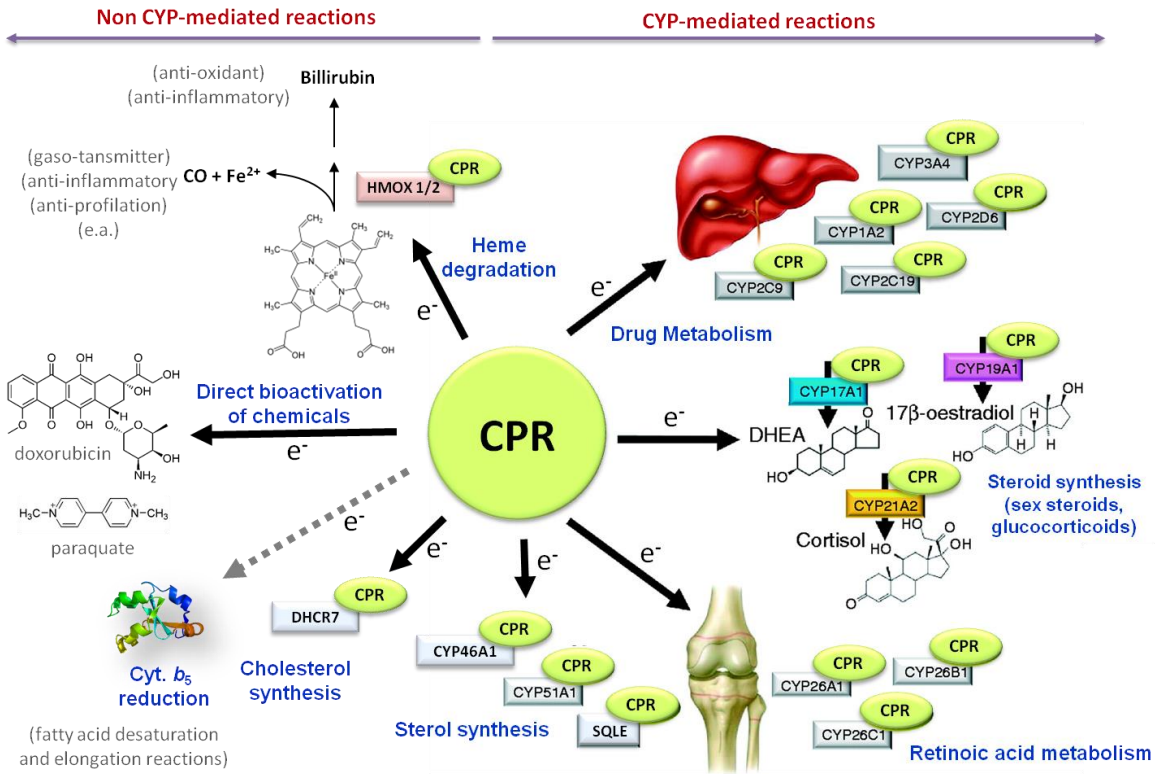

Figure 1.5. Involvement of CPR in central metabolic pathways and its physiological implications (adapted from Tomalik-Scharte *et al.*, 2010, by M. Kranendonk).

Furthermore, CPR participates in the metabolism of several other xenobiotic molecules like mitomycin C, doxorubicin, ferricyanide, paraquate, dichlorophenolindophenol (DCPIP) and nitro blue tetrazolium, either directly reducing these compounds or as an electron donor to the actual catalyst (Pandey *et al.*, 2010, 2013). The surrogate substrate cytochrome *c* is reduced by CPR and serves as a model for ET in CYP reactions as it requires two electrons donated by the FMN moiety of CPR (Pandey *et al.*, 2013).

CPR has thus a very heterogeneous group of redox partners (Figure 1.5). The mechanisms of recognition and the determinants of CPR's promiscuity in physiological acceptors remain largely unclear, although general electrostatic and hydrophobic interactions have been suggested (Hlavica *et al*., 2003; Kandel and Lampe, 2014).

1.3.6 CYP:CPR Interaction

Eukaryotic cells typically possess a multitude of different CYPs, which are tissue and cell-type specific, co-localized on the membrane of the ER and share the same protein partners CPR and CYB5 in a mixed-function oxidase system (Davydov *et al*., 2015; Reed *et al*., 2018). The membrane of the ER seems to form a scaffold, allowing proper alignment and functional interaction of these enzymes (Reed *et al*., 2013).

Interaction between CPR and CYP is necessary for NADPH-dependent ET to the heme proteins. The ratio of CYP enzymes to CPR in the liver ER is in favor of CYP, generally in excess of 5-10:1 (Paine *et al*., 1997; Venkatakrishnan *et al*., 2000). The competition of CYP for CPR implicate a structural organization of the excess CYP around limiting CPR molecules to effectively receive electrons (Davydov *et al*., 2010; Reed *et al*., 2013).

The binding of the different substrates to CYPs can enhance the affinity of CYPs for CPR or increase the CYP reduction potential, thereby providing a more efficient reduction by CPR (Das and Sligar, 2009). The structural constraints imposed by the anchoring of CPR and CYPs in the membranes provide an efficient way to form specific CPR–CYP complexes, which are needed for efficiency, since a single CPR supports multiple CYPs. Insertion of these proteins within the membrane restricts their ability to interact to two dimensions. However, owing to the flexibility of the proteins within the membrane due to the fluid mosaic model of biological membranes, their movement around their membrane-binding segments results in a greater range of motion and increases their ability to form productive complexes (Scott *et al*., 2016). The local lipid environment plays a role as constitutions of the membrane have been shown to affect interaction and ET of CPR to partner proteins (Das and Sligar, 2009). The heterogeneity in composition

of the membrane can also affect CYP function by either concentrating or segregating proteins within membrane regions (Scott *et al.*, 2016).

CPR–CYP interactions are influenced by many factors including the type of CYP, availability of substrates and ionic strength of the system (Backes and Kelley, 2003; Praporski *et al.*, 2009; Farooq and Roberts, 2010). The interaction of CPR with CYP and other electron acceptor proteins seems mainly to be guided by electrostatic interactions, but there is also some evidence for a hydrophobic component (Nadler and Strobel, 1988; Strobel *et al*., 1989). These interactions in its association with a CYP may assist in the stabilization of CPR into an effective conformation (Pochapsky *et al*., 2003).

Higher order of interactions between the components of the CYP monooxygenase system seem to allow more complex means of altering metabolism by the CYP enzymes – through the formation of CYP-CYP complexes (Davydov and Helpert 2008; Reed *et al*., 2012; Reed *et al*., 2018). Evidence seems to indicate that the CYP enzymes and CPR may exist as a mixture of various complexes in the membrane, where both homomeric (Davydov *et al*., 2010; Reed *et al*., 2011; Davydov *et al*., 2013) and heteromeric (Reed *et al*., 2010) associations of CYP enzymes with CPR are likely to occur. In several of the mentioned reports, these types of complexes were shown to alter the enzyme activity for substrates (Reed *et al*., 2018).

1.4 Heterologous expression of human biotransformation enzymes

The science of *in vitro* drug metabolism has shown remarkable progress in the recent two decades. With an increased understanding of drug-metabolizing enzymes and their roles in the metabolism of specific drugs, it is possible to apply a more mechanistic approach in assessing drug metabolism. Currently, there exists a wide array of *in vitro* methodologies to assess CYP catalysis and its modulation by xenobiotics (Ong *et al.*, 2013).

Approaches utilize simple and robust bioanalytical assay techniques to probe CYP enzyme kinetics using different enzyme sources. For example, through cloning of the cDNA of the proteins using recombinant DNA techniques and their heterologous expression in bacterial, yeast and mammalian cell systems. These *in vitro* methods allow the expression of the human enzymes directly in the target cell, increasing sensitivity in the detection, e.g. mutagenicity (Kranendonk *et al.,* 2000).

The heterologous expression of human biotransformation enzymes in bacteria, namely in *Escherichia coli* (*E. coli*), has several advantages since it is cost effective, the organism is easy to manipulate genetically and may produce high levels of protein expression (Kranendonk *et al*., 2000; Ong *et al*., 2013). However, use of *E. coli* systems are limited to enzymes that are not dependent on post-translational modifications, such as phosphorylation and glycosylation (Cain *et al*., 2014). In the case of expressing mammalian CYPs, *E. coli* does not contain any endogenous CYP which could form a confounding factor when performing activity evaluations (Kranendonk *et al*., 2000). Moreover, *E. coli* allows the simultaneous expression of human CYPs with its corresponding CPR for proper catalytic activity studies (Kranendonk et al., 1999b). However, this bacterium possesses a bacterial (cytosolic) reductase system capable of sustaining mammalian CYP activity, albeit very inefficiently (Kranendonk *et al*., 1998).

1.4.1 Bacterial system used for the functional study of CPR

A bi-plasmid system for the co-expression of CPR with a particular human CYP form in *E. coli* was previously engineered in our laboratory and developed by Kranendonk *et al*. (Kranendonk *et al.,* 1999a/b). The initial strain was engineered for mutagenicity testing and was derived from tester strain BMX100 (Kranendonk *et al.,* 1998), which detects efficiently chemical mutagenicity, monitored by the reversion to L-arginine auxotrophy, due to a mutation in the L-Arginine biosynthesis operon (genetic target *arg*E3) (Kranendonk *et al*., 1996). From this initial human CYP competent tester strain several improved derivatives were developed, of which strain BTC-CYP is currently in use (Duarte *et al*., 2005). This humanized bacterial system demonstrated to be a robust *in vitro* model for mechanistic and functional studies of CPR (Moutinho *et al*., 2012; McCammon *et al*., 2016) and CYP-variants (Palma *et al*., 2010; Palma *et al*., 2013).

BTC-CYP bacteria contain a bi-plasmid system for the co-expression of both CYP and CPR (Duarte *et al*., 2005, Kranendonk *et al*., 2008), through expression vectors pCWori-CYP (Fisher *et al*., 1992) and pLCM_POR (Kranendonk *et al.,* 1998; Kranendonk *et al*., 1999a/b) (Figure 1.6). Vector pCWori is an *E. coli* expression vector conferring ampicillin resistance. CYP expression is driven by two consecutive pTAC promoters, under the control the $LacI^q$ repressor, inducible by isopropyl β-D-thiogalactoside (IPTG) (Figure 1.6 B). Vector pLCM_POR confers kanamycin resistance and contains cDNA encoding full length human CPR. CPR expression is driven by a single pTAC promoter, controlled by the presence of the $LacI^q$ repressor (encoded by the pCWori vector), and as such co-induced by IPTG. The presence of *muc*AB operon activates the mutagenic DNA repair system (error-prone), increasing detection of mutagenicity (Kranendonk *et al*., 1998; Mortelmans and Zeiger, 2000) (Figure 1.6 A).

This bi-plasmid expression system in *E. coli* leads to the simultaneous expression of the human CYP complex proteins which are correctly inserted in the bacterial inner cell membrane and fully active, reflecting *in vivo* activities and representing the *in vivo* stoichiometry of the membrane bound enzyme complex in the ER (CPR:CYP 1:5-10) (Paine *et al*., 1997; Venkatakrishnan *et al*., 2000; Kranendonk *et al.,* 2000; Duarte *et al*., 2005).

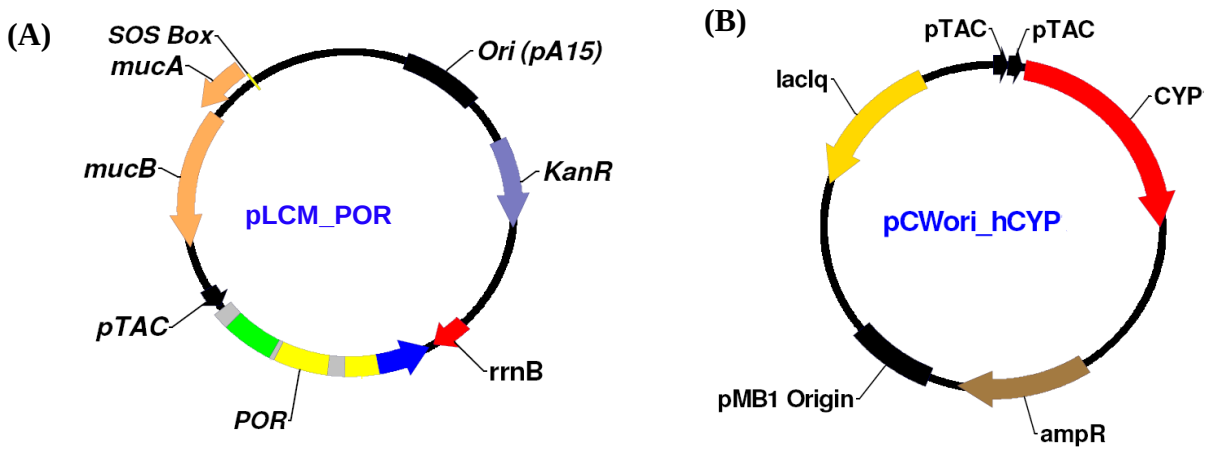

Figure 1.6. Bi-plasmid co-expression system of human CYP-competent cell model. (A) pLCM_*POR* expression vector for CPR variants. (B) Expression vector (pCWori) for different isoforms of representative human CYP (by M. Kranendonk).

The maintenance of the correct stoichiometry of the CYP complex proteins in *in vitro* approaches is important to approximate the system as close as possible to physiological conditions. The CPR/CYP stoichiometry is considered as a major determining factor in the catalytic behavior of mammalian CYPs (Moutinho *et al*., 2012). *In vivo*, the CPR/CYP ratio is in favor of CYP, i.e. CPR is in the sub-molar range relatively to CYP as mentioned above. *In vitro* molecular and mechanistic studies of CYP catalysis should therefore avoid the use of artificial CPR/CYP stoichiometries, generating kinetic data with few relevance to human *in vivo* activities. In the experimental approaches used in this thesis, the *in vivo*-like CPR:CYP stoichiometry was obtained by specific characteristics of the bi-plasmid system of BTC, using two different types (classes) of plasmids for the co-expression of the two enzymes: i) the pCWori-CYP and pLCM_POR vectors have different origin of replications, preventing plasmid incompatibility, and thus allow the coexistence of both plasmids in the same cell; ii) plasmids have different copy numbers (pCW: medium-high and pLCM_POR low copy number) and iii) each plasmid expresses its cDNA through a relatively strong (pCW: double pTAC promotor) and weak promotor (pLCM_POR: single pTAC promotor).

1.5 Aim and outline of this thesis

1.5.1 Aim

At the beginning of this PhD study in 2014, there was a scarcity in data on the structural features controlling the conformational changes in CPR's open/closed protein dynamics in its ET function. Several residues in the hinge segment had been suggested to have a pivotal role in the transition between conformations but little was known on the role of the hinge segment in the mechanism of CPR's gated ET in the interaction with its redox partners.

The aim of this thesis was to unravel the molecular mechanism of CPR's gated ET by disclosing structural determinants in its protein dynamics when sustaining structurally different redox partners in their activity. In particular, specific residues in the hinge segment were studied, to understand how these control the dynamic structural organization and conformational equilibrium of CPR in its ET function. This was pursued by changing specific hinge residues and studying their effect, both on the interaction with a frequently used, but non-physiological, surrogate redox partner of CPR, cytochrome *c*, and as well as with several natural redox partners, such as human CYP isoforms. Three specific representative human CYP isoforms involved in drug metabolism were used, and as such could contribute to the understanding of the role of CPR protein dynamics on CYP-mediated drug metabolism. This will further enhance the knowledge of pharmacokinetic/toxicokinetics of the human metabolism of drugs, xenobiotics and others.

Additionally, as CPR may be considered as a prototype of diflavin reductases, these studies may furthermore contribute to the understanding of multidomain redox systems such as nitric-oxide synthase, methionine synthase reductase, dihydropyrimidine dehydrogenase and NADPH-dependent diflavin oxidoreductase 1 (Lienhart *et al.*, 2013). This may assist in the unravelling of the precise control of the catalytic cycle of these reductases, the coupling with their redox partners and their involvement in relevant human physiological pathways, additionally helpful in understanding their role in specific disease states.

1.5.2 Outline of this thesis

Section 1: Introduction

In the first section, a general introduction to the work presented in this thesis is provided. CPR conformational model and its interaction with redox partners are discussed. In this context, the CYP superfamily and specific isoforms are outlined. Concepts like biotransformation and electron-transfer enzyme function are introduced. Heterologous human protein expression in bacteria is discussed.

Section 2.1: The hinge segment of CPR in conformational switching: the critical role of ionic strength

In section 2.1, the construction by site-directed mutagenesis and characterization of eight CPR hinge mutants, both in the soluble and membrane-bound form, are described. The reduction of the non-physiological substrate cytochrome *c* by these CPR mutants is evaluated at different salt (NaCl) concentrations, to assess the role of ionic strength in CPR's dynamics.

Section 2.2: The role of the hinge of CPR in the interaction with cytochrome P450

In section 2.2, three CPR hinge mutants selected from the original eight mutant forms were combined with three human CYPs. Several functional assays were employed to assess the role of these hinge residues in CPR interaction with these natural redox partners, including the effect of ionic strength on these interactions.

Section 3: Discussion and conclusions

Main findings of this research are discussed in section 3, regarding the role of the hinge segment of CPR in its ET function, the factors that control the protein's conformational equilibrium and CPR's capacity in sustaining activity of structural diverse redox partners. A summary and conclusions of the present research are described. Future perspectives in the study of CPR functioning are presented.

Section 4: Annexes

1.6 REFERENCES

Agrawal V, Choi JH, Giacomini KM, Miller WL. Substrate-specific modulation of CYP3A4 activity by genetic variants of cytochrome P450 oxidoreductase. Pharmacogenet Genomics. 2010; 20(10): 611-8. DOI: 10.1097/FPC.0b013e32833e0cb5.

Aigrain L, Fatemi F, Frances O, Lescop E, Truan G. Dynamic control of electron transfers in diflavin reductases. Int J Mol Sci. 2012; 13(11):15012-41. DOI: 10.3390/ijms131115012.

Aigrain L, Pompon D, Moréra S, Truan G. Structure of the open conformation of a functional chimeric NADPH cytochrome P450 reductase. EMBO Rep. 2009; 10(7): 742-7. DOI: 10.1038/embor.2009.82.

Anzenbacher P, Anzenbacherová E. Cytochromes P450 and metabolism of xenobiotics. Cell Mol Life Sci. 2001; 58(5-6): 737-47.

Backes WL, Kelley RW. Organization of multiple cytochrome P450s with NADPH-cytochrome P450 reductase in membranes. Pharmacol Ther. 2003; 98(2): 221-33.

Barnaba C, Gentry K, Sumangala N, Ramamoorthy A. The catalytic function of cytochrome P450 is entwined with its membrane-bound nature. F1000Res. 2017; 6: 662. DOI: 10.12688/f1000research.11015.1.

Bart AG, Scott EE. Structural and functional effects of cytochrome b5 interactions with human cytochrome P450 enzymes. J Biol Chem. 2017; 292(51): 20818-20833. DOI: 10.1074/jbc.RA117.000220.

Benowitz NL, Lessov-Schlaggar CN, Swan GE, Jacob P 3rd. Female sex and oral contraceptive use accelerate nicotine metabolism. Clin Pharmacol Ther. 2006; 79(5): 480-8. DOI: 10.1016/j.clpt.2006.01.008.

Cain JA, Solis N, Cordwell SJ. Beyond gene expression: the impact of protein post-translational modifications in bacteria. J Proteomics. 2014; 97: 265-86. DOI: 10.1016/j.jprot.2013.08.012.

Chen X, Pan LQ, Naranmandura H, Zeng S, Chen SQ. Influence of various polymorphic variants of cytochrome P450 oxidoreductase (POR) on drug metabolic activity of CYP3A4 and CYP2B6. PLoS One. 2012; 7(6): e38495. DOI: 10.1371/journal.pone.0038495.

Claesson A, Spjuth O. On mechanisms of reactive metabolite formation from drugs. Mini Rev Med Chem. 2013; 13(5): 720-9.

Das A, Sligar SG. Modulation of the cytochrome P450 reductase redox potential by the phospholipid bilayer. Biochemistry. 2009; 48(51): 12104-12. DOI: 10.1021/bi 9011435.

Davydov DR, Davydova NY, Sineva EV, Halpert JR. Interactions among cytochromes P450 in microsomal membranes: oligomerization of cytochromes P450 3A4, 3A5, and 2E1 and its functional consequences. J Biol Chem. 2015; 290(6): 3850-64. DOI: 10.1074/jbc.M114.615443.

Davydov DR, Davydova NY, Sineva EV, Kufareva I, Halpert JR. Pivotal role of P450-P450 interactions in CYP3A4 allostery: the case of α-naphthoflavone. Biochem J. 2013; 453(2): 219-30. DOI: 10.1042/BJ20130398.

Davydov DR, Halpert JR. Allosteric P450 mechanisms: multiple binding sites, multiple conformers or both? Expert Opin Drug Metab Toxicol. 2008; 4(12):1523-35. DOI: 10.1517/17425250802500028.

Davydov DR, Sineva EV, Sistla S, Davydova NY, Frank DJ, Sligar SG, Halpert JR. Electron transfer in the complex of membrane-bound human cytochrome P450 3A4 with the flavin domain of P450BM-3: the effect of oligomerization of the heme protein and intermittent modulation of the spin equilibrium. Biochim Biophys Acta. 2010; 1797(3): 378-90. DOI: 10.1016/j.bbabio.2009.12.008.

Denisov IG, Makris TM, Sligar SG, Schlichting I. Structure and chemistry of cytochrome P450. Chem Rev. 2005; 105(6): 2253-77. DOI: 10.1021/cr0307143.

Dhir V, Ivison HE, Krone N, Shackleton CH, Doherty AJ, Stewart PM, Arlt W. Differential inhibition of CYP17A1 and CYP21A2 activities by the P450 oxidoreductase mutant A287P. Mol Endocrinol. 2007; 21(8):1958-68. DOI: 10.1210/ me.2007-0066.

Di YM, Chow VD, Yang LP, Zhou SF. Structure, function, regulation and polymorphism of human cytochrome P450 2A6. Curr Drug Metab. 2009; 10(7): 754-80.

Duarte MP, Palma BB, Gilep AA, Laires A, Oliveira JS, Usanov SA, Rueff J, Kranendonk M. The stimulatory role of human cytochrome b5 in the bioactivation activities of human CYP1A2, 2A6 and 2E1: a new cell expression system to study cytochrome P450 mediated biotransformation. Mutagenesis. 2005b; 20(2): 93-100. DOI: 10.1093/mutage/gei012.

Duarte MP, Palma BB, Laires A, Oliveira JS, Rueff J, Kranendonk M. *Escherichia coli* BTC, a human cytochrome P450 competent tester strain with a high sensitivity towards alkylating agents: involvement of alkyltransferases in the repair of DNA damage induced by aromatic amines. Mutagenesis. 2005a; 20(3): 199-208. DOI: 10. 1093/mutage/gei028.

Ellis J, Gutierrez A, Barsukov IL, Huang WC, Grossmann JG, Roberts GC. Domain motion in cytochrome P450 reductase: conformational equilibria revealed by NMR and small-angle x-ray scattering. J Biol Chem. 2009; 284(52): 36628-37. DOI: 10. 1074/jbc.M109.054304.

Estabrook RW, Cooper DY, Rosenthal O. The light reversible carbon monoxide inhibition of the steroid c21-hydroxylase system of the adrenal cortex. Biochem Z. 1963; 338: 741-55.

Farooq Y, Roberts GC. Kinetics of electron transfer between NADPH-cytochrome P450 reductase and cytochrome P450 3A4. Biochem J. 2010; 432(3): 485-93. DOI: 10. 1042/BJ20100744.

Fisher CW, Shet MS, Caudle DL, Martin-Wixtrom CA, Estabrook RW. High-level expression in *Escherichia coli* of enzymatically active fusion proteins containing the domains of mammalian cytochromes P450 and NADPH-P450 reductase flavoprotein. Proc Natl Acad Sci U S A. 1992; 89(22): 10817–10821.

Flück CE, Mullis PE, Pandey AV. Reduction in hepatic drug metabolizing CYP3A4 activities caused by P450 oxidoreductase mutations identified in patients with disordered steroid metabolism. Biochem Biophys Res Commun. 2010; 401(1): 149-53. DOI: 10.1016/j.bbrc.2010.09.035.

Foti RS, Rock DA, Wienkers LC, Wahlstrom JL. Selection of alternative CYP3A4 probe substrates for clinical drug interaction studies using *in vitro* data and *in vivo* simulation. Drug Metab Dispos. 2010; 38(6): 981-7. DOI: 10.1124/dmd.110.032094.

Frances O, Fatemi F, Pompon D, Guittet E, Sizun C, Pérez J, Lescop E, Truan G. A well-balanced preexisting equilibrium governs electron flux efficiency of a multidomain diflavin reductase. Biophys J. 2015; 108(6): 1527-1536. DOI: 10.1016/ j.bpj.2015.01.032.

Fuhr U, Jetter A, Kirchheiner J. Appropriate phenotyping procedures for drug metabolizing enzymes and transporters in humans and their simultaneous use in the "cocktail" approach. Clin Pharmacol Ther. 2007; 81(2): 270-83. DOI: 10. 1038/sj.clpt.6100050.

Ghosal A, Hapangama N, Yuan Y, Lu X, Horne D, Patrick JE, Zbaida S. Rapid determination of enzyme activities of recombinant human cytochromes P450, human liver microsomes and hepatocytes. Biopharm Drug Dispos. 2003; 24(9): 375-84. DOI: 10.1002/bdd.374.

Gillette JR, Brodie BB, La du BN. The oxidation of drugs by liver microsomes: on the role of TPNH and oxygen. J Pharmacol Exp Ther. 1957; 119(4): 532-40.

Grunau A, Geraki K, Grossmann JG, Gutierrez A. Conformational dynamics and the energetics of protein -ligand interactions: role of interdomain loop in human cytochrome P450 reductase. Biochemistry. 2007; 46(28): 8244-55. DOI: 10.1021/bi 700596s.

Grunau A, Paine MJ, Ladbury JE, Gutierrez A. Global effects of the energetics of coenzyme binding: NADPH controls the protein interaction properties of human cytochrome P450 reductase. Biochemistry. 2006; 45(5): 1421-34. DOI: 10.1021/ bi052115r.

Guengerich FP, MacDonald JS. Applying mechanisms of chemical toxicity to predict drug safety. Chem Res Toxicol. 2007; 20(3): 344-69. DOI: 10.1021/tx600260a.

Guengerich FP, Martin MV, Sohl CD, Cheng Q. Measurement of cytochrome P450 and NADPH-cytochrome P450 reductase. Nat Protoc. 2009; 4(9): 1245-51. DOI: 10. 1038/nprot.2009.121.

Guengerich FP, Waterman MR, Egli M. Recent Structural Insights into Cytochrome P450 Function. Trends Pharmacol Sci. 2016; 37(8): 625-640. DOI: 10.1016/ j.tips.2016.05.006.

Guengerich FP. Human cytochrome P450 enzymes. In: Cytochrome P450 Structure, Mechanism and Biochemistry, P.O.d. Montellano, Editor, Kluwer, Academic/Plenum Publishers: New York; 2005: 377–530. DOI: 10.1007/b139087.

Guengerich FP. Mechanisms of cytochrome P450 substrate oxidation: MiniReview. J Biochem Mol Toxicol. 2007; 21(4): 163-8.

Guengerich FP. Reduction of cytochrome b5 by NADPH-cytochrome P450 reductase. Arch Biochem Biophys 2005; 440(2): 204-11. DOI: 10.1016/j.abb.2005.06.019.

Guengerich, F., Isin, E. Mechanisms of cytochrome P450 reactions. Acta Chimica Slovenica 2008; 55: 7–19.

Hamdane D, Xia C, Im SC, Zhang H, Kim JJ, Waskell L. Structure and function of an NADPH-cytochrome P450 oxidoreductase in an open conformation capable of reducing cytochrome P450. J Biol Chem. 2009; 284(17): 11374-84. DOI: 10.1074/ jbc.M807868200.

Hendrychová T, Anzenbacherová E, Hudeček J, Skopalík J, Lange R, Hildebrandt P, Otyepka M, Anzenbacher P. Flexibility of human cytochrome P450 enzymes: molecular dynamics and spectroscopy reveal important function-related variations. Biochim Biophys Acta. 2011; 1814(1): 58-68. DOI: 10.1016/j.bbapap.2010.07.017.

Hlavica P, Schulze J, Lewis DF. Functional interaction of cytochrome P450 with its redox partners: a critical assessment and update of the topology of predicted contact regions. J Inorg Biochem. 2003; 96(2-3): 279-97.

Huang N, Agrawal V, Giacomini KM, Miller WL. Genetics of P450 oxidoreductase: sequence variation in 842 individuals of four ethnicities and activities of 15 missense mutations. Proc Natl Acad Sci U S A. 2008; 105(5): 1733-8.

Huang N, Pandey AV, Agrawal V, Reardon W, Lapunzina PD, Mowat D, Jabs EW, Van Vliet G, Sack J, Flück CE, Miller WL. Diversity and function of mutations in p450 oxidoreductase in patients with Antley-Bixler syndrome and disordered steroidogenesis. Am J Hum Genet. 2005; 76(5): 729-49. DOI: 10.1073/pnas. 0711621105.

Huang WC, Ellis J, Moody PC, Raven EL, Roberts GC. Redox-linked domain movements in the catalytic cycle of cytochrome P450 reductase. Structure. 2013; 21(9): 1581-9. DOI: 10.1016/j.str.2013.06.022.

Ingelman-Sundberg M, Mkrtchian S, Zhou Y, Lauschke VM. Integrating rare genetic variants into pharmacogenetic drug response predictions. Hum Genomics. 2018; 12(1): 26. DOI: 10.1186/s40246-018-0157-3.

Iyanagi T, Xia C, Kim JJ. NADPH-cytochrome P450 oxidoreductase: prototypic member of the diflavin reductase family. Arch Biochem Biophys. 2012; 528(1): 72-89. DOI: 10.1016/j.abb.2012.09.002.

Jancova P, Anzenbacher P, Anzenbacherova E. Phase II drug metabolizing enzymes. Biomed Pap Med Fac Univ Palacky Olomouc Czech Repub. 2010; 154(2): 103-16.

Jenner M, Ellis J, Huang WC, Lloyd Raven E, Roberts GC, Oldham NJ. Detection of a protein conformational equilibrium by electrospray ionisation-ion mobility-mass spectrometry. Angew Chem Int Ed Engl. 2011; 50(36):8291-4. DOI: 10.1002/anie. 201101077.

Jiang Z, Dalton TP, Jin L, Wang B, Tsuneoka Y, Shertzer HG, Deka R, Nebert DW. Toward the evaluation of function in genetic variability: characterizing human SNP frequencies and establishing BAC-transgenic mice carrying the human CYP1A1_CYP1A2 locus. Hum Mutat. 2005; 25(2): 196-206. DOI: 10.1002/ humu. 20134.

Johansson I, Ingelman-Sundberg M. Genetic polymorphism and toxicology--with emphasis on cytochrome p450. Toxicol Sci. 2011; 120(1): 1-13. DOI: 10.1093/ toxsci/kfq374.

Kamdem LK, Meineke I, Gödtel-Armbrust U, Brockmöller J, Wojnowski L. Dominant contribution of P450 3A4 to the hepatic carcinogenic activation of aflatoxin B1. Chem Res Toxicol. 2006; 19(4): 577-86. DOI: 10.1021/tx050358e.

Kandel SE, Lampe JN. Role of protein-protein interactions in cytochrome P450-mediated drug metabolism and toxicity. Chem Res Toxicol. 2014; 27(9): 1474-86. DOI: 10.1021/tx500203s.

Komatsu T, Yamazaki H, Shimada N, Nakajima M, Yokoi T. Roles of cytochromes P450 1A2, 2A6, and 2C8 in 5-fluorouracil formation from tegafur, an anticancer prodrug, in human liver microsomes. Drug Metab Dispos. 2000; 28(12): 1457-63.

Kranendonk M, Carreira F, Theisen P, Laires A, Fisher CW, Rueff J, Estabrook RW, Vermeulen NP. Escherichia coli MTC, a human NADPH P450 reductase competent mutagenicity tester strain for the expression of human cytochrome P450 isoforms 1A1, 1A2, 2A6, 3A4, or 3A5: catalytic activities and mutagenicity studies. Mutat Res. 1999a; 441(1): 7383.

Kranendonk M, Fisher CW, Roda R, Carreira F, Theisen P, Laires A, Rueff J, Vermeulen NP, and Estabrook RW. *Escherichia coli* MTC, a NADPH cytochrome P450 reductase competent mutagenicity tester strain for the expression of human cytochrome P450: comparison of three types of expression systems. Mutat Res 1999b: 439: 287–300.

Kranendonk M, Laires A, Rueff J, Estabrook WR, Vermeulen NP. Heterologous expression of xenobiotic mammalian-metabolizing enzymes in mutagenicity tester bacteria: an update and practical considerations. Crit Rev Toxicol. 2000; 30(3): 287-306. DOI: 10.1080/10408440091159211.

Kranendonk M, Marohnic CC, Panda SP, Duarte MP, Oliveira JS, Masters BS, Rueff J. Impairment of human CYP1A2-mediated xenobiotic metabolism by Antley-Bixler syndrome variants of cytochrome P450 oxidoreductase. Arch Biochem Biophys. 2008; 475(2): 93-9. DOI: 10.1016/j.abb.2008.04.014.

Kranendonk M, Mesquita P, Laires A, Vermeulen NP, Rueff J. Expression of human cytochrome P450 1A2 in Escherichia coli: a system for biotransformation and genotoxicity studies of chemical carcinogens. Mutagenesis. 1998; 13(3): 263-9.

Kranendonk M, Pintado F, Mesquita P, Laires A, Vermeulen NP, Rueff J. MX100, a new *Escherichia coli* tester strain for use in genotoxicity studies. Mutagenesis. 1996; 11(4): 327-33.

La Du BN, Gaudette L, Trousof N, Brodie BB. Enzymatic dealkylation of aminopyrine (pyramidon) and other alkylamines. J Biol Chem. 1955; 214(2): 741-5.

Lamb DC, Kim Y, Yermalitskaya LV, Yermalitsky VN, Lepesheva GI, Kelly SL, Waterman MR, Podust LM. A second FMN binding site in yeast NADPH-cytochrome P450 reductase suggests a mechanism of electron transfer by diflavin reductases. Structure. 2006; 14(1): 51-61. DOI: 10.1016/j.str.2005.09.015.

Lamb DC, Waterman MR. Unusual properties of the cytochrome P450 superfamily. Philos Trans R Soc Lond B Biol Sci. 2013; 368(1612): 20120434. DOI: 10.1098/ rstb.2012.0434.

Laursen T, Jensen K, Møller BL. Conformational changes of the NADPH-dependent cytochrome P450 reductase in the course of electron transfer to cytochromes P450. Biochim Biophys Acta. 2011; 1814(1): 132-8. DOI: 10.1016/j.bbapap.2010.07.003.

Lauschke VM, Ingelman-Sundberg M. How to Consider Rare Genetic Variants in Personalized Drug Therapy. Clin Pharmacol Ther. 2018; 103(5): 745-748. DOI: 10. 1002/cpt.976.

Lienhart WD, Gudipati V, Macheroux P. The human flavoproteome. Arch Biochem Biophys. 2013; 535(2): 150-62. DOI: 10.1016/j.abb.2013.02.015.

Liu YT, Hao HP, Liu CX, Wang GJ, Xie HG. Drugs as CYP3A probes, inducers, and inhibitors. Drug Metab Rev. 2007; 39(4): 699-721. DOI: 10.1080/ 03602530701690374.

Marohnic CC, Panda SP, McCammon K, Rueff J, Masters BS, Kranendonk M. Human cytochrome P450 oxidoreductase deficiency caused by the Y181D mutation: molecular consequences and rescue of defect. Human Drug Metab Dispos. 2010; 38(2): 332-40. DOI: 10.1124/dmd.109.030445.

Masters BS, Marohnic CC. Cytochromes P450 - a family of proteins and scientists-understanding their relationships. 2006; 38(1-2): 209-25. DOI: 10.1080/ 03602530600570065.

Masters BS. The journey from NADPH-cytochrome P450 oxidoreductase to nitric oxide synthases. Biochem Biophys Res Commun. 2005; 338(1): 507-19. DOI: 10.1016/j. bbrc.2005.09.165.

McCammon KM, Panda SP, Xia C, Kim JJ, Moutinho D, Kranendonk M, Auchus RJ, Lafer EM, Ghosh D, Martasek P, Kar R, Masters BS, Roman LJ. Instability of the Human Cytochrome P450 Reductase A287P Variant Is the Major Contributor to Its Antley-Bixler Syndrome-like Phenotype. J Biol Chem. 2016; 291(39): 20487-502. DOI: 10.1074/jbc.M116.716019.

Miller WL, Agrawal V, Sandee D, Tee MK, Huang N, Choi JH, Morrissey K, Giacomini KM. Consequences of POR mutations and polymorphisms. Mol Cell Endocrinol. 2011; 336(1-2): 174-9. DOI: 10.1016/j.mce.2010.10.022.

Mortelmans K, Zeiger E. The Ames Salmonella/microsome mutagenicity assay. Mutat Res. 2000; 455(1-2): 29-60.

Moutinho D, Marohnic CC, Panda SP, Rueff J, Masters BS, Kranendonk M. Altered human CYP3A4 activity caused by Antley-Bixler syndrome-related variants of NADPH-cytochrome P450 oxidoreductase measured in a robust *in vitro* system. Drug Metab Dispos. 2012; 40(4): 754-60. DOI: 10.1124/dmd.111.042820.

Murai K, Yamazaki H, Nakagawa K, Kawai R, Kamataki T. Deactivation of anti-cancer drug letrozole to a carbinol metabolite by polymorphic cytochrome P450 2A6 in human liver microsomes. Xenobiotica. 2009; 39(11): 795-802. DOI: 10.3109/00498250903171395.

Mwenifumbo JC, Tyndale RF. Genetic variability in CYP2A6 and the pharmacokinetics of nicotine. Pharmacogenomics. 2007; 8(10): 1385-402. DOI: 10.2217/14622416.8.10.1385.

Nadler SG, Strobel HW. Role of electrostatic interactions in the reaction of NADPH-cytochrome P-450 reductase with cytochromes P-450. Arch Biochem Biophys. 1988; 261(2): 418-29.

Nakajima M, Itoh M, Sakai H, Fukami T, Katoh M, Yamazaki H, Kadlubar FF, Imaoka S, Funae Y, Yokoi T. CYP2A13 expressed in human bladder metabolically activates 4-aminobiphenyl. Int J Cancer. 2006; 119(11): 2520-6. DOI: 10.1002/ijc.22136.

Nebert DW, Dalton TP. The role of cytochrome P450 enzymes in endogenous signalling pathways and environmental carcinogenesis. Nat Rev Cancer. 2006; 6(12): 947-60. DOI: 10.1038/nrc2015.

Nelson DR, Zeldin DC, Hoffman SM, Maltais LJ, Wain HM, Nebert DW. Comparison of cytochrome P450 (CYP) genes from the mouse and human genomes, including nomenclature recommendations for genes, pseudogenes and alternative-splice variants. Pharmacogenetics. 2004; 14(1): 1-18.

Nelson DR. Cytochrome P450 nomenclature, 2004. Methods Mol Biol. 2006; 320: 1-10. DOI: 10.1385/1-59259-998-2:1.

Nicolo C, Flück CE, Mullis PE, Pandey AV. Restoration of mutant cytochrome P450 reductase activity by external flavin. Mol Cell Endocrinol. 2010; 321(2): 245-52. DOI: 10.1016/j.mce.2010.02.024.

Niwa T, Murayama N, Yamazaki H. Heterotropic cooperativity in oxidation mediated by cytochrome P450. Curr Drug Metab. 2008; 9(5): 453-62.

Omura T, Sato R. A new cytochrome in liver microsomes. J Biol Chem. 1962; 237: 1375-6.

Omura T, Sato R. The carbon monoxide-binding pigment of liver microsomes. I. Evidence for its hemoprotein nature. J Biol Chem. 1964a; 239: 2370-8.

Omura T, Sato R. The carbon monoxide-binding pigment of liver microsomes. Ii. Solubilization, purification, and properties. J Biol Chem. 1964b; 239: 2379-85.

Ong CE, Pan Y, Mak JW, Ismail R. *In vitro* approaches to investigate cytochrome P450 activities: update on current status and their applicability. Expert Opin Drug Metab Toxicol. 2013; 9(9): 1097-113. DOI: 10.1517/17425255.2013.800482.

Ono T, Bloch K. Solubilization and partial characterization of rat liver squalene epoxidase. J Biol Chem. 1975; 250(4): 1571-9.

Oshino N, Imai Y, Sato R. A function of cytochrome b5 in fatty acid desaturation by rat liver microsomes. J Biochem. 1971; 69(1): 155-67.

Paine MF, Khalighi M, Fisher JM, Shen DD, Kunze KL, Marsh CL, Perkins JD, Thummel KE. Characterization of interintestinal and intraintestinal variations in human CYP3A-dependent metabolism. J Pharmacol Exp Ther. 1997; 283(3): 1552-62.

Paine MJI, Scrutton NS, Munro AW, Gutierrez A. Roberts GCK, Wolf CR. 2005. Electron transfer partners of cytochrome P450. In: Ortiz de Montellano PR (ed) Cytochrome P450 structure, mechanism and biochemistry, 3rd ed. Kluwer Academic/ Plenum Publishers, New York, pp 115-148.

Palma BB, Silva E Sousa M, Urban P, Rueff J, Kranendonk M. Functional characterization of eight human CYP1A2 variants: the role of cytochrome b5. Pharmacogenet Genomics. 2013; 23(2): 41-52. DOI: 10.1097/FPC.0b013e32835 c2ddf.

Palma BB, Silva E Sousa M, Vosmeer CR, Lastdrager J, Rueff J, Vermeulen NP, Kranendonk M. Functional characterization of eight human cytochrome P450 1A2 gene variants by recombinant protein expression. Pharmacogenomics J. 2010; 10(6): 478-88. DOI: 10.1038/tpj.2010.2.

Pandey AV, Flück CE, Mullis PE. Altered heme catabolism by heme oxygenase-1 caused by mutations in human NADPH cytochrome P450 reductase. Biochem Biophys Res Commun. 2010; 400(3): 374-8. DOI: 10.1016/j.bbrc.2010.08.072.

Pandey AV, Flück CE. NADPH P450 oxidoreductase: structure, function, and pathology of diseases. Pharmacol Ther. 2013; 138(2): 229-54. DOI: 10.1016/j. pharmthera.2013.01.010.

Pandey AV, Sproll P. Pharmacogenomics of human P450 oxidoreductase. Front Pharmacol. 2014; 5: 103. DOI: 10.3389/fphar.2014.00103.

Papaleo E, Saladino G, Lambrughi M, Lindorff-Larsen K, Gervasio FL, Nussinov R. The Role of Protein Loops and Linkers in Conformational Dynamics and Allostery. Chem Rev. 2016; 116(11): 6391-423. DOI: 10.1021/acs.chemrev.5b00623.

Park BK, Boobis A, Clarke S, Goldring CE, Jones D, Kenna JG, Lambert C, Laverty HG, Naisbitt DJ, Nelson S, Nicoll-Griffith DA, Obach RS, Routledge P, Smith DA, Tweedie DJ, Vermeulen N, Williams DP, Wilson ID, Baillie TA. Managing the challenge of chemically reactive metabolites in drug development. Nat Rev Drug Discov. 2011; 10(4): 292-306. DOI: 10.1038/nrd3408.

Parkinson A, Ogilvie BW. 2008. Biotransformation of xenobiotics. Casarett and Doull's toxicology: The basic science of poisons (Klaasen, CD Ed.) 7th ed. New York, NY. McGraw-Hill: 161-295.

Parkinson A, Ogilvie BW; Buckley DB, Kazmi F, Czerwinski M, Parkinson O. 2013. Biotransformation of xenobiotics. Casarett and Doull's toxicology: The basic science of poisons (Klaasen, CD Ed.) 8th ed. New York, NY. McGraw-Hill: 185-366.

Pelkonen O, Pasanen M, Tolonen A, Koskinen M, Hakkola J, Abass K, Laine J, Hakkinen M, Juvonen R, Auriola S, Storvik M, Huuskonen P, Rousu T, Rahikkala M. Reactive metabolites in early drug development: predictive *in vitro* tools. Curr Med Chem. 2015; 22(4): 538-50.

Phillips AH, Langdon RG. Hepatic triphosphopyridine nucleotide-cytochrome *c* reductase: isolation, characterization, and kinetic studies. J Biol Chem. 1962; 237: 2652-60.

Pochapsky SS, Pochapsky TC, Wei JW. A model for effector activity in a highly specific biological electron transfer complex: the cytochrome P450(cam)-putidaredoxin couple. Biochemistry. 2003; 42(19): 5649-56. DOI: 10.1021/bi 034263s.

Porter TD, Beck TW, Kasper CB. NADPH-cytochrome P-450 oxidoreductase gene organization correlates with structural domains of the protein. Biochemistry. 1990; 29(42): 9814-8.

Porter TD. The roles of cytochrome b5 in cytochrome P450 reactions. J Biochem Mol Toxicol. 2002; 16(6): 311–6.

Praporski S, Ng SM, Nguyen AD, Corbin CJ, Mechler A, Zheng J, Conley AJ, Martin LL. Organization of cytochrome P450 enzymes involved in sex steroid synthesis: protein-protein interactions in lipid membranes. J Biol Chem. 2009; 284(48): 33224-32. DOI: 10.1074/jbc.M109.006064.

Pudney CR, Khara B, Johannissen LO, Scrutton NS. Coupled motions direct electrons along human microsomal P450 Chains. PLoS Biol. 2011; 9(12): e1001222. DOI: 10.1371/journal.pbio.1001222.

Raunio H, Rahnasto-Rilla M. CYP2A6: genetics, structure, regulation, and function. Drug Metabol Drug Interact. 2012; 27(2): 73-88. DOI: 10.1515/dmdi-2012-0001.

Reed JR, Cawley GF, Backes WL. Inhibition of cytochrome P450 1A2-mediated metabolism and production of reactive oxygen species by heme oxygenase-1 in rat liver microsomes. Drug Metab Lett. 2011; 5(1): 6-16.

Reed JR, Cawley GF, Backes WL. Interactions between cytochromes P450 2B4 (CYP2B4) and 1A2 (CYP1A2) lead to alterations in toluene disposition and P450 uncoupling. Biochemistry. 2013; 52(23): 4003-13. DOI: 10.1021/bi400422a.

Reed JR, Huber WJ 3rd, Backes WL. Human heme oxygenase-1 efficiently catabolizes heme in the absence of biliverdin reductase. Drug Metab Dispos. 2010; 38(11): 2060-6. DOI: 10.1124/dmd.110.034777.

Reed L, Arlt VM, Phillips DH. The role of cytochrome P450 enzymes in carcinogen activation and detoxication: an *in vivo-in vitro* paradox. Carcinogenesis. 2018; 39(7): 851-859. DOI: 10.1093/carcin/bgy058.

Rendic S, Guengerich FP. Summary of information on the effects of ionizing and non-ionizing radiation on cytochrome P450 and other drug metabolizing enzymes and transporters. Curr Drug Metab. 2012; 13(6): 787-814.

Rendic S, Guengerich FP. Survey of Human Oxidoreductases and Cytochrome P450 Enzymes Involved in the Metabolism of Xenobiotic and Natural Chemicals. Chem Res Toxicol. 2015; 28(1): 38-42. DOI: 10.1021/tx500444e.

Roberts AG, Yang J, Halpert JR, Nelson SD, Thummel KT, Atkins WM. The structural basis for homotropic and heterotropic cooperativity of midazolam metabolism by human cytochrome P450 3A4. Biochemistry. 2011; 50(50): 10804-18. DOI: 10. 1021/bi200924t.

Rossini A, de Almeida Simão T, Albano RM, Pinto LF. CYP2A6 polymorphisms and risk for tobacco-related cancers. Pharmacogenomics. 2008; 9(11): 1737-52. DOI: 10. 2217/14622416.9.11.1737.

Sansen S, Hsu MH, Stout CD, Johnson EF. Structural insight into the altered substrate specificity of human cytochrome P450 2A6 mutants. Arch Biochem Biophys. 2007b; 464(2): 197-206. DOI: 10.1016/j.abb.2007.04.028.

Sansen S, Yano JK, Reynald RL, Schoch GA, Griffin KJ, Stout CD, Johnson EF. Adaptations for the oxidation of polycyclic aromatic hydrocarbons exhibited by the structure of human P450 1A2. J Biol Chem. 2007a; 282(19): 14348-55. DOI: 10. 1074/jbc.M611692200.

Schacter BA, Nelson EB, Marver HS, Masters BS. Immunochemical evidence for an association of heme oxygenase with the microsomal electron transport system. J Biol Chem. 1972; 247(11): 3601-7.

Scott EE, Halpert JR. Structures of cytochrome P450 3A4. Trends Biochem Sci. 2005; 30(1): 5-7. DOI: 10.1016/j.tibs.2004.11.004.

Scott EE, Wolf CR, Otyepka M, Humphreys SC, Reed JR, Henderson CJ, McLaughlin LA, Paloncýová M, Navrátilová V, Berka K, Anzenbacher P, Dahal UP, Barnaba C, Brozik JA, Jones JP, Estrada DF, Laurence JS, Park JW, Backes WL. The Role of Protein-Protein and Protein-Membrane Interactions on P450 Function. Drug Metab Dispos. 2016; 44(4): 576-90. DOI: 10.1124/dmd.115.068569.

Šrejber M, Navrátilová V, Paloncýová M, Bazgier V, Berka K, Anzenbacher P, Otyepka M. Membrane-attached mammalian cytochromes P450: An overview of the membrane's effects on structure, drug binding, and interactions with redox partners. J Inorg Biochem. 2018; 183: 117-136. DOI: 10.1016/j.jinorgbio.2018.03.002.

Strobel HW, Nadler SG, Nelson DR. Cytochrome P-450: cytochrome P-450 reductase interactions. Drug Metab Rev. 1989; 20(2-4): 519-33. DOI: 10.1038/nprot.2009.121.

Su T, Bao Z, Zhang QY, Smith TJ, Hong JY, Ding X. Human cytochrome P450 CYP2A13: predominant expression in the respiratory tract and its high efficiency metabolic activation of a tobacco-specific carcinogen, 4-(methylnitrosamino)-1-(3-pyridyl)-1-butanone. Cancer Res. 2000; 60(18): 5074-9.

Sugishima M, Sato H, Higashimoto Y, Harada J, Wada K, Fukuyama K, Noguchi M. Structural basis for the electron transfer from an open form of NADPH-cytochrome P450 oxidoreductase to heme oxygenase. Proc Natl Acad Sci U S A. 2014; 111(7): 2524-9. DOI: 10.1073/pnas.1322034111.

Sündermann A, Oostenbrink C. Molecular dynamics simulations give insight into the conformational change, complex formation, and electron transfer pathway for cytochrome P450 reductase. Protein Sci. 2013; 22(9): 1183-95. DOI: 10.1002/pro. 2307.

Tomalik-Scharte D, Maiter D, Kirchheiner J, Ivison HE, Fuhr U, Arlt W. Impaired hepatic drug and steroid metabolism in congenital adrenal hyperplasia due to P450 oxidoreductase deficiency. Eur J Endocrinol. 2010; 163(6): 919-24. DOI: 10.1530/ EJE-10-0764.

Venkatakrishnan K, von Moltke LL, Court MH, Harmatz JS, Crespi CL, Greenblatt DJ. Comparison between cytochrome P450 (CYP) content and relative activity approaches to scaling from cDNA-expressed CYPs to human liver microsomes: ratios of accessory proteins as sources of discrepancies between the approaches. Drug Metab Dispos. 2000; 28(12): 1493-504.

Vergéres G, Waskell L. Cytochrome b5, its functions, structure and membrane topology. Biochimie. 1995; 77(7-8): 604-20.

Vincent B, Morellet N, Fatemi F, Aigrain L, Truan G, Guittet E, Lescop E. The closed and compact domain organization of the 70-kDa human cytochrome P450 reductase in its oxidized state as revealed by NMR. J Mol Biol. 2012; 420(4-5): 296-309. DOI: 10.1016/j.jmb.2012.03.022.

Wang M, Roberts DL, Paschke R, Shea TM, Masters BS, Kim JJ. Three-dimensional structure of NADPH-cytochrome P450 reductase: prototype for FMN- and FAD-containing enzymes. Proc Natl Acad Sci USA. 1997; 94(16): 8411-6.

Waskell L, Kim JJP. 2015. Electron-transfer Partners of Cytochrome P450. In: Ortiz de Montellano PR (ed). Cytochrome P450 structure, mechanism and biochemistry, 4th ed. Springer International Publishing, Switzerland, pp 33–68. DOI: 10.1007/978-3-319-12108-6

Williams CH Jr, Kamin H. Microsomal triphosphopyridine nucleotide-cytochrome *c* reductase of liver. J Biol Chem. 1962; 237: 587-95.

Xia C, Hamdane D, Shen AL, Choi V, Kasper CB, Pearl NM, Zhang H, Im SC, Waskell L, Kim JJ. Conformational changes of NADPH-cytochrome P450 oxidoreductase are essential for catalysis and cofactor binding. J Biol Chem. 2011a; 286(18): 16246-60. DOI: 10.1074/jbc.M111.230532.

Xia C, Panda SP, Marohnic CC, Martásek P, Masters BS, Kim JJ. Structural basis for human NADPH-cytochrome P450 oxidoreductase deficiency. Proc Natl Acad Sci U S A. 2011b; 108(33): 13486-91. DOI: 10.1073/pnas.1106632108.

Xu C, Li CY, Kong AN. Induction of phase I, II and III drug metabolism/transport by xenobiotics. Arch Pharm Res. 2005; 28(3): 249-68.

Zanger UM, Schwab M. Cytochrome P450 enzymes in drug metabolism: regulation of gene expression, enzyme activities, and impact of genetic variation. Pharmacol Ther. 2013; 138(1): 103-41. DOI: 10.1016/j.pharmthera.2012.12.007.

Zanger UM, Turpeinen M, Klein K, Schwab M. Functional pharmacogenetics/genomics of human cytochromes P450 involved in drug biotransformation. Anal Bioanal Chem. 2008; 392(6): 1093-108. DOI: 10.1007/s00216-008-2291-6.

Zhou H, Josephy PD, Kim D, Guengerich FP. Functional characterization of four allelic variants of human cytochrome P450 1A2. Arch Biochem Biophys. 2004; 422(1): 23-30.

Zhou Y, Ingelman-Sundberg M, Lauschke VM. Worldwide Distribution of Cytochrome P450 Alleles: A Meta-analysis of Population-scale Sequencing Projects. Clin Pharmacol Ther. 2017; 102(4): 688-700. DOI: 10.1002/cpt.690.

2. RESULTS

2.1 The Hinge Segment of Human CPR in Conformational Switching: The Critical Role of Ionic Strength

This section was transcribed from a peer-reviewed paper, featured in an e-book published by Frontiers in Pharmacology:

D. Campelo, *et al.* (2017). "The hinge segment of human NADPH cytochrome P450 reductase in conformational switching: the critical role of ionic strength". Front Pharmacol. 8:755. DOI: 10.3389/fphar.2017.00755.

D. Campelo, *et al.* (2018). "The Hinge Segment of Human NADPH-Cytochrome P450 Reductase in Conformational Switching: The Critical Role of Ionic Strength" In Pandey, A. V., Henderson, C. J., Ishii, Y., Kranendonk, M., Backes, W. L., Zanger, U. M., eds. Role of Protein-Protein Interactions in Metabolism: Genetics, Structure, Function. (pp-125-137). Lausanne: Frontiers Media. DOI: 10.3389/978-2-88945-385-6. ISBN 978-2-88945-385-6.

CONTENT

2.1.1 ABSTRACT

NADPH-cytochrome P450 reductase (CPR) is a redox partner of microsomal cytochrome P450 and is a prototype of the diflavin reductase family. CPR contains 3 distinct functional domains: a FMN-binding domain (acceptor reduction), a linker (hinge), and a connecting/FAD domain (NADPH oxidation). It has been demonstrated that the mechanism of CPR exhibits an important step in which it switches from a compact, closed conformation (locked state) to an ensemble of open conformations (unlocked state), the latter enabling ET to redox partners. The conformational equilibrium between the locked and unlocked states has been shown to be highly dependent on ionic strength, reinforcing the hypothesis of the presence of critical salt interactions at the interface between the FMN and connecting FAD domains. Here we show that specific residues of the hinge segment are important in the control of the conformational equilibrium of CPR. We constructed six single mutants and two double mutants of the human CPR, targeting residues G240, S243, I245 and R246 of the hinge segment, with the aim of modifying the flexibility or the potential ionic interactions of the hinge segment. We measured the reduction of cytochrome *c* at various salt concentrations of these 8 mutants, either in the soluble or membrane bound form of human CPR. All mutants were found capable of reducing cytochrome *c* yet with different efficiency and their maximal rates of cytochrome *c* reduction were shifted to lower salt concentration. In particular, residue R246 seems to play a key role in a salt bridge network present at the interface of the hinge and the connecting domain. Interestingly, the effects of mutations, although similar, demonstrated specific differences when present in the soluble or membrane-bound context. Our results demonstrate that the electrostatic and flexibility properties of the hinge segment are critical for ET from CPR to its redox partners.

Keywords: diflavin reductase, protein dynamics, multidomain proteins, conformational exchange, electron transfer, protein–protein interaction

2.1.2 INTRODUCTION

Monooxygenase enzymes occur in all kingdoms of life and CYPs represent the largest superfamily of them (Lamb and Waterman, 2013; Munro *et al.,* 2013). In mammals, microsomal CYPs catalyze the oxidation of a wide variety of essential endogenous and xenobiotic compounds (Coon, 2005; Rendic and Guengerich, 2015) by a two-electron activation of molecular oxygen, whereby one atom of oxygen is inserted into the organic substrate and the other is reduced to water (Guengerich, 2007). The catalytic cycle of CYP enzymes depends on redox partners for electron delivery. The CPR is strictly required for the activity of microsomal CYPs, while CYB5 can potentially be a donor molecule, albeit only for the second ET step (Scott *et al.*, 2016).

Human CPR, encoded by the *POR* gene, is a 78-kDa multidomain diflavin reductase that binds both FMN and FAD and is attached to the cytoplasmic side of the ER via a transmembrane segment at its N-terminus. The domains that bear the two cofactors are: a flavodoxin like FMN-binding domain and a ferredoxin-NADPC reductase like FAD-binding domain. The third domain, called the hinge segment, links the FMN and the connecting/FAD domain. Electrons flow through CPR from NADPH to oxidized FAD as a hydride ion transfer to the FAD N5 atom, then, one by one, from the FAD to the FMN, then from the FMN hydroquinone to external acceptors, with the FMN cycling mainly between the hydroquinone and the blue semiquinone states (Murataliev *et al.*,1999).

Although studies of CPR have predominantly focused on its role in CYP catalysis, CPR also support ET to other enzymes like HO (Schacter *et al.*, 1972), SQLE (Ono and Bloch, 1975), dehydrocholesterol reductase (DHCR) (Nishino and Ishibashi, 2000), and though not uniquely, CYB5, involved also in fatty acid desaturation and elongation reactions (Oshino *et al.*, 1971). The determinants of this promiscuity in physiological acceptors are not yet known, however, they might indicate that the mechanisms of recognition of this heterogenic group of redox partners by CPR are probably not highly stringent.

The first X-ray diffraction studies on soluble rat CPR showed a surprising compact structure in which the distance of FAD to FMN was about 4 Å, the two isoalloxazine rings almost coplanar and some parts of the FMN domain tightly packed against the rest of the CPR protein (Wang *et al.*, 1997). This conformation, referred thereafter as part of

a locked state, was easily ascribed to the conformation allowing ET from FAD to FMN. Several other X-ray structures of CPR displaying the same spatial organization were subsequently obtained (Lamb *et al.*, 2006; Xia *et al.*, 2011b; McCammon *et al.*, 2016). This conformational state as obtained in crystals, also occurs in solution (Vincent *et al.*, 2012). Furthermore, a CPR mutant in which the FMN domain was linked to the FAD domain via a disulfide bridge was competent for ET to the FMN moiety, ultimately proving that the locked state is fit for the internal flavin ET but is unable to reduce external cytochrome acceptors unless the disulfide bridge is reduced (Xia *et al.*, 2011a). This led to the hypothesis that interdomain motions have to take place to render the FMN domain accessible to electron acceptors.

The crystal structure of a mutant CPR in which the hinge segment was shortened by deletion of four residues (ΔTGEE) shows three different molecules per asymmetric unit. In each of them, the FMN domain is in a different position, more and more distant from the rest of the protein, whereas their connecting and FAD-binding domains are strictly superimposable, demonstrating a marked reorientation of the FMN domain relative to the FAD domain (Hamdane *et al.*, 2009). Another evidence for domain mobility has come from the structural study of a chimeric enzyme consisting of the FMN-binding domain of yeast CPR and the remainder of the molecule, including the hinge segment, from human CPR (Aigrain *et al.*, 2009). This chimeric enzyme, which is active in NADPH reduction of cytochromes *c* and CYP, displays a single, well-defined, molecule in the asymmetric unit. In this structure, the FMN domain is no longer making any interface with the connecting and FAD domains. Hence, large domain movements can happen in CPR (86 Å distance between the two flavins). Furthermore, the redox potential of the flavins exhibit changes that maybe attributed to this large conformational change (Aigrain *et al.*, 2011). The various conformations in which the FMN domain is no longer making an interface with the FAD domain represent an ensemble of structures that can be designated as the unlocked state. SAXS studies on human CPR have also been crucial in demonstrating that, in solution, human CPR is in equilibrium between a closed, compact and a series of open, extended conformations (Ellis *et al.*, 2009; Huang *et al.*, 2013; Frances *et al.*, 2015). The abovementioned mutant CPR containing a disulfide bond, though capable of NADPH mediated ferricyanide reduction, is essentially incapable of supporting CYP activity unless the disulfide bond is reduced (Xia *et al.*, 2011a).

The ability of both flavin domains to move relatively back and forth from each other is thus a prerequisite for the FMN domain to interact with its physiological acceptors. However, the structural determinants that guide this conformational transition between open and closed forms, a process demonstrated to be essential for gating the interflavin ET in CPR and thus to its redox partners, are still not fully identified.

It has long been known that ET from CPR to CYP displays a strong ionic strength dependency which demonstrated that the ET complex between the CPR and a CYP is, beside hydrophobic interactions, strongly based on charge pair interactions (Tamburini and Schenkman, 1986; Nadler and Strobel, 1988, 1991; Davydov *et al.*, 1996, 2000; Bridges *et al.*, 1998). Most of these studies evidenced that ionic interactions between CPR and its redox partners were the major determinants of the salt effects on CYPs activities and are reviewed in (Hlavica *et al.*, 2003). However, we also demonstrated that the ionic strength effect on cytochrome *c* reduction by the soluble form of human CPR depends on the conformational equilibrium between the locked and unlocked states (Frances *et al.*, 2015). From the comparative studies of the open conformation seen in the chimeric yeast-human CPR, two residues in the hinge, G240 and S243, were proposed to be important molecular determinants for the large conformational changes (Aigrain *et al.*, 2009). Beside these two residues, I245 and R246 were also recently identified, in a molecular dynamics simulation study, as two essential residues of the hinge segment, forming a part of the conformational axis and involved in a rotational movement of the FMN domain relative to the rest of the protein (Sündermann and Oostenbrink, 2013). S243 and R246 were also found to display large chemical shifts during the change in the conformational equilibrium between the locked and unlocked states (Frances *et al.*, 2015). Additionally, the hinge segment was also found to be directly controlling ET to cytochrome *c* from the reductase domain of nNOS (Haque *et al.*, 2007, 2012) as well as in CPR (Grunau *et al.*, 2007).

In this work we have targeted four specific residues of the hinge segment indicated above, for site-directed mutagenesis to test their potential role in the conformational equilibrium of human CPR. By analyzing the salt-dependent changes of the cytochrome *c* reductase activity in the context of both soluble and membrane-bound forms of CPR, we propose

several hypotheses on the role played by these residues on the transition between the locked to the unlocked state, and thus in the ET mechanism of CPR.

2.1.3 MATERIALS AND METHODS

Reagents

DCPIP and potassium ferricyanide were from Fluka (Buchs, Switzerland). L-Arginine, ampicillin, kanamycin sulfate, chloramphenicol, cytochrome *c* (horse heart), IPTG (dioxane-free), thiamine, glucose 6-phosphate, glucose 6-phosphate dehydrogenase, $NADP^+$ and NADPH were obtained from Sigma–Aldrich (St. Louis, MO, United States). Phenylmethanesulfonyl fluoride (PMSF) was purchased from Gerbu Biotechnik GmbH (Heidelberg, Germany). Bacto agar, Bacto peptone and Bacto tryptone were obtained from BD Biosciences (San Jose, CA, United States). Bacto yeast extract was obtained from Formedium (Norwich, England). A polyclonal antibody from rabbit serum raised against recombinant human CPR obtained from Genetex (Irvine, CA, United States) was used for immunodetection of the membrane-bound CPR, while the respective antibody used the in the case of the soluble form of the enzyme was obtained from Thermofisher Scientific (Waltham, MA, United States).

Construction and Cloning of the Different Mutants

Soluble Forms of Human CPR

Soluble CPR mutants, deleted of their first 44 N-terminal amino acids, were cloned by the Gibson method using a synthetic DNA fragment containing the desired mutation, with a compatible divergent PCR amplification of the plasmid pET15b expressing the soluble form of the human CPR, containing a N-terminal 6xHis tag. DNA sequencing confirmed the absence of any undesired mutations. The constructed plasmids were transformed into competent *E. coli* BL21 (DE3) cells for expression.

Membrane-Bound Forms of Human CPR

Plasmid pLCM_POR (Kranendonk *et al*., 2008) was used for the expression of the membrane-bound, full-length forms of human CPR. Mutants containing alanine substitutions of residues I245 and R246 were initially obtained through standard site-directed mutagenesis, using the sub-cloning vector pUC_POR, containing the initial segment (1–1269 bp) of human *POR* cDNA comprising the FMN and hinge domains (based on National Center for Biotechnology Information sequence NM_000941, encoding the CPR consensus protein sequence (NP_000932)). The mutated segments were obtained from the different mutated pUC_*POR* plasmids, using *Eco*RI + *Aat*II restriction enzymes and cloned back into full-length CPR expression vector pLCM_POR. CPR mutants containing proline substitutions of residues G240, S243, I245 and R246 were obtained by the Gibson method using a synthetic DNA fragment containing the desired mutation and a compatible divergent PCR amplification of the plasmid pET15b expressing the soluble form of human CPR. The mutated gene fragments were sub-cloned in vector pUC_POR using Megaprimer PCR of whole plasmid (MEGAWHOP) (Miyazaki and Takenouchi, 2002), followed by *Dpn*I treatment. The mutated segments were obtained using *Eco*81I + *Sac*I restriction enzymes and cloned back into the CPR expression vector pLCM_POR. The different constructed pLCM_POR plasmids were transformed into DH5a *E. coli* cells for plasmid propagation. *POR* cDNA of plasmids was fully sequenced to confirm the introductions of the designed mutations and the absence of any undesired mutations. CPR mutants were expressed in *E. coli* BTC, using the specialized bi-plasmid system for co-expression of CPR with human CYPs (Duarte *et al*., 2005). The pLCM_POR and the CYP-void plasmid pCWΔ (Kranendonk *et al*., 2008) were transfected through standard electroporation procedures (see annex 1).

Protein Expression and Isolation

Soluble Forms of CPR

Protein expression in BL21 (DE3) cells was carried out at 29 ºC in Terrific Broth medium complemented with 1 $mg.L^{-1}$ riboflavin and 100 $mg.mL^{-1}$ ampicillin during 36 h (Frances *et al.*, 2015). Cultures were spun down for 10 min at 7200 g and suspended in 20 mM

Na/K phosphate buffer pH 7.4 (buffer A). Cell lysis was achieved by 4 cycles of sonication (30 s of burst followed by intervals of 2 min for cooling) in buffer A containing a protease inhibitor cocktail (aprotinin 0.3 mM, leupeptin 1 mM, pepstatin A 1.5 mM, benzamidine 100 mM, metabisulfite 100 mM). Cell debris were removed by centrifugation at 8200 g for 1 h at 4 ºC. His-tagged proteins were bound on a TALON polyhistidine-TAG Purification Resin (Clontech, Mountain View, CA, United States), equilibrated with buffer A, containing 0.25 M NaCl and 0.25 M KCl, washed with this equilibrium buffer and eluted with a 0.25 M imidazole step gradient. Imidazole was eliminated from the eluted fraction by sequential washes in buffer A using a Vivaspin-15 centrifugal concentrator (Sartorius, Goettingen, Germany). The protein solution was stored at 4 ºC in buffer A, containing 1 mM of both FMN and FAD. Purity of the sample was determined by SDS–PAGE and examination of the 280/450 nm ratio measured by optical spectroscopy.

Membrane-Bound Forms of CPR

Expression of the full-length membrane bound CPR mutants was obtained in BTC bacteria and membrane fractions of the different strains were prepared and characterized for protein content as described previously (Marohnic *et al*., 2010; Palma *et al*., 2013). CPR content of membrane fractions was quantified by immunodetection against a standard curve of purified human, full-length wild-type (WT) CPR, using polyclonal rabbit anti-CPR primary antibody and biotin-goat anti-rabbit antibody in combination with the fluorescent streptavidin conjugate (WesternDot 625 Western Blot Kit; Invitrogen). Densitometry of CPR signals was performed using LabWorks 4.6 software (UVP, Cambridge, United Kingdom) (see annex 1).

DCPIP and Ferricyanide Reduction Assay and Cytochrome *c* Reduction Microplate Assay

DCPIP and Ferricyanide Reduction

With DCPIP, assays were performed in 20 mM Tris-HCl buffer containing 1 mM EDTA, and various NaCl concentrations (from 50 mM up to 1.4 M), pH 7,4 at 25 ºC in the presence of 70 mM DCPIP. Initial rates were monitored at 600 nm using $\Delta\varepsilon_M$ = 21000 $M^{-1}.cm^{-1}$. With ferricyanide, assays were performed in the same conditions as described above, but in the presence of 1 mM ferricyanide. Initial rates were monitored at 420 nm using $\Delta\varepsilon_M$ = 1020 $M^{-1}.cm^{-1}$.

Cytochrome *c* Reduction Activities

Initial experiments were performed with soluble CPR. Cytochrome *c* reductase activity was followed at 550 nm ($\Delta\varepsilon_M$ = 21000 $M^{-1}.cm^{-1}$) with CPR concentrations ranging from 2 to 20 nM. In cuvette assays, cytochrome *c* (100 mM final) and NADPH (200 mM final) were mixed in 20 mM Tris-HCl buffer containing 1 mM EDTA, and various NaCl concentrations (from 50 mM up to 1.4 M), pH 7.4 at 25 ºC. The reaction was initiated by adding CPR. A set of preliminary rate assays were performed in a microtiter plate format to optimize linearity of the reaction traces for the mutants, with conditions close to the traditional *cuvette* approach. In particular, the concentrations of CPR, cytochrome *c* and NADPH were varied in several control experiments to ensure linearity. In these assays, CPR and NADPH (200 mM final) were mixed and the reaction was started by diluting directly this mix in microplate wells containing 20 mM Tris-HCl buffer pH 7.4, supplemented with cytochrome *c* (100 or 200 mM) and the *ad hoc* NaCl final concentration (from 50 mM to 1.25 M) at 37 ºC. The reaction was monitored at 550 nm for 5 min in a PowerWave X select microplate reader (Biotek Instruments, Winooski, VT, United States).

A first set of kinetic measurements was performed in triplicate using the two cytochrome *c* concentrations indicated above. A second set of triplicate experiments was repeated with another batch of purified CPR. Reduction velocities were found virtually equal when using cytochrome *c* at 100 or 200 mM (data not shown). Cytochrome *c* was subsequently

used in the microplate format at 200 mM (final concentration) for all kinetic measurements. CPR samples (soluble forms) were diluted up to concentrations giving linear velocity traces to compensate for lower or increased velocities, see Supplementary Table S2.1. Each k_{obs} value is the average of six measurements: one triplicate using a first batch of enzyme and a second triplicate, using a second batch of purified CPR.

The conditions of the microplate rate assay were then verified for the membrane-bound CPRs, to ensure linearity of the reaction traces. Reactions were followed for 4 min in a multi-mode microtiter plate reader (SpectraMax i3x, Molecular Devices) and each sample was assayed at least in triplicate. The optimal dilution of the membrane bound WT CPR was determined (0.5 pmol/mL), using 200 mM of cytochrome *c*, NADPH regenerating system (NADPH 200 mM, glucose 6-phosphate 500 mM and glucose 6-phosphate dehydrogenase 0,04 U/mL, final concentrations) and 372 mM NaCl in a 100 mM Tris buffer (pH 7.4). The same CPR dilution was applied in the cuvette assay under the same conditions except for cytochrome *c* (50 mM) and NADPH (200 mM, without regeneration) and was measured during 60 s, which resulted in virtually the same k_{obs} as with the microtiter plate format assay. Finally, the membrane bound mutants were assayed with CPR well-concentrations, proportionally diluted as those determined for the soluble forms (see Sup. Table S2.1). Control experiments with *E. coli* (BTC) membranes without CPR expression demonstrated no cytochrome *c* reduction upon dilution (see annex 1).

2.1.4 RESULTS

Ionic Strength Dependency of the ET of the Soluble Form of Human CPR to Three Artificial Acceptors

In order to further understand the role of the ionic strength in ET from CPR to acceptors such as cytochrome *c* and discriminate between the two major hypotheses (salt-dependent conformational equilibrium or electrostatic interactions with the substrates), we analyzed and compared the ionic strength dependency of CPR toward DCPIP and ferricyanide with that of cytochrome *c*. DCPIP and ferricyanide have unique characteristics in term of charge and electron receiving capabilities (redox potential). **Figure 2.1** shows the activity profiles of the soluble, WT form of human CPR in function of the ionic strength for cytochrome *c*-, DCPIP- and ferricyanide-reduction.

Cytochrome *c* and DCPIP related graphs share the same bell-shaped curve. For cytochrome *c*, the concentration of NaCl giving the maximal k_{obs} is around 400 mM, a value quite comparable to the one measured in our previous study (Frances *et al.*, 2015). However, the maximum of k_{obs} is different for DCPIP (575 mM). This difference might be attributed to the fact that DCPIP is an obligate two electrons (hydride) acceptor, which may have a different overall ET scheme compared to cytochrome *c*. The ionic strength dependent variation of k_{obs} measured for the reduction of DCPIP and cytochrome *c* by soluble human CPR display both a bell-shaped profile. However, these substrates are different in term of net charge (cytochrome *c* contains + 9,5 charges at pH 7,0 while DCPIP is neutral). This result thus strengthens the hypothesis that the ionic strength dependency of electron flow from CPR to acceptors is mainly determined by the conformational equilibrium between the locked and unlocked states of CPR and only in a minor manner by electrostatic interactions between the FMN domain and the acceptor.

We also analyzed the reduction of ferricyanide, another nonnatural substrate. Interestingly, the salt-dependent k_{obs} profile is totally different from the ones seen with cytochrome *c* or DCPIP, being composed of two straight lines crossing at a NaCl concentration of around 450 mM. The constant rise of the k_{obs} might be attributed to a gradual increase of the redox potential of ferricyanide due to the increase of ionic strength

in Tris-based buffers (O'Reilly, 1973). Therefore, the ferricyanide reduction, which mainly occurs at the FAD cofactor (Vermilion *et al.*, 1981), may be relatively independent from the salt concentration and hence from the conformational equilibrium, a result that was previously observed with the ΔTGEE mutant (Hamdane *et al.*, 2009). Interestingly, the inflection occurs around a salt concentration quite similar to the one yielding the maximum k_{obs} with cytochrome *c*. However, we do not have any coherent explanation for the peculiar salt profile observed with this substrate.

Based on these latter results, we decided to use cytochrome *c* reduction as an appropriate reporter to probe salt-mediated conformational equilibrium changes in ET of specific CPR mutants.

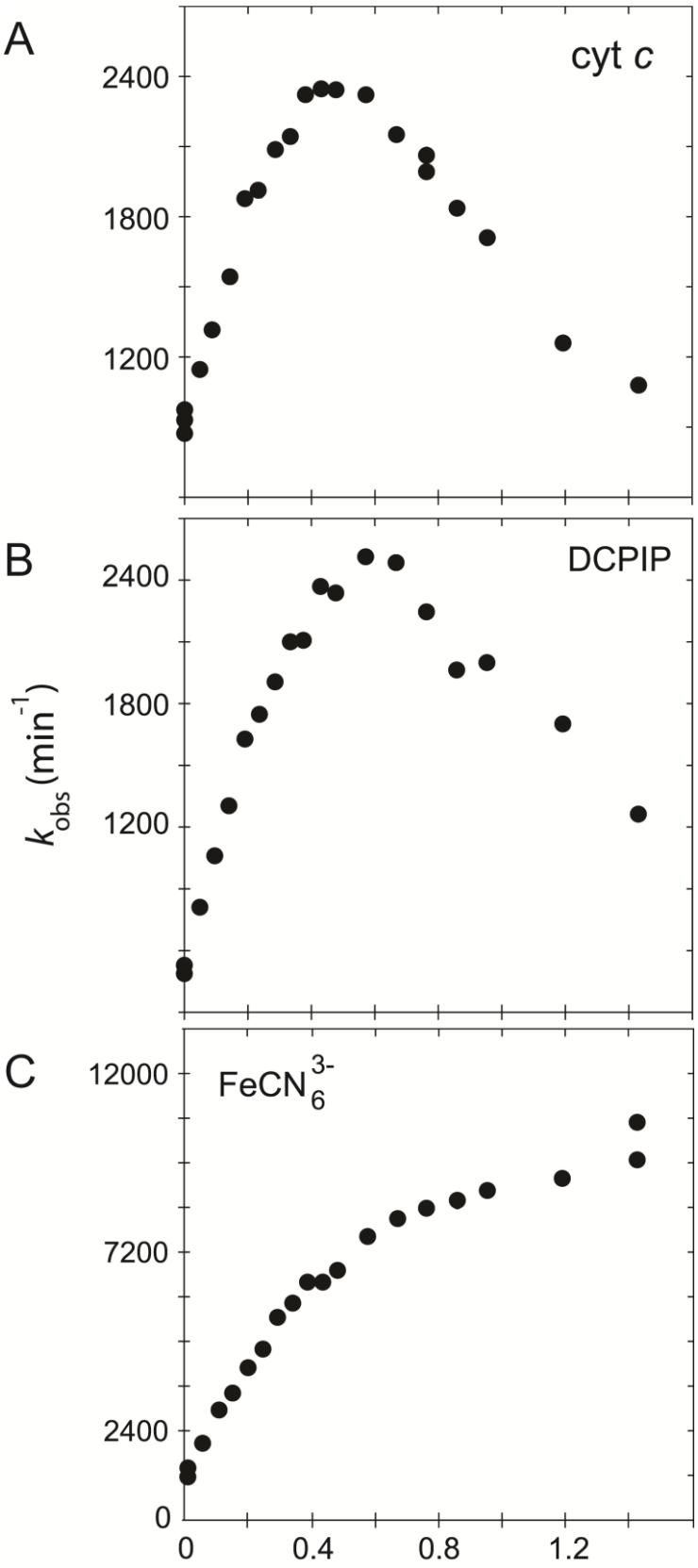

Figure 2.1 Variation of k_{obs} in function of the ionic strength. The activity of the soluble, WT form of human CPR was assayed with various acceptors, namely cytochrome *c* **(A)**, DCPIP **(B)** or ferricyanide **(C)**.

Design of the Different Mutants

The hinge segment is defined by a stretch of 14–15 amino acids that does not display any particularly defined secondary structure. It is also the only part of the CPR structure where evident structural changes can be seen when comparing the two open conformations of CPR (crystallographic structures of the ΔTGEE mutant and the yeast/human chimera) and the other closed conformations of CPR (yeast, human, rat). Residues G240 and S243 (numbering according to the human CPR consensus amino acid sequence NP_000932) correspond to positions with strongly modified phi and psi angles between the closed and open forms (Aigrain *et al.*, 2009). These two residues were therefore mutated into prolines in order to test if and how geometrical constraints modify the conformational equilibrium of CPR. Residues I245 and R246 were selected based on the observation that the backbone atoms of both residues were rotated in the ΔTGEE mutant or in the closed to open transition visualized by molecular modeling (Hamdane *et al.*, 2009; Sündermann and Oostenbrink, 2013). For this last residue, we evidently switched the cationic Arg residue into a non-charged one (either Ala or Pro) while for the previous Ile residue, we preferred mutations affecting either the mobility/rigidity (Ile to Ala or Pro). Two double mutants, cumulating charge and flexibility changes were also designed for residues 245/246. Finally, as the physiological form of CPR is membrane-bound and the membrane anchoring segment may have a profound influence on the equilibrium between locked and unlocked states or the open-closed exchange rates, we analyzed the effects of these mutations in both the soluble and membrane bound context.

Based on these rationales, six single mutants (G240P, S243P, I245A, I245P, R246A and R246P) and two double mutants (I245A/R246A and I245R/R246I) were produced both in the soluble and membrane-bound (full-length) forms of CPR. **Figure 2.2** provides a representation of the positions of the four targeted amino acids in the structure of the closed conformation of human CPR (5FA6, chain A) and on the structure of the open conformation of the yeast/human chimeric CPR (3FJO). The two structures (5FA6, chain A and 3FJO) were aligned onto the FAD domain (**Figure 2.2A**) or the FMN domain (**Figure 2.2B**). Both views provide the rationale for the design of our mutants: G240 corresponds to the position where the hinge is tilted in the open conformation compared to the closed conformation (**Figure 2.2A**); S243 side chain orientation is different

between the two forms (**Figure 2.2A**); I245 and R246 show an interesting proximity and potential interaction with the connecting domain (**Figures 2.2 A, B**).

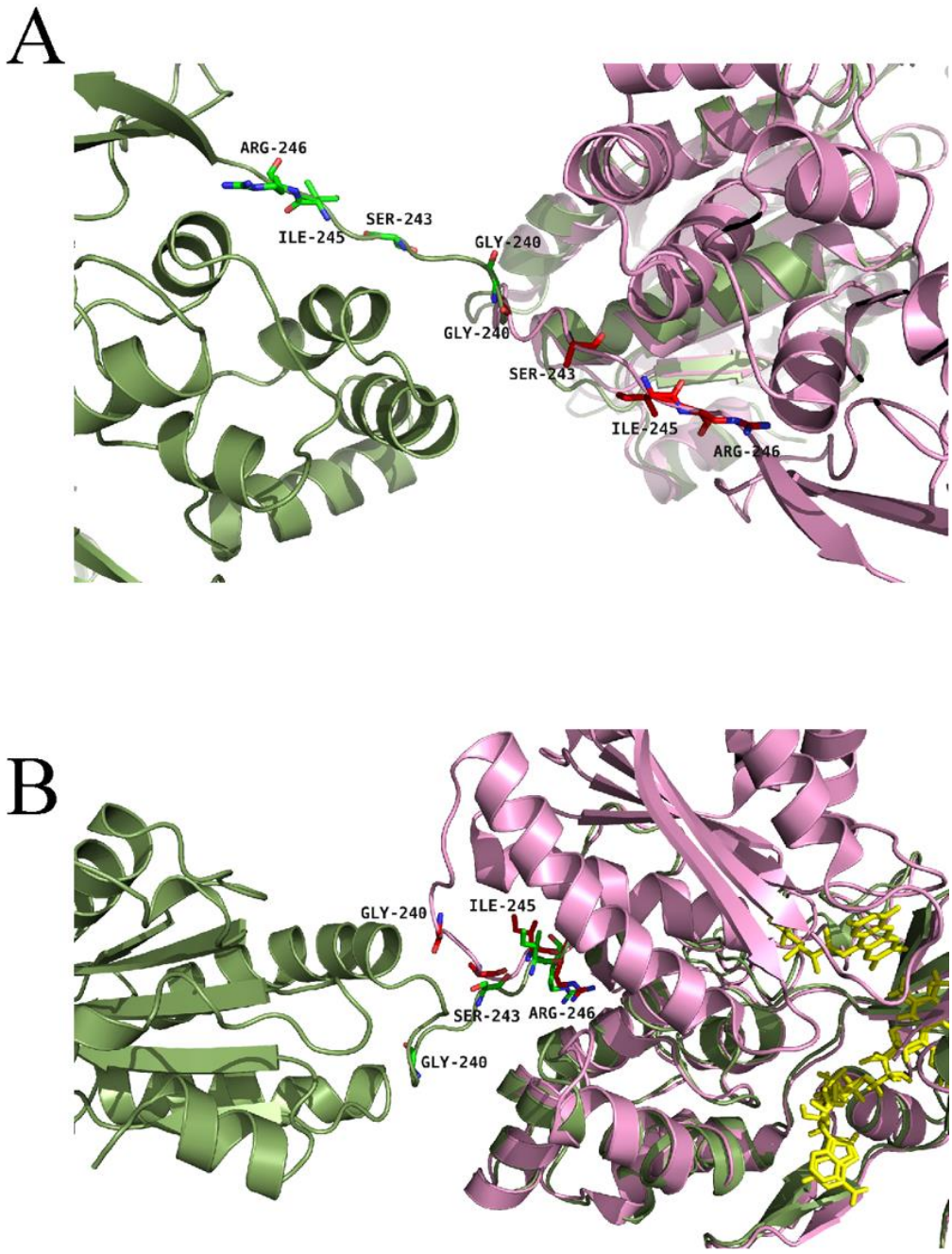

Figure 2.2 Positions of the studied mutations in CPR. The structure of the yeast-human open form CPR chimera (3FJO, in dark green) and the WT soluble human closed form CPR (5FA6, chain A, in pink) were used to analyze the variations in the hinge segment between the closed and open form of CPR. Mutated residues are displayed as sticks of either green or magenta colors according to the structures. **(A)** Both structures were aligned onto their FMN domains. **(B)** Both structures were aligned onto their connecting/FAD domains. The figure was prepared using the PyMol software (Schrödinger, 2015).

Production of the Various Mutants of Human CPR

Soluble Forms

Eight different plasmids encoding the soluble CPR mutants G240P, S243P, I245A, I245P, R246A, R246P, I245A/R246A and I245R/R246I were introduced into *E. coli* and the various proteins expressed and purified as described in Section "Material and Methods." SDS-PAGE gel analysis shows that the different mutant proteins present the same profile than the wild type (WT), with a major band just below 70 kDa which corresponds to the soluble form of the CPR (69 kDa). Biological duplication of the entire expression and purification stages was performed to ensure repeatability. Some discrete bands, at lower molecular weights compared to WT CPR were detected either with Coomassie staining or by western blot analysis (see Supplementary **Figure S2.1**), indicating some minor degradation of the purified enzymes. However, these represent less than 5% of the full-length soluble CPR and hence would have a minor impact on the kinetic assays. All CPR mutants presented the same absorbance spectra as the WT soluble enzyme, with a maximum of absorption at 450 nm, indicating no or minor changes in the chemical surrounding of both flavins. Last, all mutants were obtained in the semiquinone form, like the WT CPR, indicating no major changes in the absolute redox potential values of the flavins in the mutant forms. These results emphasize that the introduced mutations did not apparently modify the surroundings of the flavins.

Membrane-Bound Forms

The eight different mutants were introduced in the *E. coli* BTC strain, expressed and bacterial microsomes were isolated, as described previously (Kranendonk *et al.*, 2008). No expression problems were encountered, except for mutant G240P for which the level of expression was substantially lower than for the other mutants. Immunodetection of CPR in isolated microsomes showed only trace amounts of the G240P mutant protein, not sufficient for subsequent analysis. Other CPR mutants demonstrated expression levels comparable with the WT form (see Supplementary **Figure S2.1**).

Mutations Affect Differently the Soluble and Membrane-Bound Forms of CPR

Assay Conditions

Our study was designed to test the variation of cytochrome *c* reduction in various salt concentration conditions for nine CPR enzymes variants (WT + eight mutants) in the context of the soluble or membrane bound forms. We therefore developed and optimized a 96-well plate format assay to follow cytochrome *c* reduction. These experiments were performed at 37 ºC, contrarily to the primary test realized at room temperature in *cuvette* with the WT, soluble form of human CPR (**Figure 2.1**). Optimal conditions of the microplate rate assay were determined to ensure the linearity of the reaction traces. Initially, assays were performed at two cytochrome *c* concentrations (100 and 200 mM) in order to ensure that saturation was reached at all salt concentrations, which virtually gave the same velocities (data not shown). Subsequently cytochrome *c* was used at 200 mM. CPR concentrations in the tests were also optimized to obtain linear traces for each mutant (both for the soluble and membrane bound forms) in order to compensate for lower or higher activities (see Supplementary Table S2.1). We verified that salt profiles were equivalent between the tests performed in the *cuvette* and in the 96-well plate format (data not shown). **Figure 2.3A** displays the salt profile of the WT as well as mutants in the context of their soluble form at 37 ºC. Clearly the WT profile is superimposable to the one in **Figure 2.1**, although minor differences can be seen, notably for the concentration of salt that gives the maximal value of k_{obs} (425 mM at 25 ºC instead of 395 mM at 37 ºC). This minor variation could be explained by the temperature shift from 25 ºC to 37 ºC, probably favoring the opening mechanism and therefore the unlocked state. Apart from this difference, no other changes were noted and the comparison of the salt profiles of the mutants either in their soluble or membrane bound forms was pursued at 37 ºC, with the 96 well plate assay format.

The Hinge Partly Controls the Conformational Equilibrium of the Soluble CPR Form

As mentioned earlier, the ionic strength dependency of cytochrome *c* reduction by CPR can be partly considered as a direct measure of the proportion of the locked *vs.* unlocked states (Frances *et al.*, 2015) and the bell-shaped curve of this ionic strength dependence has been also reported in the ET from the flavodoxin of *Desulfovibrio vulgaris* to cytochrome *b*553 (Sadeghi *et al.*, 2000). We therefore performed a full analysis of the ionic strength dependency of cytochrome *c* reduction for all single and double mutants (**Figure 2.3**). **Figure 2.3A** depicts the 8 different ionic strength profiles obtained with the various mutants compared with the WT one. All curves of the k_{obs} *vs*. ionic strength display the same typical bell-shaped curve seen with the WT CPR. With the exception of the S243P mutant, all ionic strength profiles are shifted to the left (lower NaCl concentrations). Moreover, nearly all of them (except S243P and I245A) have lower maximal k_{obs} values. This result indicates that the various introduced mutations have pronounced effects either on the conformational equilibrium or the ET efficiency, yet all of them are still active (lowest k_{obs} is 30% of the one observed with WT CPR). The redox potentials of both flavins and cytochrome *c* are known to depend to some extent on the ionic strength. While for cytochrome *c* these changes are known and relatively small (Gopal *et al.*, 1988), it is difficult to predict the changes that would occur for the flavins. Based on our observation that the microenvironment of flavins is probably not significantly altered between mutants and WT CPR (equal absorption spectra) we have based our working hypotheses on the assumption that the redox potential of the flavins are not functionally different between the mutants and the WT soluble or membrane-bound forms of CPR.

From **Figure 2.3A**, maximal k_{obs} values were extracted and used to generate a graph comparing the salt concentration at which the maximum k_{obs} occur and the maximal k_{obs} value itself (**Figure 2.3B**). The case of S243P and I245A is interesting. Both have approximately the same k_{obs} (slightly higher than the WT for S243P). However, I245A denotes a clear difference in term of optimal ionic strength contrarily to S243P and WT. Another example is the situation for I245A, G240P and I245P, for which the optimal ionic strengths are identical, yet the three mutants have different maximal k_{obs} values. Hence

these data seem to indicate a separation between the efficiency of cytochrome *c* reduction and the conformational equilibrium of CPR (represented by the salt concentration at which the maximal k_{obs} occurs). However, globally, when the profiles are shifted to lower ionic strength the maximal k_{obs} values are lower.

The effects on the conformational equilibrium are interesting and merit further analysis. With the exception of S243P, all mutants either favored the unlocked state or stabilized the locked state. The introduction of a proline residue (G240P, I245P and R246P) probably imposes strong constraints on the hinge and may therefore stabilize discrete conformations of the unlocked state. The removal of the positive charge of the arginine residue at position 246 (R246A) may loosen the potential interactions between the hinge and the connecting domain and also destabilize the locked state. It should also be noted that the double mutants present the maximal displacements in term of salt profile and that the charge suppression at position 246 cannot be compensated by the introduction of an arginine at position 245 (see the double mutant I245R/R246I).

Lower maximal k_{obs} values are probably associated to some decrease in the rate constants of one or several ET steps. We already demonstrated that conformational exchange occurs at a much faster rate than ET (Frances *et al.*, 2015). Hence, during the course of steady state activity, CPR opens and closes several times before electrons are transferred from FAD to FMN. This also means that the locked state might actually have several closed conformations, not all of them productive for inter-flavin ET, a feature that has already been described (Hay *et al.*, 2010). Therefore, the mutants might disfavor the occurrence of productive conformations in the locked state, hereby reducing the maximal k_{obs} value. Hence, although there would not be a direct relationship between conformational equilibrium and maximal k_{obs}, the effects of some of the mutations on the destabilization of the locked state could also change the rate limiting step.

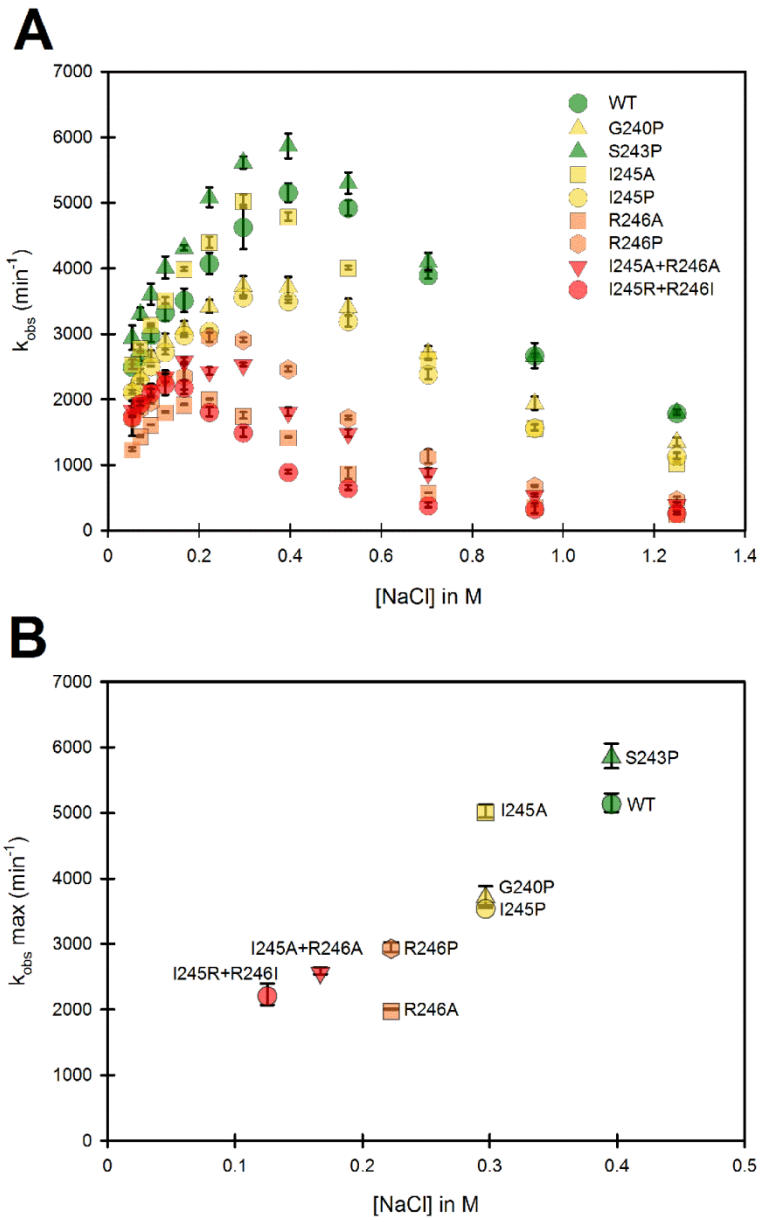

Figure 2.3 Variation of the k_{obs} for cytochrome *c* reduction in function of the ionic strength for the WT and mutants of the soluble forms of human CPR. Cytochrome *c* reduction assays were performed in triplicate in 96 well microtiter plates as described in the Material and Methods section. **(A)** Salt dependent profile of the k_{obs} with the WT and the mutants. Symbols depicting the different mutants are included in the panel. **(B)** Maximal k_{obs} values were extracted from panel A and plotted as a function of the salt concentration. Symbols depicting the different mutants are identical as the ones in **(A)**. k_{obs} values represent the average of three replicates and the error bars depict the standard deviation.

The Hinge Controls the Conformational Equilibrium of the Membrane Bound CPR

The same mutants, when present in the full-length, membrane anchored form, were subsequently studied. **Figure 2.4** presents the same analysis of both the variation of k_{obs} and the optimal ionic strength value for each of the mutants in the context of the membrane bound form. Our first striking result is that the ionic strength giving the maximum k_{obs} for the WT membrane bound form is shifted to higher salt concentrations compared to the WT soluble form, indicating a stronger interaction between the two domains (**Figure 2.4A**). Various hypotheses can be formulated to account for this fact. First, the presence of the negatively charged phospholipid heads of the membrane probably modifies the electrostatic potential around the FMN domain, potentially strengthening the interactions between the two flavin domains and thus favoring the equilibrium toward the locked state. Second, the presence of the membrane close to the FMN domain might impeach movements of the FAD domain compared to those attainable with the soluble form. This restriction of movement could favor the closing mechanism, hereby stabilizing the locked state.

Despite the above peculiarity of membranous CPR, **Figure 2.4A** shows that, as seen with the majority of the soluble forms, all mutants have their salt profiles shifted to lower ionic strengths when compared to the WT. This result confirms that the generated mutants have a greater tendency to favor the unlocked state, independently of the presence or absence of the membrane. Although differences exist between individual mutants depending on the context (soluble or membrane bound forms), again the maximal effects are seen with the R246 mutations and the double mutants containing mutations at the positions 246 and 245.

Maximal k_{obs} values were also extracted and plotted against the corresponding salt concentration (**Figure 2.4B**). Overall, the salt concentration at which k_{obs} is maximal covers a larger range with the membrane bound forms compared to the soluble forms. This indicates that the influence of salt on the conformational equilibrium is greater when CPR is attached to the membrane than when the various domains have more degree of liberty, i.e., when in the soluble form.

Interestingly, **Figure 2.4B** shows marked differences in the clustering of mutants compared to **Figure 2.3B**. This suggests again that the salt concentration giving the highest possible k_{obs} (1:1 proportion of locked/unlocked states) does not correlate with the value of the k_{obs} itself. This is particularly evident with the membrane-bound forms of the S243 and I245 mutants.

Some parallels can be drawn between mutants in the soluble and the membrane bound forms from comparison of **Figures 2.3B, 2.4B**: (i) the group which had lower cytochrome *c* reduction rates in the soluble form (R246A, R246P, I245R/R246I and I245A/R246A) have almost the same k_{obs} than the WT in the membrane bound form and, (ii) the group that had similar cytochrome *c* reduction rates than the WT in the soluble form (S243P, I245A and I245P), display a greater efficiency of ET to cytochrome *c* in the membrane bound form.

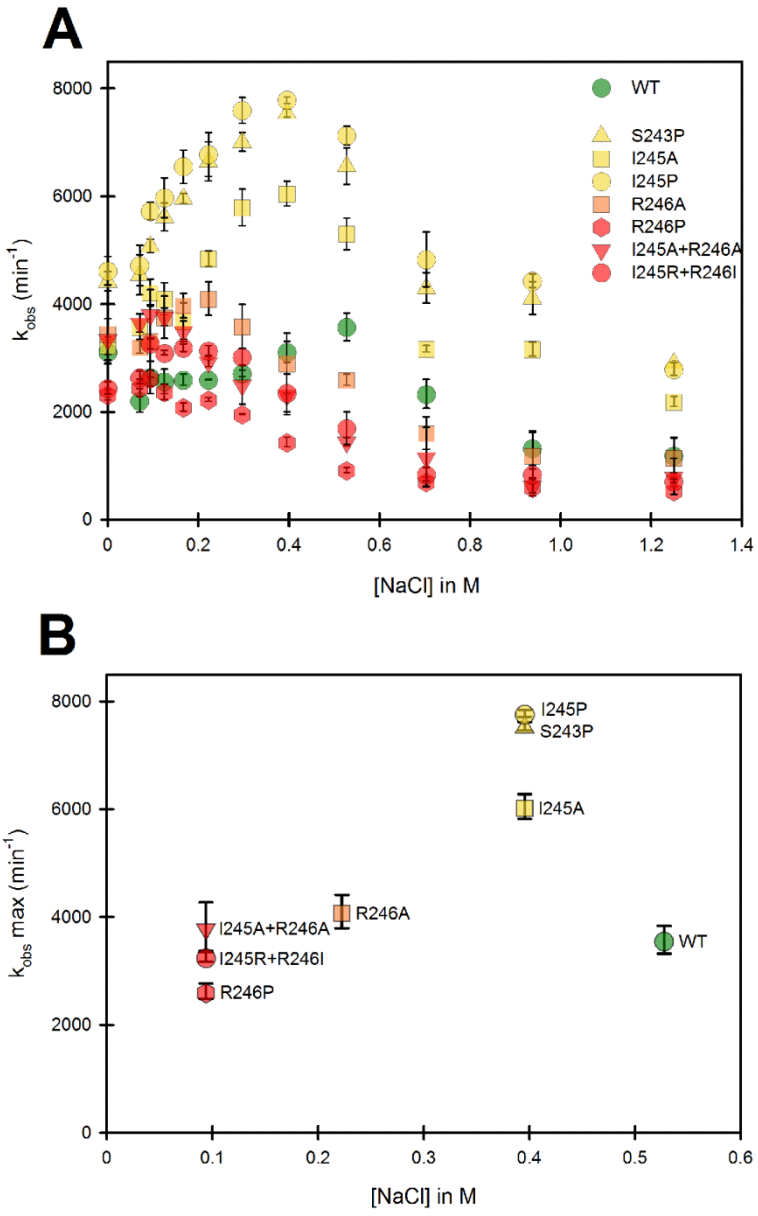

Figure 2.4 Variation of the k_{obs} for cytochrome *c* reduction in function of the ionic strength for the WT and mutants of the membrane bound forms of human CPR. Cytochrome *c* reduction assays were performed in triplicate in 96 well microtiter plates as described in the Material and Methods section. **(A)** Salt dependent profile of the k_{obs} with the WT and the mutants. Symbols depicting the different mutants are included in the panel. **(B)** Maximal k_{obs} values were extracted from panel A and plotted as a function of the salt concentration. Symbols depicting the different mutants are identical as the ones in **(A)**. k_{obs} values represent the average of three replicates and the error bars depict the standard deviation.

2.1.5 DISCUSSION

The role of the hinge segment in diflavin reductase enzymes was studied both in NOS enzymes (Haque *et al.*, 2007, 2012) and in CPR (Hamdane *et al.*, 2009), using either lengthening or shortening of the primary sequence. Our study was designed to address the role of specific residues of the hinge segment of CPR (G240, S243, I245 and R246) without modifying its length. We have analyzed the salt-induced changes in the conformational equilibrium between the locked and unlocked states, via cytochrome *c* reduction, in the context of both the soluble and membrane-bound forms of CPR. In our first set of experiments using the soluble form of WT CPR, we compared the ionic strength profiles of the k_{obs} with three artificial substrates. Our results confirmed that the well-known salt dependency of either cytochrome *c* or CYP reductions (Voznesensky and Schenkman, 1992) can be mostly attributed to a change in the conformational equilibrium of CPR, between the locked state, non-competent in ET to cytochrome *c* and the unlocked state capable of transferring electrons from the reduced FMN to acceptors. However, as explained in Section "The Hinge Partly Controls the Conformational Equilibrium of the Soluble CPR Form" we cannot rule out that the redox potentials of the flavins in the mutants forms of CPR are equivalent. Still, as mentioned before, the fact that the absorption spectra of the different WT and mutant CPRs are indistinguishable indicates that the chemical environment of the flavins is similar in all studied proteins. In the rest of the discussion, we therefore assumed that these redox potentials are equal between all CPR forms studied, bearing in mind that the various properties of the mutants (especially the rate constants) might, to some extent, be attributed to these putative redox potentials changes.

In the membrane bound form of WT CPR, the k_{obs} is lower than the one measured with the soluble form, a feature already seen upon solubilization of CPR (Phillips and Langdon, 1962). A possible explanation is a potential restrictive access of cytochrome *c* to the FMN domain caused by the membrane, giving rise to the observed differences between the effects of mutations when present in the soluble or membrane bound forms. Interestingly, none of the introduced mutations were capable of completely abolishing the CPR ET to cytochrome *c* but rather displayed several intermediate features, either changing the salt profile or the efficiency of ET, or both. We thus hypothesize that the

targeted positions, although important, are only a part of the structural determinants promoting the conformational exchange between the locked and unlocked states. It is also worth noting that the ionic strength profiles obtained with all mutant forms (soluble and membrane bound, except for the soluble form of the S243P mutant) were shifted to lower salt concentrations compared to that of the WT CPR. This clearly indicates that the majority of changes that were introduced displaced the equilibrium toward the unlocked state. This is not completely surprising for the mutations that potentially enhance the flexibility (I245A) or removed salt bridges between the hinge and the connecting domain (R246A). However, for the mutations introducing proline residues in the hinge (G240P, S243P, I245P, R246P) the shift in the ionic strength profile might indicate that rigidifying these positions could result either in the destabilization of the locked state or the stabilization of the unlocked state. Still, the maintenance of a rather effective cytochrome *c* reduction in all cases might indicate that the loss of flexibility in the mutants bearing a proline residue may also be partly compensated by the hinge flexibility involving residues at other positions.

The second interesting feature of our mutants is that we can separate the ionic strength profile from the efficiency of the ET to cytochrome *c*, i.e., there is no evident direct relationship between the salt concentration at which k_{obs} is maximal and the value of k_{obs} itself (**Figures 2.3B, 2.4B**). Thus, in our conditions, the rate limiting steps remain independent of the conformational equilibrium. The conformational exchange frequency between the locked and unlocked states is at minimum 600 s^{-1} (Frances *et al.*, 2015), a value 10 times greater than the k_{obs} observed with cytochrome *c* and coherent with the one determined by Haque *et al.*, (2014). This also means that the locked state might actually have several closed conformations, not all of them productive for inter-flavin ET, a feature that has already been described (Hay *et al.*, 2010). Hence, there would not be a direct relationship between conformational equilibrium and maximal k_{obs} and the effects of our introduced mutations, destabilization of the locked state, could also affect the rate limiting step giving rise to either equal, lower or higher k_{obs} values compared to the WT forms.

In the soluble form of human CPR, only the S243P and possibly the I245A mutations have no effect on the rate of cytochrome *c* reduction. However, in the membrane bound

form, these two mutants, along with I245P, present cytochrome *c* reduction rates higher than the WT form, and higher than the soluble counterparts. To our knowledge, this is the first report of k_{obs} values up to 8.000 min^{-1} for ET to cytochrome *c* with CPR. However, these features were already observed in some mutants affecting the charge pairing between the FMN and FAD domains of nNOS (Haque *et al.*, 2013) and in a C-terminal-truncated version of murine iNOS in which cytochrome *c* reduction attained 31.467 min^{-1} (Roman *et al.*, 2000). In the nNOS mutants, the increase of k_{obs} for cytochrome *c* reduction was attributed to a change of the conformational behavior. However, in our case, the maximal k_{obs} was determined at a salt concentration where the conformational equilibrium corresponds to a 1:1 ratio of locked/unlocked states, as we demonstrated before (Frances *et al.*, 2015). Therefore, the high maximal k_{obs} values observed in the mutants may be attributed to a change in the FAD to FMN ET rate limiting step, because, in the case of cytochrome *c* reduction by CPR, this step is considered the slowest. Still, it should be reminded here that natural redox partners of CPR such as microsomal CYP, may have specific structural requisites to bind CPR and form productive electron-transfer complexes with its membrane anchored redox partners, a situation evidently different with soluble partners such as cytochrome *c*. The differences in our results for the soluble and membrane-bound forms seem to indicate that residues S243 and I245 of human CPR are playing a role in this specific aspect.

Figure 2.5 depicts the position of the R246 amino acid in the structure of the WT, soluble form of human CPR (McCammon *et al.*, 2016). The R246 is in close contact with two acidic residues (D445 and E449) present in the connecting domain (**Figure 2.5A**). Mutations at position 246 abolish a charge pairing with these two acidic residues. The distances of the three nitrogen atoms of R246 (NE, NH1 and NH2) with both terminal oxygens of D445 and E449 and the carbonyl oxygen of D445 are compatible with hydrogen bonds (**Figure 2.5B**). Furthermore, one terminal oxygen atom of E449 is also in a distance compatible to form a hydrogen bond with the amide nitrogen atom of Q247. This relatively strong hydrogen bonding network is evidently disrupted in the mutants changing R246 into any non-charged residue. The addition of a charge at the previous residue (in the double mutant I245R/R246I) does not restore the WT phenotype because I245 side-chain is clearly not oriented favorably in order to substitute for R246 in the complex hydrogen bonding network. This result is reminiscent of the mutations analyzed

by Shen and coworkers demonstrating a similar shift in the salt profile when removing potential ionic interactions between the FMN and the connecting domains by mutating E216 into a glutamine residue (Shen and Kasper, 1995). Our results thus demonstrate that the hinge segment also actively participates in the construction of the FMN/FAD interface. When the loss of critical ionic interactions modifies the equilibrium between the locked and unlocked states, the ionic strength at which the maximal value of k_{obs} occurs is evidently lower, yet the maximum k_{obs} value may remain roughly constant, as demonstrated by several of the mutant CPRs.

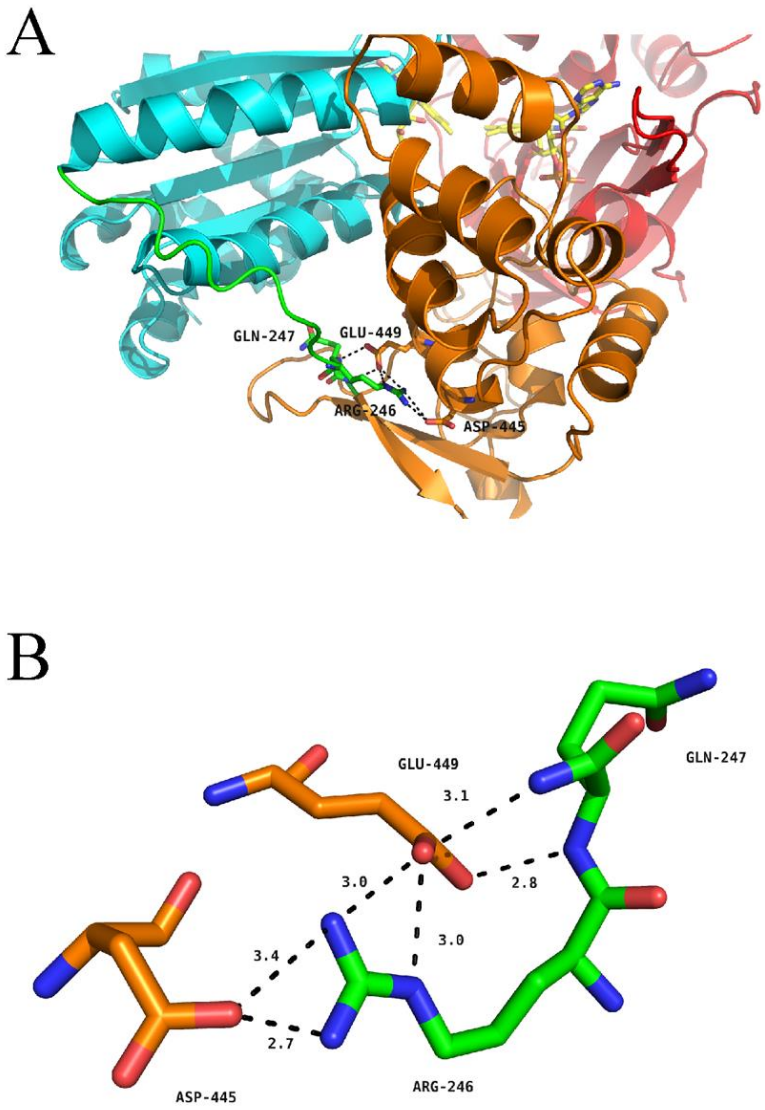

Figure 2.5 Hydrogen bond network around residue R246 of human CPR. (A) Position of R246, Q247, D445 and E449 in the structure of the soluble form of WT human CPR. The color coding is as follows: FMN domain, cyan; hinge segment, green; connecting domain, orange; FAD domain, red. Flavins are depicted in yellow sticks, the various positions as stick in the same color code of the domain to which they belong. **(B)** Detailed view of the hydrogen bonding network. The color coding is the same as in **(A)**.

A final remark should be made concerning the salt concentration at which the maximal k_{obs} was observed for the WT, membrane bound form of CPR, which is around 500 mM NaCl. It is clear that the ionic strength at this salt concentration is much higher than the physiological one, 154 mM KCl (physiological serum). As such it seems that the conformational equilibrium of CPR, *in vivo*, is probably in favor of the locked state, thereby reinforcing the idea of an external trigger for opening CPR (Grunau *et al.*, 2006, 2007), such as the presence of membrane-bound CYPs which are physiologically outnumbering CPR molecules by a factor of 5–10 in the liver. How this competition for CPR is affected by the conformational equilibrium is still an open and intriguing question.

2.1.6 AUTHOR CONTRIBUTIONS

Experimental design: all authors; experimental work: DC, TL, PU, FE, and SB; data analysis and interpretation: all authors; writing, reviewing and editing of the manuscript: all authors; funding acquisition: GT and MK.

2.1.7 FUNDING

This work was in part funded by a joint ANR/FCT program; France: ANR-13-ISV5-0001 (DODYCOEL), and Portuguese national funds, through the Fundação para a Ciência e a Tecnologia (Project FCT-ANR/BEXBCM/0002/2013).

2.1.8 ACKNOWLEDGMENT

We are grateful to Solène Galinier for technical assistance on the CPR soluble form enzymatic assays.

2.1.9 SUPPLEMENTARY MATERIAL

Table S2.1: CPR concentrations used in cytochrome *c* reduction microplate assays.

	Soluble CPR (nM)	Membrane-bound CPR (nM)
WT	6,1	0,50
G240P	11,6	0,95
S243P	2,8	0,23
I245A	9,2	0,75
I245P	4,4	0,36
R246A	8,8	0,72
R246P	9,4	0,77
I245R+R246I	19,2	1,57
I245A+R246A	4,4	0,36

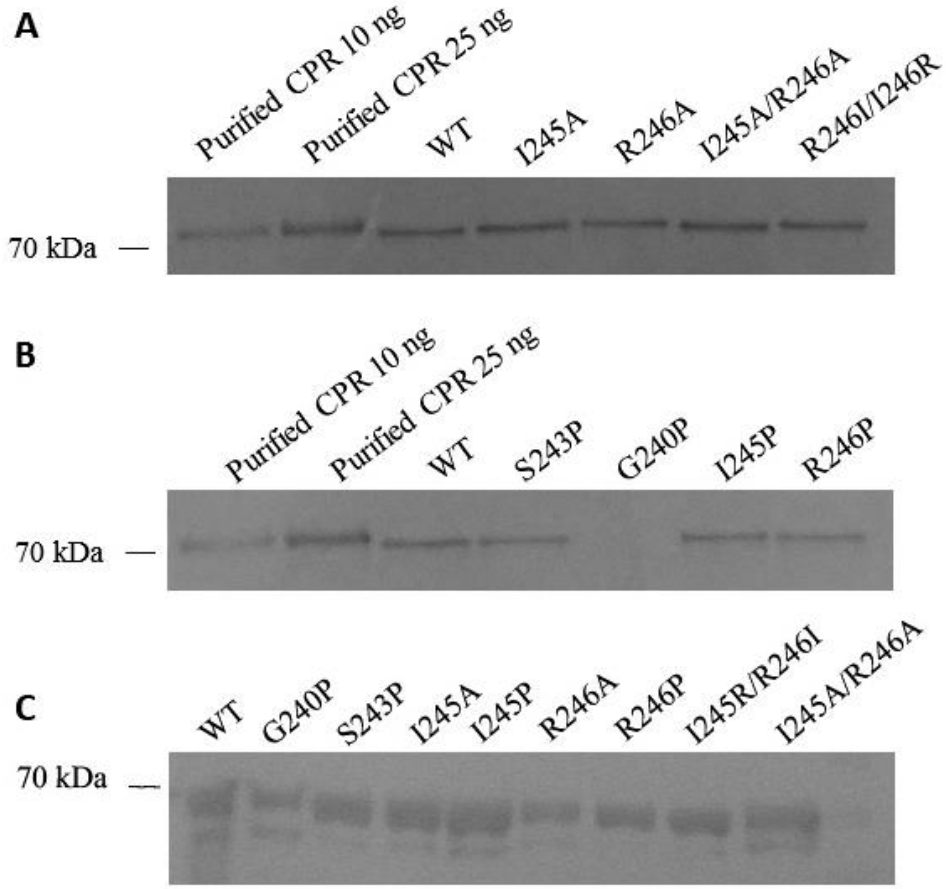

Figure S2.1: Immuno-detection of membrane-bound (**A, B**) and soluble forms of human CPR (**C**).

2.1.10 REFERENCES

Aigrain, L., Pompon, D., Moréra, S., and Truan, G. (2009). Structure of the open conformation of a functional chimeric NADPH cytochrome P450 reductase. *EMBO Rep*. 10, 742–747. doi: 10.1038/embor.2009.82

Aigrain, L., Pompon, D., and Truan, G. (2011). Role of the interface between the FMN and FAD domains in the control of redox potential and electronic transfer of NADPH–cytochrome P450 reductase. *Biochem. J*. 435, 197–206. doi: 10.1042/BJ20101984

Bridges, A., Gruenke, L., Chang, Y.-T., Vakser, I. A., Loew, G., and Waskell, L. (1998). Identification of the binding site on cytochrome P450 2B4 for cytochrome b 5 and cytochrome P450 reductase. *J. Biol. Chem*. 273, 17036–17049. doi: 10.1074/jbc.273.27.17036

Coon, M. J. (2005). Cytochrome P450: nature's most versatile biological catalyst. *Annu. Rev. Pharmacol. Toxicol*. 45, 1–25. doi: 10.1146/annurev.pharmtox.45. 120403.100030

Davydov, D. R., Kariakin, A. A., Petushkova, N. A., and Peterson, J. A. (2000). Association of cytochromes P450 with their reductases: opposite sign of the electrostatic interactions in P450BM-3 as compared with the microsomal 2B4 system. *Biochemistry* 39, 6489–6497. doi: 10.1021/bi992936u

Davydov, D. R., Knyushko, T. V., Kanaeva, I. P., Koen, Y. M., Samenkova, N. F., Archakov, A. I., et al. (1996). Interactions of cytochrome P450 2B4 with NADPH-cytochrome P450 reductase studied by fluorescent probe. *Biochimie* 78, 734–743. doi: 10.1016/S0300-9084(97)82531-X

Duarte, M. P., Palma, B. B., Laires, A., Oliveira, J. S., Rueff, J., and Kranendonk, M. (2005). *Escherichia coli* BTC, a human cytochrome P450 competent tester strain with a high sensitivity towards alkylating agents: involvement of alkyltransferases in the repair of DNA damage induced by aromatic amines. *Mutagenesis* 20, 199–208. doi: 10.1093/mutage/gei028

Ellis, J., Gutierrez, A., Barsukov, I. L., Huang, W.-C., Grossmann, J. G., and Roberts, G. C. K. (2009). Domain motion in cytochrome P450 reductase: conformational equilibria revealed by NMR and small-angle x-ray scattering. *J. Biol. Chem*. 284, 36628–36637. doi: 10.1074/jbc.M109.054304

Frances, O., Fatemi, F., Pompon, D., Guittet, E., Sizun, C., Pérez, J., et al. (2015). A well-balanced preexisting equilibrium governs electron flux efficiency of a multi-domain diflavin reductase. *Biophys. J.* 108, 1527–1536. doi:10.1016/j.bpj.2015.01.032

Gopal, D., Wilson, G. S., Earl, R. A., and Cusanovich, M. A. (1988). Cytochrome c: ion binding and redox properties. Studies on ferri and ferro forms of horse, bovine, and tuna cytochrome c. *J. Biol. Chem*. 263, 11652–11656.

Grunau, A., Geraki, K., Grossmann, J. G., and Gutierrez, A. (2007). Conformational dynamics and the energetics of protein-ligand interactions: role of interdomain loop in human cytochrome P450 reductase†. *Biochemistry* 46, 8244–8255. doi: 10.1021/bi700596s

Grunau, A., Paine, M. J., Ladbury, J. E., and Gutierrez, A. (2006). Global effects of the energetics of coenzyme binding: NADPH controls the protein interaction properties of human cytochrome P450 reductase†. Biochemistry 45, 1421–1434. doi: 10.1021/bi052115r

Guengerich, F. P. (2007). Mechanisms of cytochrome P450 substrate oxidation: MiniReview. *J. Biochem. Mol. Toxicol*. 21, 163–168. doi: 10.1002/jbt.20174

Hamdane, D., Xia, C., Im, S.-C., Zhang, H., Kim, J.-J. P., and Waskell, L. (2009). Structure and function of an NADPH-cytochrome P450 oxidoreductase in an open conformation capable of reducing cytochrome P450. *J. Biol. Chem*. 284, 11374–11384. doi: 10.1074/jbc.M807868200

Haque, M. M., Bayachou, M., Tejero, J., Kenney, C. T., Pearl, N. M., Im, S.-C., et al. (2014). Distinct conformational behaviors of four mammalian dualflavin reductases (cytochrome P450 reductase, methionine synthase reductase, neuronal nitric oxide synthase, endothelial nitric oxide synthase) determine their unique catalytic profiles. *FEBS J*. 281, 5325–5340. doi: 10.1111/febs.13073

Haque, M. M., Fadlalla, M. A., Aulak, K. S., Ghosh, A., Durra, D., and Stuehr, D. J. (2012). Control of electron transfer and catalysis in neuronal nitric-oxide synthase (nNOS) by a hinge connecting its FMN and FAD-NADPH domains. *J. Biol. Chem*. 287, 30105–30116. doi: 10.1074/jbc.M112.339697

Haque, M. M., Panda, K., Tejero, J., Aulak, K. S., Fadlalla, M. A., Mustovich, A. T., et al. (2007). A connecting hinge represses the activity of endothelial nitric oxide synthase. *Proc. Natl. Acad. Sci. U.S.A.* 104, 9254–9259.doi:10.1073/pnas.0700332104

Haque, M. M., Tejero, J., Bayachou, M., Wang, Z.-Q., Fadlalla, M., and Stuehr, D. J. (2013). Thermodynamic characterization of five key kinetic parameters that define neuronal nitric oxide synthase catalysis. *FEBS J.* 280, 4439–4453. doi: 10.1111/febs.12404

Hay, S., Brenner, S., Khara, B., Quinn, A. M., Rigby, S. E. J., and Scrutton, N. S. (2010). Nature of the energy landscape for gated electron transfer in a dynamic redox protein. *J. Am. Chem. Soc*. 132, 9738–9745. doi: 10.1021/ja1016206

Hlavica, P., Schulze, J., and Lewis, D. F. V. (2003). Functional interaction of cytochrome P450 with its redox partners: a critical assessment and update of the topology of predicted contact regions. *J. Inorg. Biochem*. 96, 279–297. doi: 10.1016/S0162-0134(03)00152-1

Huang, W.-C., Ellis, J., Moody, P. C. E., Raven, E. L., and Roberts, G. C. K. (2013). Redox-linked domain movements in the catalytic cycle of cytochrome P450 reductase. *Structure* 21, 1581–1589. doi: 10.1016/j.str.2013.06.022

Kranendonk, M., Marohnic, C. C., Panda, S. P., Duarte, M. P., Oliveira, J. S., Masters, B. S. S., et al. (2008). Impairment of human CYP1A2-mediated xenobiotic metabolism by Antley-Bixler syndrome variants of cytochrome P450 oxidoreductase. *Arch. Biochem. Biophys*. 475, 93–99. doi: 10.1016/j.abb.2008.04.014

Lamb, D. C., Kim, Y., Yermalitskaya, L. V., Yermalitsky, V. N., Lepesheva, G. I., Kelly, S. L., et al. (2006). A second FMN binding site in yeast NADPH cytochrome P450 reductase suggests a mechanism of electron transfer by diflavin reductases. *Structure* 14, 51–61. doi: 10.1016/j.str.2005.09.015

Lamb, D. C., and Waterman, M. R. (2013). Unusual properties of the cytochrome P450 superfamily. *Philos. Trans. R. Soc. Lond. B. Biol. Sci*. 368:20120434. doi:10.1098/rstb.2012.0434

Marohnic, C. C., Panda, S. P., McCammon, K., Rueff, J., Masters, B. S. S., and Kranendonk, M. (2010). Human cytochrome P450 oxidoreductase deficiency caused by the Y181D mutation: molecular consequences and rescue of defect. *Drug Metab. Dispos*. 38, 332–340. doi: 10.1124/dmd.109.030445

McCammon, K. M., Panda, S. P., Xia, C., Kim, J.-J. P., Moutinho, D., Kranendonk, M., et al. (2016). Instability of the human cytochrome P450 reductase A287P variant is the major contributor to its antley-bixler syndrome like phenotype. *J. Biol. Chem.* 291, 20487–20502. doi: 10.1074/jbc.M116.716019

Miyazaki, K., and Takenouchi, M. (2002). Creating random mutagenesis libraries using megaprimer PCR of whole plasmid. *BioTechniques* 33, 1036–1038.

Munro, A. W., Girvan, H. M., Mason, A. E., Dunford, A. J., and McLean, K. J. (2013). What makes a P450 tick? *Trends Biochem. Sci.* 38, 140–150. doi: 10.1016/j.tibs.2012.11.006

Murataliev, M. B., Ariño, A., Guzov, V. M., and Feyereisen, R. (1999). Kinetic mechanism of cytochrome P450 reductase from the house fly (*Musca domestica*). *Insect. Biochem. Mol. Biol.* 29, 233–242. doi: 10.1016/S0965-1748(98)00131-3

Nadler, S. G., and Strobel, H. W. (1988). Role of electrostatic interactions in the reaction of NADPH-cytochrome P-450 reductase with cytochromes P-450. *Arch. Biochem. Biophys.* 261, 418–429. doi: 10.1016/0003-9861(88)90358-X

Nadler, S. G., and Strobel, H. W. (1991). Identification and characterization of an NADPH-cytochrome P450 reductase derived peptide involved in binding to cytochrome P450. *Arch. Biochem. Biophys.* 290, 277–284. doi: 10.1016/0003-9861(91)90542-Q

Nishino, H., and Ishibashi, T. (2000). Evidence for requirement of NADPHcytochrome P450 oxidoreductase in the microsomal NADPH-sterol Delta7-reductase system. *Arch. Biochem. Biophys*. 374, 293–298. doi: 10.1006/abbi.1999.1602

Ono, T., and Bloch, K. (1975). Solubilization and partial characterization of rat liver squalene epoxidase. *J. Biol. Chem.* 250, 1571–1579.

O'Reilly, J. E. (1973). Oxidation-reduction potential of the ferro-ferricyanide system in buffer solutions. *Biochim. Biophys. Acta* 292, 509–515. doi: 10.1016/0005-2728(73)90001-7

Oshino, N., Imai, Y., and Sato, R. (1971). A function of cytochrome b5 in fatty acid desaturation by rat liver microsomes. *J. Biochem.* 69, 155–167. doi: 10.1093/oxfordjournals.jbchem.a129444

Palma, B. B., Silva, E., Sousa, M., Urban, P., Rueff, J., and Kranendonk, M. (2013). Functional characterization of eight human CYP1A2 variants: the role of cytochrome b5. *Pharmacogenet. Genomics* 23, 41–52. doi: 10.1097/FPC.0b013e32835c2ddf

Phillips, A. H., and Langdon, R. G. (1962). Hepatic triphosphopyridine nucleotidecytochrome c reductase: isolation, characterization, and kinetic studies. *J. Biol. Chem.* 237, 2652–2660.

Rendic, S., and Guengerich, F. P. (2015). Survey of human oxidoreductases and cytochrome P450 enzymes involved in the metabolism of xenobiotic and natural chemicals. *Chem. Res. Toxicol*. 28, 38–42. doi: 10.1021/tx500444e

Roman, L. J., Miller, R. T., de la Garza, M. A., Kim, J.-J. P., and Masters, B. S. S. (2000). The C terminus of mouse macrophage inducible nitric-oxide synthase attenuates electron flow through the flavin domain. *J. Biol. Chem*. 275, 21914–21919. doi: 10.1074/jbc.M002449200

Sadeghi, S. J., Valetti, F., Cunha, C. A., Romão, M. J., Soares, C. M., and Gilardi, G. (2000). Ionic strength dependence of the non-physiological electron transfer between flavodoxin and cytochrome c553 from *D. vulgaris*. *J. Biol. Inorg. Chem.* 5, 730–737. doi: 10.1007/s007750000162

Schacter, B. A., Nelson, E. B., Marver, H. S., and Masters, B. S. (1972). Immunochemical evidence for an association of heme oxygenase with the microsomal electron transport system. J. Biol. Chem. 247, 3601–3607.

Schrödinger (2015). The PyMOL Molecular Graphics System, Version 1.8. New York, NY: Schrödinger.

Scott, E. E., Wolf, C. R., Otyepka, M., Humphreys, S. C., Reed, J. R., Henderson, C. J., et al. (2016). The role of protein-protein and protein-membrane interactions on P450 function. *Drug Metab. Dispos*. 44, 576–590. doi: 10.1124/dmd.115.068569

Shen, A. L., and Kasper, C. B. (1995). Role of acidic residues in the interaction of NADPH-cytochrome P450 oxidoreductase with cytochrome P450 and cytochrome *c*. *J. Biol. Chem*. 270, 27475–27480. doi: 10.1074/jbc.270.46.27475

Sündermann, A., and Oostenbrink, C. (2013). Molecular dynamics simulations give insight into the conformational change, complex formation, and electron transfer pathway for cytochrome P450 reductase. *Protein Sci*. 22, 1183–1195. doi: 10.1002/pro.2307

Tamburini, P. P., and Schenkman, J. B. (1986). Differences in the mechanism of functional interaction between NADPH-cytochrome P-450 reductase and its redox partners. *Mol. Pharmacol*. 30, 178–185.

Vermilion, J. L., Ballou, D. P., Massey, V., and Coon, M. J. (1981). Separate roles for FMN and FAD in catalysis by liver microsomal NADPH-cytochrome P-450 reductase. *J. Biol. Chem.* 256, 266–277.

Vincent, B., Morellet, N., Fatemi, F., Aigrain, L., Truan, G., Guittet, E., et al. (2012). The closed and compact domain organization of the 70-kDa human cytochrome P450 reductase in its oxidized state as revealed by NMR. *J. Mol. Biol.* 420, 296–309. doi: 10.1016/j.jmb.2012.03.022

Voznesensky, A. I., and Schenkman, J. B. (1992). The cytochrome P450 2B4- NADPH cytochrome P450 reductase electron transfer complex is not formed by charge-pairing. *J. Biol. Chem.* 267, 14669–14676.

Wang, M., Roberts, D. L., Paschke, R., Shea, T. M.,Masters, B. S. S., and Kim, J.-J. P. (1997). Three-dimensional structure of NADPH–cytochrome P450 reductase: prototype for FMN- and FAD-containing enzymes. *Proc. Natl. Acad. Sci. U.S.A.* 94, 8411–8416. doi: 10.1073/pnas.94.16.8411

Xia, C., Hamdane, D., Shen, A. L., Choi, V., Kasper, C. B., Pearl, N. M., et al. (2011a). Conformational changes of NADPH-cytochrome P450 oxidoreductase are essential for catalysis and cofactor binding. *J. Biol. Chem*. 286, 16246–16260. doi: 10.1074/jbc.M111.230532

Xia, C., Panda, S. P., Marohnic, C. C., Martásek, P., Masters, B. S., and Kim, J.-J. P. (2011b). Structural basis for human NADPH-cytochrome P450 oxidoreductase deficiency. *Proc. Natl. Acad. Sci. U.S.A.* 108, 13486–13491. doi: 10.1073/pnas.1106632108

2.2 Probing the Role of the Hinge Segment of Cytochrome P450 Oxidoreductase in the Interaction with Cytochrome P450

This section was transcribed from the following peer-reviewed paper:

D. Campelo, *et al.* (2018). "Probing the role of the hinge segment of cytochrome P450 oxidoreductase in the interaction with cytochrome P450". Int J Mol Sci. 19 (12). DOI: 10.3390/ijms19123914.

CONTENT

2.2.1 ABSTRACT

NADPH-cytochrome P450 reductase (CPR) is the unique redox partner of microsomal cytochrome P450s (CYPs). CPR exists in a conformational equilibrium between open and closed conformations throughout its electron transfer (ET) function. Previously, we have shown that electrostatic and flexibility properties of the hinge segment of CPR are critical for ET. Three mutants of human CPR were studied (S243P, I245P and R246A) and combined with representative human drug-metabolizing CYPs (isoforms 1A2, 2A6 and 3A4). To probe the effect of these hinge mutations different experimental approaches were employed: CYP bioactivation capacity of pre-carcinogens, enzyme kinetic analysis, and effect of the ionic strength and cytochrome b5 (CYB5) on CYP activity. The hinge mutations influenced the bioactivation of pre-carcinogens, which seemed CYP isoform and substrate dependent. The deviations of Michaelis-Menten kinetic parameters uncovered tend to confirm this discrepancy, which was confirmed by CYP and hinge mutant specific salt/activity profiles. CPR/CYB5 competition experiments indicated a less important role of affinity in CPR/CYP interaction. Overall, our data suggest that the highly flexible hinge of CPR is responsible for the existence of a conformational aggregate of different open CPR conformers enabling ET-interaction with structural varied redox partners.

Keywords: NADPH-cytochrome P450 reductase (CPR); microsomal cytochrome P450 (CYP); Cytochrome b5 (CYB5); protein dynamics; electron-transfer (ET); protein–protein interaction.

2.2.2 INTRODUCTION

Microsomal cytochrome P450 (CYP) metabolism requires a coupled supply of electrons, which are donated by the auxiliary protein NADPH cytochrome P450 oxidoreductase (CPR). CPR, encoded by the *POR* gene, is a ~78-kDa electron-transferring diflavin enzyme anchored to the membrane of the ER [1]. CPR mediates a two-electron transfer (ET) per reaction cycle, originated from NADPH enabling CYP-mediated metabolism of many compounds. These include endobiotics, e.g., steroids, bile acids, vitamins and arachidonic acid metabolites, as well as many xenobiotics, including therapeutic drugs and environmental toxins [2,3]. Moreover, CPR is the unique electron supplier of heme oxygenase, squalene monooxygenase and fatty acid elongase [4], sustaining exclusively the activity of these enzymes. Cytochrome b5 (CYB5) can donate the second electron to CYP, competing with CPR for the binding site on the proximal side of CYP [5]. CYB5's interaction may have either a stimulating, inhibiting or having no effect over CYP catalytic activity, which seems to be CYP isoform and even substrate dependent [6].

CPR comprises a number of structurally distinct domains namely an N-terminal hydrophobic membrane anchoring domain; two flavin binding domains for flavin adenine dinucleotide (FAD) and flavin mononucleotide (FMN); a LD joining the FMN and FAD domains, as the provider of structural flexibility; and an NADPH binding domain [7]. The hinge segment, a highly flexible stretch with no defined secondary structure links the FMN and the connecting/FAD domain [8–10]. Electrons are transferred from NADPH through FAD (reductase) and FMN (transporter) coenzymes of CPR to redox partners, such as to the heme group in the reactive center of CYP [11].

Initial structural studies of CPR identified compact conformations that allowed internal (inter-flavin) ET, but were unable to reduce external acceptors [8,12,13]. Subsequently, three separate studies identified different open structures of CPR that allowed ET to redox partners, indicative of domain motion of CPR [10,14,15]. It is now fairly established that CPR exists in a conformational equilibrium between open and closed states in its ET function, which is highly dependent on ionic strength conditions [10,16,17]. The transition between these states appears to occur through a rapid swinging and rotational movement [17,18]. Certain residues in the hinge region have been suggested to be of

importance for these large conformational changes [19], and seem to form a conformational axis, involved in a partial rotational movement of the FMN domain relative to the remainder of the protein [10,18].

Analysis of CPR domain dynamics is pertinent to understand its role in the interactions with its natural redox partners and its gated ET function. The affinities between CPR and CYP have been indicated among the factors modulating the protein dynamics of CPR. Different CYP isoforms may be differently served by CPR gating its ET differentially [20,21]. Although advances obtained during the last decade, CPR's structural features controlling ET are not yet properly identified. CPR mutations may perturb specific structural requisites, necessary for the optimal transition between open and closed conformations, as well as disturb the interaction of CPR with its redox partners [10,20–22].

Previously, we have studied the effect of mutations in CPR on its redox partners [20,22,23] and the effect of alterations in the hinge segment in CPR-dependent cytochrome *c* reduction [24]. These hinge mutations showed differential effects on the conformational equilibrium of CPR and ET efficiency to cytochrome *c,* a non-physiological redox partner of CPR. Through modulation of the ionic strength conditions we demonstrated that electrostatic and flexibility properties of the hinge are critical for ET function, in which CPR's membrane anchoring was shown to play an important role [24]. Although frequently used as a surrogate, the soluble cytochrome *c* has been indicated to interact differently with CPR, when compared with interactions of natural membrane-bound partners, such as CYP [25]. The use of cytochrome *c* as redox partner may have obscured additional important clues on structural features of the hinge segment involved in CPR's open/closed dynamics and its gated ET function. To address this issue, three hinge mutants were selected from the initial eight mutants of our former study, based on their specific phenotypes in cytochrome *c* reduction. Human membrane bound CPR mutants S243P, I245P and R246A (numbering according to the human CPR consensus amino acid sequence NP_000932) were each combined with three different human CYPs, namely CYP1A2, 2A6 or 3A4, representatives of three major CYP families involved in drug metabolism [2,3]. The effect of the structural deviations of the three mutants was

probed to obtain further insights on the role of the hinge segment of CPR in the interaction and ET with these physiological redox partners, using different experimental approaches.

2.2.3 RESULTS

Bacterial co-expression of CPR mutants and CYP

Wild-type CPR and CPR hinge mutants S243P, I245P and R246A were separately introduced in the *E. coli* BTC strain and co-expressed with CYP1A2, 2A6 or 3A4, using methods described previously [26,27]. CYP expression levels were determined in bacterial whole-cells (Table 2.1). When co-expressed with CPR variants, CYP expression levels varied between 109–241 nM, 96–130 nM and 105–143 nM for CYP1A2, 2A6 and 3A4, respectively. Expression levels for these CYPs were comparable with those found previously with BTC strains [22,28,29]. More importantly, no large deviations were found in the CPR:CYP ratio between the four CPR variants, when expressed with each of the three CYPs (see Table 2.1). This enabled us to ascribe differences in activities of the CPR variants to the mutations, and not to variations in the stoichiometry between the two enzymes. These ratios were actually similar to those observed in our previous studies [22,28,29] and are in the range of those observed in human liver microsomes [30,31].

Table 2.1 Microsomal cytochrome P450 (CYP) and NADPH cytochrome P450 oxidoreductase (CPR) contents of BTC cultures and membrane fractions.

CYP Isoform	CPR Form	Whole-Cells	Membrane Fractions		
		CYP [1] (nM)	CYP [1]	CPR [1] (pmol/mg Protein)	CPR:CYP Ratios
CYP1A2	WT	109 ± 4	54 ± 1	4.1 ± 1.5	1:13
	S243P	241 ± 4	73 ± 4	7.7 ± 0.2	1:9
	I245P	206 ± 11	102 ± 1	6.1 ± 0.5	1:17
	R246A	176 ± 3	91 ± 2	5.4 ± 0.2	1:17
CYP2A6	WT	130 ± 2	139 ± 1	10.5 ± 1.3	1:13
	S243P	98 ± 1	106 ± 3	11.2 ± 0.5	1:9
	I245P	96 ± 7	102 ± 1	9.5 ± 0.9	1:11
	R246A	98 ± 2	146 ± 1	10.6 ± 1.5	1:14
CYP3A4	WT	105 ± 2	83 ± 3	19.8 ± 0.2	1:4
	S243P	122 ± 3	77 ± 2	22.5 ± 2.6	1:3
	I245P	128 ± 3	78 ± 2	18.3 ± 0.7	1:4
	R246A	143 ± 5	78 ± 1	21.4 ± 0.3	1:4

[1] CYP and CPR contents are mean ± sd.

CYP-Activities When Combined with the Three CPR Hinge Domain Mutant

Whole-cell Bioactivation assays

A whole cell/bioactivation assay was used for the first evaluation of the effect of the three hinge mutations on the activity of the three CYPs. This approach made use of the applicability of the BTC-CYP bacteria in mutagenicity testing [26,28]. The levels in CYP-dependent bioactivation of different pre-carcinogens, namely 2AA (2-aminoanthracene), IQ (2-amino-3-methylimidazo(4,5-f)quinolone), NNdEA (N-nitrosodiethylamine), NNK (4-(methylnitrosamino)-1-(3-pyridyl)-1-butanone) and AfB1) were determined (Table 2.2; Figure 2.6). Interestingly, two of the three CPR hinge mutants lead to bioactivation capacities, which were either stimulated or equal, in comparison when CYPs were sustained by WT CPR, except for mutant I245P. This hinge mutant demonstrated a decrease for CYP1A2 and CYP3A4 mediated bioactivation of 2AA and AfB1, respectively. In contrast, CYP1A2 and CYP2A6 bioactivation capacities (for IQ and NNdEA, respectively) were increased when assayed with this mutant, with no significant differences in CYP2A6 bioactivation of NNK. Seemingly, the effect of

CPR mutant I245P was CYP isoform and substrate dependent. The bioactivation capacity of all three CYPs was consistently augmented when assayed with CPR mutant R246A, i.e. all tested compounds demonstrated increased mutagenicity levels, in comparison with CYPs sustained by WT CPR. Mutant S243P demonstrated no significant differences in the bioactivation capacity of the three CYPs for the tested compounds, when compared with WT CPR.

Table 2.2 CYP-mediated bioactivation of pre-carcinogens.

CYP Isoform	Mutagen	CPR form			
		WT	S243P	I245P	R246A
CYP1A2	2AA [1]	5643 ± 271	5666 ± 177	3339 ± 145	6274 ± 106
	IQ [1]	335 ± 8	323 ± 7	521 ± 104	1103 ± 253
CYP2A6	NNdEA [2]	537 ± 14	543 ± 21	885 ± 122	929 ± 118
	NNK [2]	770 ± 121	799 ± 110	788 ± 57	1014 ± 29
CYP3A4	AfB1 [1]	1129 ± 97	1109 ± 115	661 ± 185	1616 ± 163

Values are mean ± sd of three independent experiments, expressed as the number of revertant colonies per nmol [1] or per µmol [2] of pre-carcinogen.

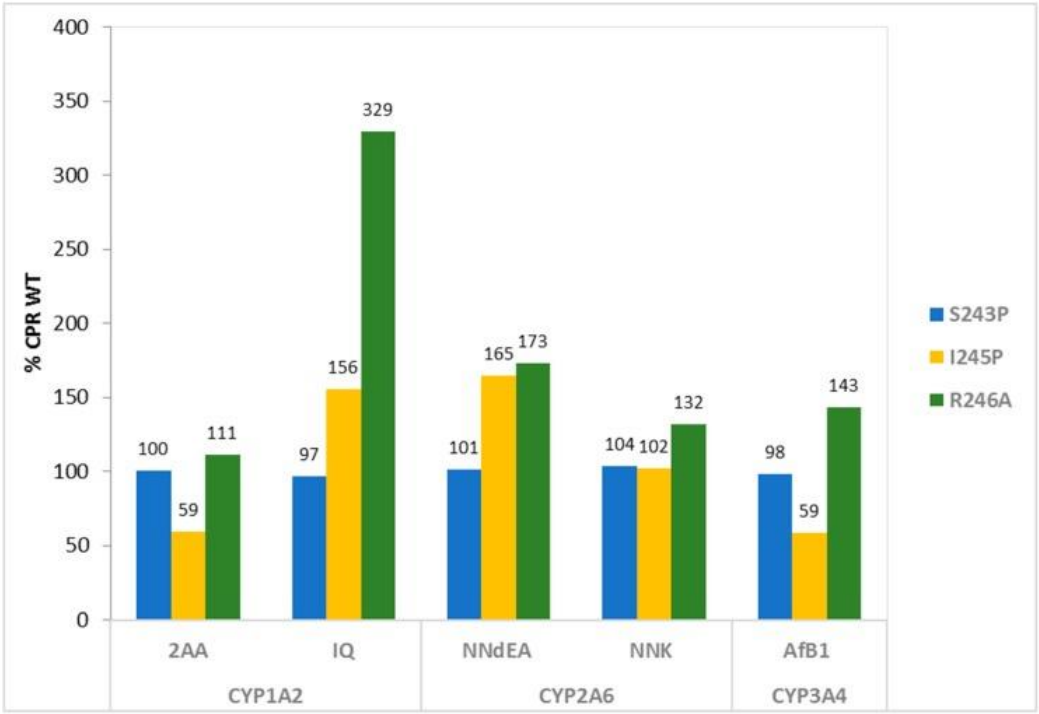

Figure 2.6 Bioactivation of pre-carcinogens mediated by CYP 1A2, 2A6 or 3A4 when combined with the three CPR hinge mutants. Bioactivation capacities were normalized with the one observed when CYPs were combined with WT CPR. (2AA: 2-aminoanthracene; IQ: 2-amino-3-methylimidazo(4,5-f)quinoline; NNdEA: N-nitrosodiethylamine; NNK: 4-(methylnitrosamino)-1-(3-pyridyl)-1-butanone; AfB1: aflatoxin B1).

Membrane Preparations

CYP-Enzyme Kinetic Analysis

Enzyme activities of CYP1A2, 2A6 and 3A4 were measured using specific fluorogenic probe substrates ethoxyresorufin (EthR), coumarin and dibenzylfluorescein (DBF), respectively). Reaction velocities could be plotted according to the Michaelis-Menten equation and kinetic parameters (k_{cat} and K_M) could be derived (Table 2.3). In general, CYP activities promoted by CPR mutants showed lower turn-over rates (k_{cat}) and affinities (K_M) when compared with WT that were also CYP form dependent. However, differences were minor in both constants and k_{cat}/K_M values were not significantly different from WT values for all tested CYPs (Table 2.3).

Table 2.3 Michaelis-Menten kinetic parameters of CYP activities.

CYP Isoform	CPR Form	k_{cat} [1] (Product Formed pmol.min^{-1}.pmol^{-1} CYP)	K_M [1] (µM)	Efficiency (k_{cat}/K_m) (% WT)
CYP1A2	WT	0.62 ± 0.02	1.94 ± 0.16	0.32 (1.00)
	S243P	0.63 ± 0.01	1.23 ± 0.05	0.51 (1.59)
	I245P	0.40 ± 0.01	0.89 ± 0.04	0.46 (1.44)
	R246A	0.43 ± 0.01	0.74 ± 0.06	0.59 (1.84)
CYP2A6	WT	1.37 ± 0.07	1.99 ± 0.34	0.69 (1.00)
	S243P	1.17 ± 0.08	2.03 ± 0.40	0.58 (0.84)
	I245P	1.20 ± 0.09	1.78 ± 0.39	0.67 (0.97)
	R246A	1.53 ± 0.08	1.98 ± 0.33	0.77 (1.12)
CYP3A4	WT	2.53 ± 0.16	3.75 ± 0.55	0.67 (1.00)
	S243P	1.83 ± 0.08	3.07 ± 0.34	0.60 (0.88)
	I245P	1.89 ± 0.13	2.85 ± 0.50	0.66 (0.98)
	R246A	2.18 ± 0.22	3.82 ± 0.87	0.57 (0.85)

[1] k_{cat} and K_m values are expressed as mean values of three independent experiments ± sd, determined at 0 M NaCl.

Ionic strength effect on CPR:CYP interaction

We previously demonstrated that mutations in the hinge region of human CPR strongly influences ionic strength profiles of ET to cytochrome *c* [24]. Ionic strength dependency of CPR's ET was thus analyzed via CYP activities measurement in presence of increasing NaCl concentrations (0–1.25 M) (Figures 2.7 and 2.8). Control experiments showed no effect of the salt concentration on the fluorescence of the formed products (Figure S2.3) or on the pH of the reaction mixture (data not shown). Interestingly, the maximum velocities of the three CYPs seem to occur at lower ionic strength conditions for all CPR (WT or variants) when compared to their maximum velocities in cytochrome *c* reduction reported in our previous study [24].

The salt dependence of CYP1A2 activity demonstrated a bell-shaped EthR O-deethylase activity curve with all CPR tested (Figure 2.7A), analogous to the ones described in our former study when measuring cytochrome *c* reduction [24]. The maximum activity (maximum k_{obs}) was obtained, on average, at 100 mM NaCl. CYP1A2 activities dropped close to zero at the highest salt concentrations (1.25 M) for all CPR variants. CPR mutant S243P was more active than the WT, while other mutants showed lower activities when compared with WT.

For CYP2A6 (Figure 2.7B), the coumarin hydroxylase activity profiles showed less dependence on ionic strength as with CYP1A2 and showed no drop in activity at the highest salt concentrations. Maximum velocities were obtained approximately at 150 mM NaCl. All CPR mutants presented lower activities when compared with WT CPR.

CYP3A4 DBF O-debenzylase activity profiles (Figure 2.7C) were also bell-shaped, like CYP1A2, except for the CPR mutant R246A. The maximum activity was obtained, on average, at 100 mM NaCl. The activity dropped close to zero at the highest salt concentrations as was observed with CYP1A2. Interestingly, the CPR mutant R246A revealed a different salt profile with CYP3A4, leading to a continuous decrease of activity with increasing salt concentration, the maximal activity being even greater that the one obtained with WT CPR.

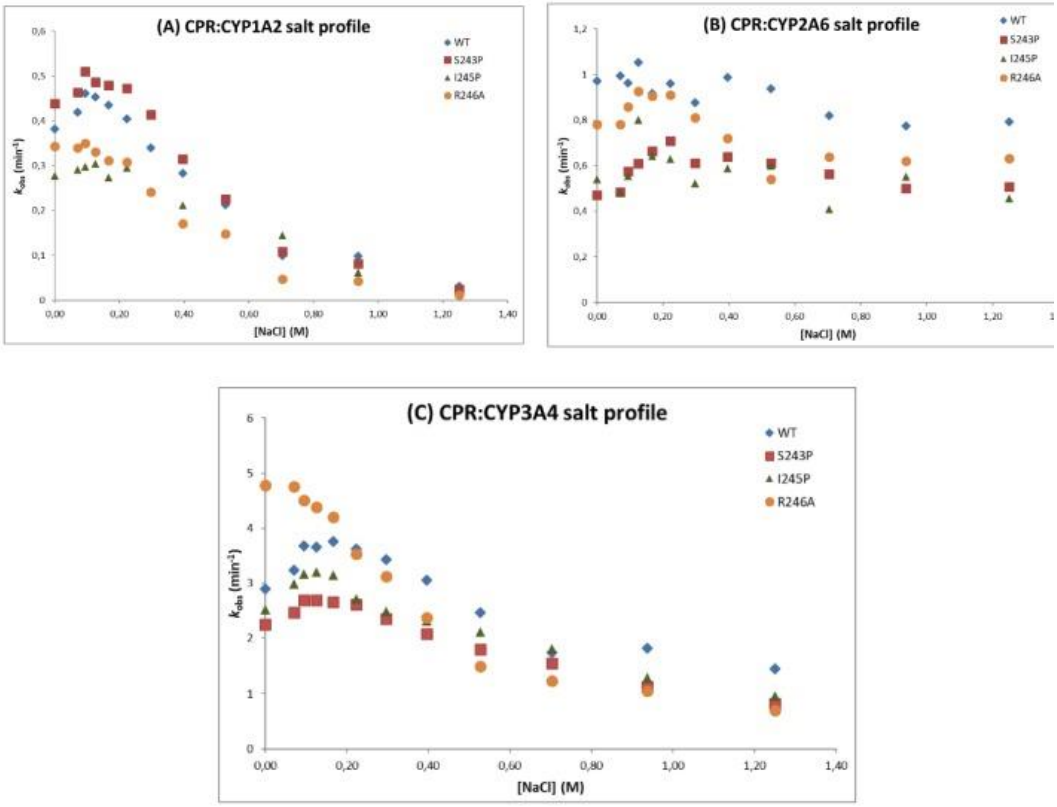

Figure 2.7 CYP reaction velocity (k_{obs}) in of the NaCl concentration, for the WT and mutant forms of CPR with CYP1A2 (A), CYP2A6 (B) or CYP3A4 (C).

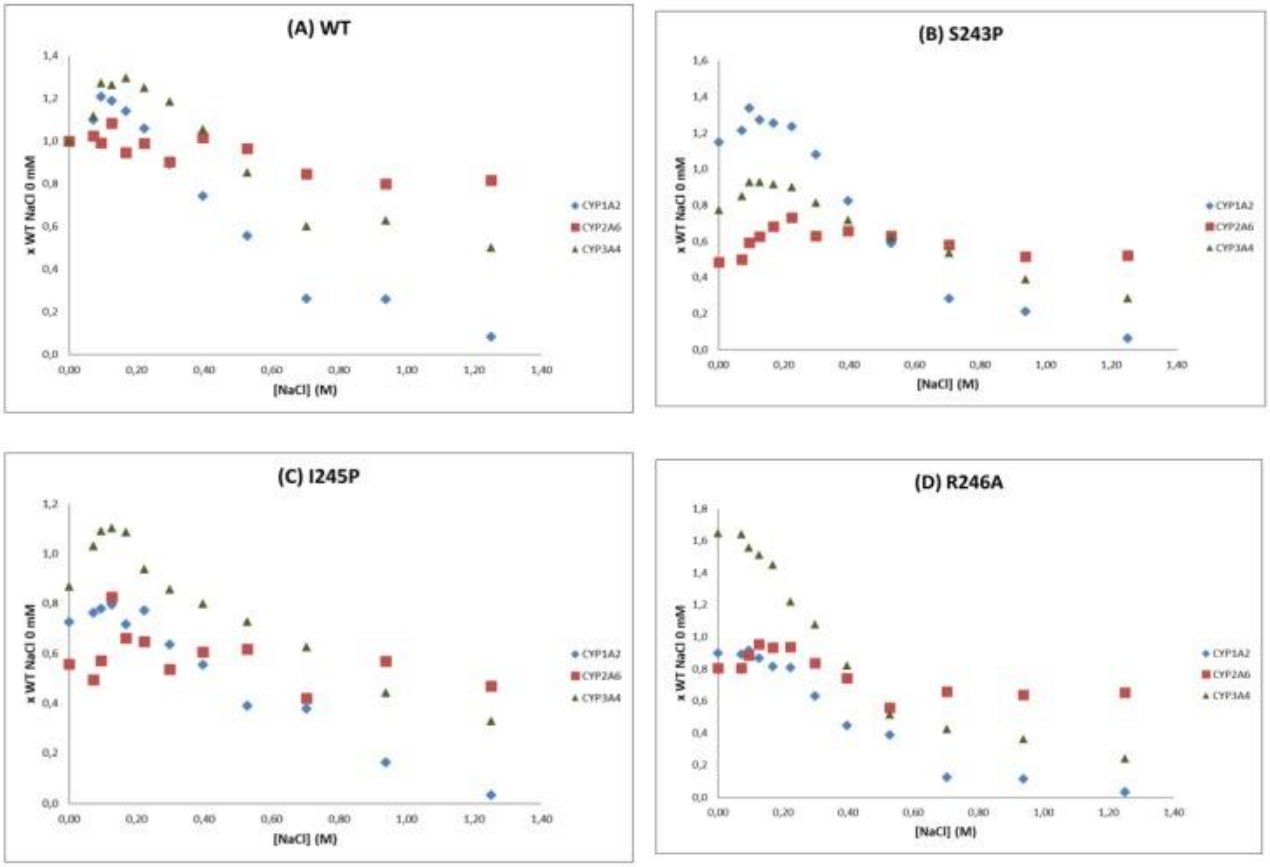

Figure 2.8 Relative CYP-reaction velocities (k_{obs}) of CYP1A2, 2A6 and 3A4 in function of the NaCl concentration, when combined with CPR WT (A) or mutants S234P (B), I245P (C) and R246A (D). Velocities were normalized with the one observed when combined with WT CPR at 0 M NaCl.

CYB5 effect on activity of CYP1A2, 2A6 and 3A4

CYB5 may act as an alternative donor of the second electron in the CYP catalytic cycle. We thus studied the effect of CPR hinge mutations when associated with CYB5, to determine if the presence of an alternative electron donor partner, capable of competing with CPR for CYPs is an important issue in the function of the hinge segment. The effects of CYB5 on CPR/CYP combinations were analyzed through enzyme activity assays in the presence of increasing concentrations of CYB5 and thus different CYB5:CPR ratios (Figure 2.9 and Table 2.4). Enzyme activities were normalized to the activity measured in the absence of CYB5. While the effect of CYB5 on CYP activities was not major, some interesting differences could be seen, notably in the CYB5 concentration giving the best stimulus. While for CYP1A2, the maximal effect was observed at 150 nM of CYB5, for CYP2A6 the concentration of CYB5 giving this maximal effect was dependent on the mutation, ranging from 50 nM with the WT CPR to 400 nM for the R246A mutant of CPR. For CYP3A4, the effect was relatively constant between all CPR mutants, but the concentration of CYB5 needed to obtain the maximal stimulation was much higher (400 nM). Overall, while CYP1A2 does not seem very sensitive to the presence of CYB5, a slight inhibition could be observed at high concentrations of CYB5. For the two other CYPs, the stimulation was quite pronounced, ranging from 2.6 to 3.4 or 1.8 to 2.6 for CYP2A6 and CYP3A4, respectively (Figure 2.9). No major differences were observed between CPR WT and mutants for each CPR/CYP combinations in term of the concentration of CYB5 to achieve the maximal effect, however, the intensity of the stimuli was different between CPR mutants.

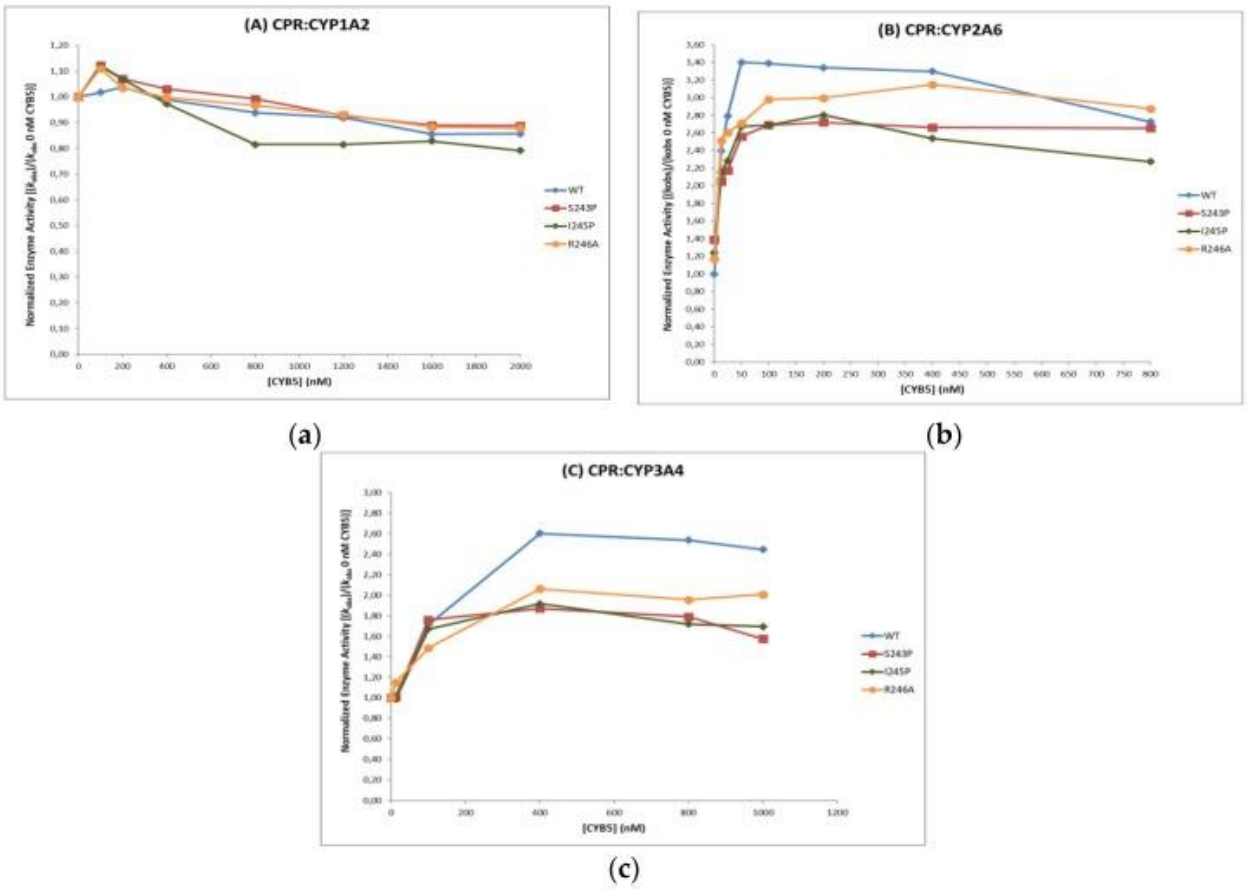

Figure 2.9 Effect of CYB5 concentration on maximum reaction velocities of CYP1A2 (A), 2A6 (B) and 3A4 (C) when sustained by WT CPR and the three hinge mutants. Activities were normalized to the one without CYB5 for each CPR mutant in comparison to WT.

Table 2.4 Effect of CYB5 on CPR/CYP combinations.

CYP Isoform	CPR Form	Maximal k_{obs} [1]	CYB5 Stimulus [2] (%)	CYB5:CPR Ratio [3]
CYP1A2	WT	1.04 ± 0.01	100	163
	S243P	1.11 ± 0.02	107	118
	I245P	1.12 ± 0.04	108	208
	R246A	1.12 ± 0.02	108	211
CYP2A6	WT	3.40 ± 0.04	100	26
	S243P	2.72 ± 0.05	80	106
	I245P	2.69 ± 0.04	79	43
	R246A	3.15 ± 0.04	93	211
CYP3A4	WT	2.60 ± 0.01	100	66
	S243P	1.87 ± 0.02	72	55
	I245P	1.92 ± 0.00	74	68
	R246A	2.06 ± 0.02	79	67

[1] Normalized maximum enzyme activity: (k_{obs})/(k_{obs} at 0 nM CYB5). Values are expressed as the mean of three independent experiments ± sd. [2] Maximum CYB5 stimulus of enzyme activity when CYPs were combined with mutant CPRs, relative to the ones obtained with CPR WT. [3] The ratio at which maximum k_{obs} was reached. Grey shaded values: Maximum fold stimulation of enzyme activity by CYB5 when CYPs were combined with WT CPR.

2.2.4 DISCUSSION

Microsomal CYP-mediated metabolism is dependent on ET through protein:protein interaction with its primary redox partner CPR. Traditionally, membrane anchoring and a negatively-charged surface patch of CPR have been considered to be major determinants of the proper alignment in this interaction, in which hydrophobic interactions have also been implicated [32,33]. Still, the view on CPR:CYP interaction for ET has become increasingly more complex with the recognition of CPR protein dynamics in ET, presenting an equilibrium between closed/locked and open/unlocked conformers in its function, in which the flexible hinge region seems to have a determinant role [10,16–18]. In a recent report we have shown the importance of this hinge segment and the effect of ionic strength in ET to the non-physiological redox partner cytochrome *c*, using eight different CPR mutants targeting four critical residues [24]. Data from this report lead us to hypothesize a hydrogen H-bond network around R246, important for the function of the open/closed dynamics.

Although the use of the soluble surrogate redox partner cytochrome *c* has been informative, the open/closed dynamics and thus ET may occur differently with CPR's natural membrane-bound electron acceptors, such as CYPs. Three hinge mutants were selected from our former set, namely mutant R246A, for R246's role in the suggested H-bond network, and mutants S243P and I245P demonstrating augmented cytochrome *c* reduction capabilities when compared with WT CPR. The CPR variants were combined with three different CYPs, representatives of three major CYP-families involved in drug metabolism. CYP families 1, 2 and 3 are responsible for 75% of all phase I metabolism of clinically used drugs: CYP3A4 is the major enzyme, and together these three CYPs are involved in almost 50% of metabolism of drugs [34]. Different experimental approaches were used to probe the effect of these hinge mutations.

The first general observation is that none of the three mutations caused a complete inactivation of CYP activity (i.e., obliterated CPR electron transfer to CYP), consistent with the data obtained using cytochrome *c* as electron acceptor [24]. We thus confirm that the three targeted positions in the hinge region are certainly part of a set of residues capable of controlling the CPR function and thus the effects of the mutations on internal and external ET are partially compensated by a larger network involved in the structural transitions (opening/closing).

The second interesting feature that these mutants demonstrated was their relative selectivity in inducing CYP-isoform dependent effects. This was first observed with CYP mediated bioactivation of pre-carcinogens, which seemed CYP isoform and in some cases substrate dependent. Still, the measurement of mutagenicity might be a quite indirect measurement of CYP activity, in generating DNA damaging metabolites. However, the specific features of CPR hinge mutants were more clearly demonstrated by the ionic strength dependency of CYP activities. Salt activity profiles were deviated differently by the three CPR hinge mutations, in a CYP-isoform dependent manner (Figures 2.7 and 2.8). We previously demonstrated that the salt concentration at which the overall CPR to acceptor ET occurs depends on the relative difference in the rate of reduction of CPR and the rate of reduction of the electron acceptor [17]. The fact that all hinge mutations affect the salt concentration at which this maximal activity occur indicate that these CPR mutations modify the conformational equilibria. However, as noted above, all mutations

have distinct salt-dependent signatures (Figure 2.8). We can thus hypothesize that the induced differences in conformational equilibria affect differently the three tested CYPs. Interestingly, all V_{max} and K_M values measured for the three CYPs were nearly identical between CPR mutants. This reinforces our current hypotheses addressing the conformational equilibria: The single hinge CPR mutants modify the salt-dependent conformational equilibria and not the intrinsic CYP properties. As such, they uncover the dependence of CYPs toward these conformational equilibria and provide a potential explanation of the mechanism by which CPR could, in certain conditions, favor one CYP over another.

An additional interesting feature of these salt profiles concerns the optimal salt concentration for CYP activity. Previously, when membrane-bound, WT CPR and the three mutants demonstrated very different salt concentrations for optimal cytochrome *c* reduction (ranging from 220–550 mM NaCl [24]). However, in the current study when combined with CYP1A2, 2A6 or 3A4, optimal activities were found at 100–200 mM NaCl, which together with the K/P reaction buffer approaches the ionic strength of physiological serum (154 mM KCl). This current data set exemplifies the difference in ET between the soluble surrogate electron acceptor cytochrome *c* and CPR's natural membrane-bound redox partners. Maximum ET rates of soluble WT CPR in cytochrome *c* reduction was found to occur when CPR was equally distributed between open and closed conformers at approximately 375 mM NaCl [17]. With membrane bound WT CPR, maximum cytochrome *c* reduction rates were shifted above 500 mM NaCl, namely at 527 mM [24]. As such, data from our previous and current study suggests that optimal ET to various acceptors, either natural or artificial, occurs at very different ionic strengths. However, under physiological conditions, membrane bound CPR is present in an equilibrium, which is mostly in the locked state, however maintaining a very fast rate in alternating between open and closed conformations. This reinforce the idea that additional factors, such as the presence of membrane bound redox-partners, with stoichiometry's favoring the electron acceptors (as is the case for CYPs, outnumbering CPR by a factor of 5–10), modulate the open/closed dynamics, as we put forward in our previous study [24].

As mentioned above, our data showed differences in the salt effect of the three different CYPs when combined with WT CPR, corroborating the study by Yun *et al*. [35] that ascribed the ionic strength effect observed mostly to CPR:CYP "interaction" while having relative minor effects on CYP protein conformation [36]. Still, results of the study of Voznesensky and Schenkman [37] indicated that charge pairing between CPR and CYP may not be the major determinant of the salt effect. Our current data, as well as that of our previous study [24] confirms that the CPR:CYP interaction (i.e., electronic flow) dependency on ionic strength is mainly determined by its effect on the conformational equilibrium between locked and unlocked states of CPR and only in a minor manner by electrostatic interactions (affinity) between the FMN domain and the acceptor. Due to this major salt effect on CPR's open/closed dynamics, the identification of potential electrostatic interactions between CPR and CYP have therefore been obscured. In retrospect, the seminal studies of Voznesensky and Schenkman [37,38] and of others (reviewed in [32]) on the salt effect of CYP catalysis in the quest for electrostatic interactions between CPR and CYP have been hampered by the lack of knowledge, at that time, on the salt-dependent protein dynamics of CPR.

In vivo, under constant ionic strengths conditions, affinity parameters may become determining in the CPR:CYP interaction, modulating the open/closed dynamics as indicated above. CYB5, the optional electron donor, demonstrated also stimulation/inhibition profiles that were dependent on CYPs, as well as on the various CPR used. This may also sign a relatively minor role for the affinity between CPR/CYP and CYB5/CYP interactions. Although CPR and CYB5 share similar, but not identical, binding-sites on the proximal side of CYP [39], the competition between the two electron donors does not seem to be a major factor in controlling CYP activities. Still, subtle differences in electrostatic interactions between the CPR/CYP and CYB5/CYP complexes have been shown [40,41], which seem even to be depending on substrate binding [42], indicating specific features in the sampling of the ensemble of open conformers of CPR.

Overall, our data point out that salt profiles are specific to CYP isoforms dependent interaction with CPR. The idea emerges for the existence of an ensemble of different unlocked CPR conformers that may be required for CYP-specific interactions. The highly

flexible hinge region allows for a large ensemble of open conformations from which only a few or a subset may be required for ET to CYPs. CPR hinge mutants, by modifying the conformational equilibrium (as seen in salt profiles) may either promote or hinder specific conformations of the unlocked state, thus allowing or preventing interactions with (structurally) different redox partners. Such a selection of specific open conformations could explain the differential effect of the three hinge mutations on the activity of the different CYPs. Moreover, the soluble cytochrome *c* will sample these conformers quite differently when compared with the membrane-bound CYP redox partner, a plausible explanation for the difference in effects of the three hinge mutants when measuring ET to cytochrome *c* [24] or CYPs (this study).

From a structural perspective, it is clear that different CYP isoforms must share a common functional CPR binding surface. Although mitochondrial CYPs seem to have a signature of key basic amino acids on the proximal side for their interaction with the iron–sulfur protein adrenodoxin, such signature sequences do not exist for microsomal CYPs in their interaction with CPR [43]. This implies diversity in critical amino acids on their proximal side and suggests the possibility of affinity differences of microsomal CYPs for CPR, a plausible key element in the sampling of the open CPR conformers.

The conformational plasticity of CYPs could additionally play a role in this respect. Substrate binding has been shown to cause (subtle) conformational changes at the proximal site of CYPs, reviewed in Kandel and Lampe, 2014 [33], which may influence the affinity and thus sampling of open conformers of CPR for effective ET. In fact, this seems to be corroborated by our data of the hinge mutations, causing beside CYP-isoform dependent seemingly also substrate dependent effects, as described above.

It is tempting to speculate that CPR's protein dynamics, containing different ensembles of closed and open conformations, was Nature's way to enable CPR to be the "degenerated" electron supplier of so many (structural and functional) different redox-partners. In this respect it would be of interest to obtain insight on the evolutionary gain and thus the physiological relevance of such a universal electron donor for enzymes, involved in some many different and crucial metabolic pathways. In parallel to other central enzymes, the possibility may exist of a central hub- or central controller-function of CPR, for the fine tuning of multiple metabolic pathways and energy (NADPH) usage.

2.2.5 MATERIALS AND METHODS

Reagents

L-Arginine, thiamine, chloramphenicol, ampicillin, kanamycin sulfate, isopropyl β-D-thiogalactoside (IPTG) (dioxane-free), δ-aminolevulinic acid (δ-Ala), cytochrome *c* (horse heart), glucose 6-phosphate, glucose 6-phosphate dehydrogenase, nicotinamide adenine dinucleotide phosphate ($NADP^+$ and NADPH), 2-aminoanthracene (2AA), N-nitrosodiethylamine (NNdEA), 4-(methylnitrosamino)-1-(3-pyridyl)-1-butanone (NNK), aflatoxin B1 (AfB1), resorufin (R), 7-hydroxy coumarine (7-OH C) and fluorescein (F) were obtained from Sigma-Aldrich (St. Louis, MO, USA). 2-amino-3-methylimidazo(4,5-f)quinolone (IQ) was obtained from Toronto Research Chemicals (North York, ON, Canada). LB Broth (Formedium, Norfolk, UK), bacto tryptone and bacto peptone were purchased from BD Biosciences (San Jose, CA, USA). Bacto yeast extract was obtained from Formedium (Norwich, England). EthR and coumarin were obtained from BD Biosciences (San Jose, CA, USA) and DBF from Santa Cruz Biotechnology (Santa Cruz, CA, USA). A polyclonal antibody from rabbit serum raised against recombinant human CPR obtained from Genetex (GTX101099) (Irvine, CA, USA) was used for immunodetection of the membrane-bound CPR.

Bacterial Expression of Human CYB5 and Purification

The cDNA of the open reading frame of human full length CYB5 was cloned in pET15b, as described in Nunez *et al*., 2010 [44], except that the full sequence was used instead of only the soluble part of it. The resulting plasmid was transformed into BL21-DE3 for expression. A single colony was grown in Terrific Browth medium containing 100 µg/mL ampicillin for 72 h with shaking at 22 ºC. Cells were harvested by centrifugation at 4000x g, and the resulting pellet was resuspended and incubated for 30 min in 50 mM Tris-HCl, pH 7.4, containing 1 mM PMSF and 1 mg/mL lysozyme. Cells were lysed by sonication. Then 0.02 mg/mL RNase and 0.05 mg/mL DNase were added, and CYB5 was solubilized at 4 ºC with 1% (w/v) sodium cholate, pH 7.4, for 1 h with moderate shaking. Supernatant was loaded onto a DEAE-cellulose anion-exchange column equilibrated with 0.2% (w/v) sodium cholate, 20 mM sodium/potassium phosphate buffer, pH 7.4. CYB5 was eluted

with 0.5 M NaCl, 0.2% cholate, and 20 mM sodium/potassium phosphate buffer, pH 7.4. Fractions containing CYB5 were applied to a hydroxylapatite column equilibrated with 0.5 M NaCl and 20 mM sodium/potassium phosphate buffer, pH 7.4. Pure CYB5 was eluted with 0.1% (w/v) sodium cholate and 0.5 M sodium/potassium phosphate buffer and dialyzed against 0.1% (w/v) sodium cholate, 1 mM PMSF, and 20 mM sodium/potassium phosphate buffer. CYB5 content of samples was determined by spectrophotometric techniques as described previously [28,29]. CYB5 was concentrated and stored at -20 ºC.

Bacterial Co-Expression of Human CPR Mutants and CYPs

CPR forms were expressed as a full-length membrane bound proteins using a dedicated *E. coli* host, the BTC strain, using the specialized bi-plasmid system adequate for co-expression of CPR with representative human CYP [26,27]. Plasmid pLCM_POR [20] was used for the expression of the membrane-bound, full-length WT form and mutants of human CPR [24]. The expression of human CYP-isoforms in the cell model was accomplished with plasmid pCWori containing human wildtype CYP cDNA (pCWh_1A2, pCWh_2A6 or pCWh_3A4) [45]. The pLCM_POR and the CYP plasmids pCWh were transfected through standard electroporation procedures [22]. Each strain was cultured in TB medium supplemented with peptone (2 g/L), thiamine (1 µg/mL), ampicillin (50 µg/mL), kanamycin (15 µg/mL), chloramphenicol (10 µg/mL), trace elements solution [46] (0.4 µL/mL), IPTG (0.2 mmol/L) and δ-Ala (100 µmol/L), final concentrations. Cultures were started with -80 ºC glycerol stocks and cells were grown for 16 h at 28 ºC with moderate agitation. CYP content of bacterial whole-cells preparations was determined using standard CO-difference spectrophotometry [47] (see annex 1).

Whole-Cell Mutagenicity Assays

The mutagenicity assays were performed as described previously [20,23,45,47] using the liquid pre-incubation assay technique [48,49]). Briefly, BTC bacteria were grown for 18 h in TB medium supplemented with peptone (2 g/L), thiamine (1 µg/mL), ampicillin (50 µg/mL), kanamycin (15 µg/mL), a mixture of trace elements solution [46]

(0.4 µL/mL) and IPTG (0.2 µmol/L), final concentrations. Pre-incubation was performed for 45 min in an orbital shaker at 37 ºC before plating. Incubation buffer contained 10 mM glucose. Stock solutions of carcinogens were freshly made in dimethyl sulfoxide (DMSO) and working solutions were obtained by dilution in water. DMSO concentration in preincubations were ≤1.3%. Experiments were performed at least in triplicate. Revertant colonies on L-Arg selector plates were counted after 48 h incubation at 37 ºC. Revertant colonies were determined by ProtoCOL 3 colony counter (Synbiosis, Cambridge, UK) using ProtoCOL V0 1.0.6 Software. CYP-mediated bioactivation was expressed in terms of mutagenic activity [L-arginine prototrophic (revertant) colonies per nmole of test compound, or in revertant colonies per µmole of test compound], determined from the slope of the linear portion of the dose–response curve.

Membrane Preparation and Characterization

Membrane preparations were isolated as previously described [22,24]. Briefly, cultures were harvested at 2772x g for 20 min at 4 ºC. The pellet was resuspended in Tris-sucrose buffer (50 mM Tris-HCl, 250 mM sucrose, pH 7.8). Lysozyme was added to a final concentration of 0.5 mg/mL, EDTA (0.5 mM), phenylmethanesulfonyl fluoride (0.5 mM) and benzonase (12.5 U/mL). Cells were incubated on a roller bench for 30 min at 4 ºC. Cell lyses was performed by freezing (-80 ºC) and thawing (1 cycle) and by subsequent several short rounds (30 s) of low-intensity sonication, interspersed with 60 s of ice-bath submersion. The suspension was centrifuged at 2772x g, for 20 min at 4 ºC to eliminate unbroken cells. Membranes were pelleted by ultracentrifugation of the supernatant at 100,000x g at 4 ºC for 60 min. Membranes were resuspended in TGE buffer (75 mM Tris-HCl, 10% (v/v) glycerol, 25 mM EDTA, pH 7.5) using a Potter homogenizer and stored at -80 ºC. Protein concentrations were determined using the method described by Bradford, following the manufacturer's protocol from Bio-Rad (San Francisco, CA, USA), using bovine serum albumin as the standard. CYP contents of membrane preparations were determined using CO-difference spectrophotometry (see annex 1). Membrane proteins were separated by SDS–PAGE gel electrophoresis (10% polyacrylamide gel) and either stained with Coomassie blue or electro-transferred to PVDF membranes and further processed. CPR content of membrane fractions was

quantified by immunodetection against a standard curve of purified human, full-length WT CPR, using polyclonal rabbit anti-CPR primary antibody and biotin-goat anti-rabbit antibody in combination with the fluorescent streptavidin conjugate (WesternDot 625Western Blot Kit; Invitrogen, Eugene, OR, USA) (see Figure S2.2). Densitometry of CPR signals was performed using LabWorks 4.6 software (UVP, Cambridge, UK).

CYP-Enzyme Assays

Using membrane preparations, CYP-activities were assessed through determination of product formation by EthR O-deethylation (EROD; CYP1A2) (excitation 530 nm; emission 580 nm), coumarin 7-hydroxylation (CYP2A6) (excitation 330 nm; emission 460 nm) or O-debenzylation of DBF (CYP3A4) (excitation 485 nm; emission 535 nm) [20,22,26]. Assays were performed in 96-well format with a multi-mode microtiter plate reader (SpectraMax®i3x, Molecular Devices, USA) using SoftMax Pro 2.0 Software. Experiments were conducted with 8 nM CYP1A2, 100 nM CYP2A6, and 25 nM CYP3A4 (final well concentrations). Reactions were performed in 100 mM potassium phosphate buffer (without NaCl) (pH 7.6) supplemented with 3 mM $MgCl_2$ and an NADPH regenerating system (NADPH 200 µM, glucose 6-phosphate 500 µM and glucose 6-phosphate dehydrogenase 40 $U.L^{-1}$, final concentrations). Stock solutions of EthR were prepared in DMSO, while coumarin and DBF were prepared in acetonitrile (ACN). Final solvents concentrations were maintained constant throughout the experiment (0.2% (v/v) DMSO or 0.1% (v/v) ACN). Product formation was followed for 10 min at 37 ºC and rates were calculated by using a standard curve of the products. Reactions were performed in triplicate with substrate concentrations ranging up to 5 µM EthR (CYP1A2), 20 µM coumarin (CYP2A6) or 10 µM DBF (CYP3A4). Velocity data were plotted according to the Michaelis–Menten equation with high confidence (r^2 > 0.95) using GraphPad Prism 5.01 Software (La Jolla, CA, USA) and kinetic parameters (k_{cat} and K_M) were derived [20,22,47]. Variance in data was analyzed using one-way ANOVA with Bonferroni's multiple comparison tests, with 95% confidence interval - GraphPad Prism 5.01 Software (La Jolla, CA, USA).

Ionic Strength Effect

Catalytic activity of CYP1A2, 2A6, and 3A4, sustained by WTCPR and CPR mutants, was assessed at various NaCl concentrations (0–1.25 M), using 5 µM EthR, 20 µM coumarin and 10 µM DBF, respectively, in 100 mM potassium phosphate buffer (pH 7.6), and NADPH regenerating system (NADPH 200 µM, glucose 6-phosphate 500 µM and glucose 6-phosphate dehydrogenase 40 $U.L^{-1}$, final concentrations). Velocities were measured in triplicate in 96-well format using multi-mode microtiter plate reader (SpectraMax®i3x, Molecular Devices, San José, CA, USA; SoftMax Pro 2.0). Initial rates (picomoles of fluorescent product formed per picomoles of CYP per minute) were derived from the linear part of the kinetic traces using a standard curve of the respective products. Control experiments were conducted to assess the effect of ionic strength on the pH of the reaction matrix and the fluorescence of products.

CYP Activity Titration with CYB5

The CYB5 titration assay was performed in microplate format (96 wells) using the same enzyme assay conditions as described above (without NaCl), except substrate concentrations were hold constant (5 µM EthR, 20 µM coumarin or 7.5 µM DBF), applying a gradient of CYB5 (0–2000, 0–800 and 0–1000 nM for CYP1A2, 2A6 and 3A4, respectively).

2.2.6 SUPPLEMENTARY MATERIALS

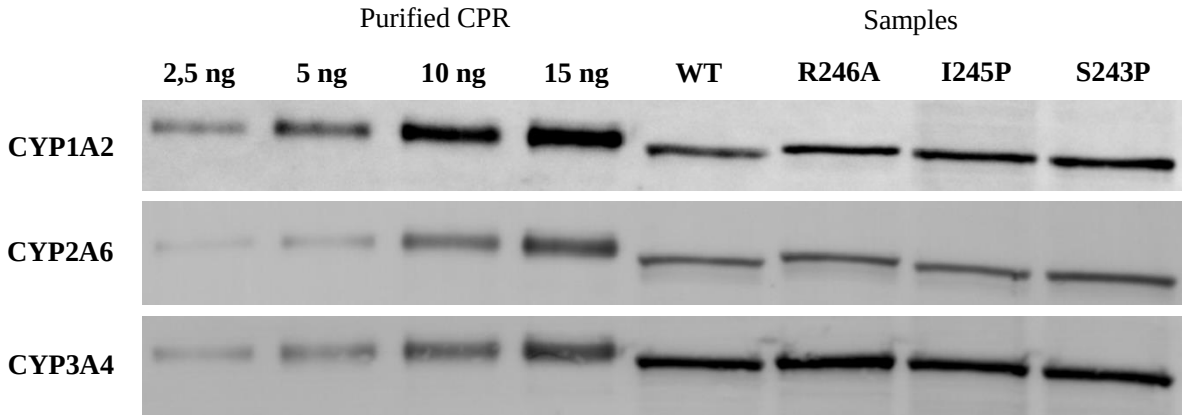

Figure S2.2: Immuno-detection of human CPR variants in membrane preparations.

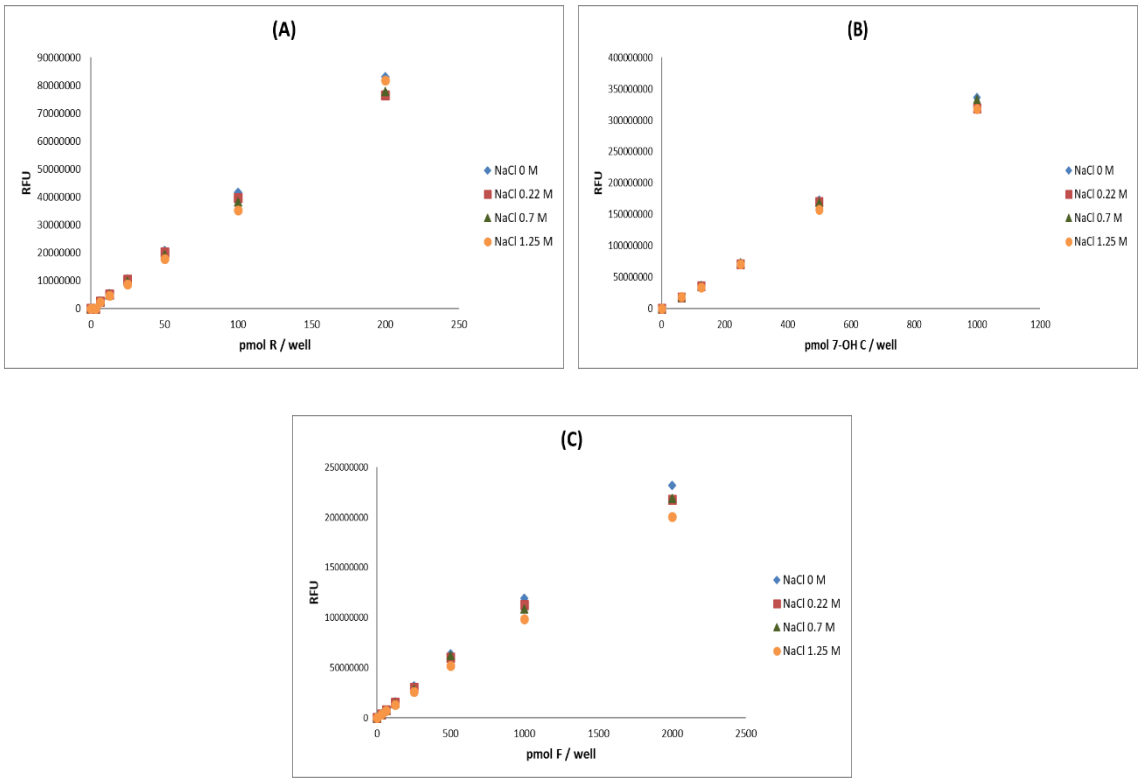

Figure S2.3: Fluorescence of resorufin (R), 7-hydroxy coumarin (7-OH C) and fluorescein (F) with increasing NaCl concentrations, in panel A, B and C, respectively.

2.2.7 AUTHOR CONTRIBUTIONS

Conceptualization, M.K. and G.T.; methodology, D.C., B.C.G., B.B.P. and F.E.; formal analysis, M.K., G.T., T.L., P.U. and J.R.; writing - original draft preparation, D.C. and M.K.; writing - review and editing, all authors; project administration, M.K. and G.T.; funding acquisition, M.K. and G.T.

2.2.8 FUNDING

This work was in part financed by a joint project, funded by the Portuguese Fundação para a Ciência e a Tecnologia [Grant FCT-ANR/ BEXBCM/0002/2013, as well as Grant UID/BIM/0009/2016 of the Research Center for Toxicogenomics and Human Health (ToxOmics)] and the L'Agence Nationale de la Recherche [Grant ANR-13-ISV5-0001]. F.E. was supported with a post-doctoral fellowship grant of the Portuguese Fundação para a Ciência e a Tecnologia [Grant SFRH/BPD/110633/2015].

2.2.9 CONFLICTS OF INTEREST

The authors declare no conflict of interest.

2.2.10 REFERENCES

1. Yasukochi, Y.; Masters, B.S. Some properties of a detergent-solubilized NADPH-cytochrome *c* (cytochrome P-450) reductase purified by biospecific affinity chromatography. *J. Biol. Chem.* **1976**, *251*, 5337–5344.
2. Rendic, S.; Guengerich, F.P. Survey of Human Oxidoreductases and Cytochrome P450 Enzymes Involved in the Metabolism of Xenobiotic and Natural Chemicals. *Chem. Res. Toxicol*. **2015**, *28*, 38–42, doi:10.1021/tx500444e.
3. Guengerich, F.P. Human Cytochrome P450 Enzymes. In *Cytochrome P450: Structure, Mechanism, and Biochemistry*, 4th ed.; De Montellano, P.R.O., Ed.; Springer International Publishing: Basel, Switzerland, 2015, pp. 523–785.
4. Pandey, A.V.; Flück, C.E. NADPH P450 oxidoreductase: Structure, function, and pathology of diseases. *Pharmacol. Ther.* **2013**, *138*, 229–254, doi:10.1016/j. pharmthera.2013.01.010.
5. Vergéres, G.; Waskell, L. Cytochrome b5, its functions, structure and membrane topology. *Biochimie* **1995**, *77*, 604–620.
6. Bart, A.G.; Scott, E.E. Structural and functional effects of cytochrome b5 interactions with human cytochrome P450 enzymes. *J. Biol. Chem*. **2017**, *292*, 20818–20833, doi:10.1074/jbc.RA117.000220.
7. Murataliev, M.B.; Feyereisen, R.; Walker, F.A. Electron transfer by diflavin reductases. *Biochim. Biophys. Acta* **2004**, *1698*, 1–26, doi:10.1016/j.bbapap. 2003.10.003.
8. Wang, M.; Roberts, D.L.; Paschke, R.; Shea, T.M.; Masters, B.S.; Kim, J.J. Three-dimensional structure of NADPH-cytochrome P450reductase: Prototype for FMN- and FAD-containing enzymes. *Proc. Natl. Acad. Sci. USA* **1997**, *94*, 8411–8416.
9. Grunau, A.; Geraki, K.; Grossmann, J.G.; Gutierrez, A. Conformational dynamics and the energetics of protein ligand interactions: role of interdomain loop in human cytochrome P450 reductase. *Biochemistry* **2007**, *46*, 8244–8255, doi:10.1021/bi 700596s.
10. Ellis, J.; Gutierrez, A.; Barsukov, I.L.; Huang, W.C.; Grossmann, J.G.; Roberts, G.C. Domain motion in cytochrome P450 reductase: Conformational equilibria revealed by NMR and small angle xray scattering. *J. Biol. Chem*. **2009**, *284*, 36628–36637, doi:10.1074/jbc.M109.054304.

11. Paine, M.J.I.; Scrutton, N.S.; Munro, A.W.; Gutierrez, A.; Roberts, G.C.K.; Wolf, C.R. Electron transfer partners of cytochrome P450. In *Cytochrome P450: Structure, Mechanism, and Biochemistry*, 3th ed.; De Montellano, P.R.O., Ed.; Springer International Publishing: Basel, Switzerland, 2005, pp. 115–148.
12. Xia, C.; Hamdane, D.; Shen, A.L.; Choi, V.; Kasper, C.B.; Pearl, N.M.; Zhang, H.; Im, S.C.; Waskell, L.; Kim, J.J. Conformational changes of NADPH-cytochrome P450 oxidoreductase are essential for catalysis and cofactor binding. *J. Biol. Chem*. **2011**, *286*, 16246–16260, doi:10.1074/jbc.M111.230532
13. Vincent, B.; Morellet, N.; Fatemi, F.; Aigrain, L.; Truan, G.; Guittet, E.; Lescop, E. The closed and compact domain organization of the 70-kDa human cytochrome P450 reductase in its oxidized state as revealed by NMR. *J. Mol. Biol*. **2012**, *420*, 296–309, doi:10.1016/j.jmb.2012.03.022.
14. Hamdane, D.; Xia, C.; Im, S.C., Zhang, H.; Kim, J.; Waskell, L. Structure and function of an NADPH cytochrome P450 oxidoreductase in an open conformation capable of reducing cytochrome P450. *J. Biol. Chem*. **2009**, *284*, 11374–11384, doi:10.1074/jbc.M807868200.
15. Aigrain, L.; Pompon, D.; Truan, G.; Morera, S. Cloning, purification, crystallization and preliminary Xray analysis of a chimeric NADPH cytochrome P450 reductase. *Acta Crystallogr. Sect. F Struct. Biol. Cryst. Commun*. **2009**, *65(Pt 3)*, 210–212, doi:10.1107/S1744309109000700.
16. Huang, W.C.; Ellis, J.; Moody, P.C.; Raven, E.L.; Roberts, G.C. Redox linked domain movements in the catalytic cycle of cytochrome P450 reductase. *Structure* **2013**, *21*, 1581–1589, doi:10.1016/j.str.2013.06.022.
17. Frances, O.; Fatemi, F.; Pompon, D.; Guittet, E.; Sizun, C.; Pérez, J.; Lescop, E.; Truan, G. A Well-Balanced Preexisting Equilibrium Governs Electron Flux Efficiency of a Multidomain Diflavin Reductase. *Biophys. J.* **2015**, *108*, 1527–1536, doi:10.1016/j.bpj.2015.01.032.
18. Sündermann, A.; Oostenbrink, C. Molecular dynamics simulations give insight into the conformational change, complex formation, and electron transfer pathway for cytochrome P450 reductase. *Protein Sci.* **2013**, *22*, 1183–1195, doi:10.1002/ pro.2307.

19. Aigrain, L.; Pompon, D.; Truan, G. Role of the interface between the FMN and FAD domains in the control of redox potential and electronic transfer of NADPH-cytochrome P450 reductase. *Biochem. J.* **2011**, *435*, 197–206, doi:10.1042/BJ20101984.
20. Kranendonk, M.; Marohnic, C.C.; Panda, S.P.; Duarte, M.P.; Oliveira, J.S.; Masters, B.S.; Rueff, J. Impairment of human CYP1A2mediated xenobiotic metabolism by Antley Bixler syndrome variants of cytochrome P450 oxidoreductase. *Arch. Biochem. Biophys.* **2008**, *475*, 93–99, doi:10.1016/j.abb.2008.04.014.
21. Miller, W.L.; Agrawal, V.; Sandee, D.; Tee, M.K.; Huang, N.; Choi, J.H.; Morrissey, K.; Giacomini, K.M. Consequences of POR mutations and polymorphisms. *Mol. Cell. Endocrinol.* **2011**, *336*, 174–9, doi:10.1016/j.mce.2010.10.022.
22. Moutinho, D.; Marohnic, C.C.; Panda, S.P.; Rueff, J.; Masters, B.S.; Kranendonk, M. Altered human CYP3A4 activity caused by Antley Bixler syndrome related variants of NADPH cytochrome P450 oxidoreductase measured in a robust *in vitro* system. *Drug Metab. Dispos.* **2012**, *40*, 754–760, doi:10.1124/dmd.111.042820.
23. Marohnic, C.C.; Panda, S.P.; McCammon, K.; Rueff, J.; Masters, B.S.; Kranendonk, M. Human cytochrome P450 oxidoreductase deficiency caused by the Y181D mutation: Molecular consequences and rescue of defect. *Drug Metab. Dispos.* **2010**, *38*, 332–340, doi:10.1124/dmd.109.030445
24. Campelo, D.; Lautier, T.; Urban, P.; Esteves, F.; Bozonnet, S.; Truan, G.; Kranendonk, M. The Hinge Segment of Human NADPH-Cytochrome P450 Reductase in Conformational Switching: The Critical Role of Ionic Strength. *Front. Pharmacol.* **2017**, *8*, 755, doi:10.3389/fphar.2017.00755.
25. Shen, A.L., Kasper, C.B. Role of acidic residues in the interaction of NADPH-cytochrome P450 oxidoreductase with cytochrome P450 and cytochrome *c*. *J. Biol. Chem.* **1995**, *270*, 27475–27480.
26. Duarte, M.P.; Palma, B.B.; Gilep, A.A., Laires, A.; Oliveira, J.S.; Usanov, S.A., Rueff, J.; Kranendonk, M. The stimulatory role of human cytochrome b5 in the bioactivation activities of human CYP1A2, 2A6 and 2E1: A new cell expression system to study cytochrome P450 mediated biotransformation. *Mutagenesis* **2005**, *20*, 93–100, doi:10.1093/mutage/gei012.

27. McCammon, K.M.; Panda, S.; Xia, C.; Kim, J.J.; Moutinho, D.; Kranendonk, M.; Auchus, R.J.; Lafer, E.M.; Ghosh, D.; Martasek, P.; et al. Instability of the Human Cytochrome P450 Reductase A287P Variant Is the Major Contributor to Its Antley-Bixler Syndrome-like Phenotype. *J. Biol. Chem.* **2016**, *291*, 20487–20502, doi:10.1074/jbc.M116.716019.
28. Duarte, M.P.; Palma, B.B.; Laires, A.; Oliveira, J.S.; Rueff, J.; Kranendonk, M. *Escherichia coli* BTC, a human cytochrome P450 competent tester strain with a high sensitivity towards alkylating agents: Involvement of alkyltransferases in the repair of DNA damage induced by aromatic amines. *Mutagenesis* **2005**, *20*, 199–208, doi:10.1093/mutage/gei028.
29. Palma, B.B.; Silva, E.S.M.; Urban, P.; Rueff, J.; Kranendonk, M. Functional characterization of eight human CYP1A2 variants: The role of cytochrome b5. *Pharmacogenet. Genomics* **2013**, *23*, 41–52, doi:10.1097/FPC.0b013e32835c2ddf.
30. Venkatakrishnan, K.; von Moltke, L.L.; Court, M.H.; Harmatz, J.S.; Crespi, C.L.; Greenblatt, D.J. Comparison between cytochrome P450 (CYP) content and relative activity approaches to scaling from cDNA-expressed CYPs to human liver microsomes: ratios of accessory proteins as sources of discrepancies between the approaches. *Drug Metab. Dispos*. **2000**, *28*, 1493–1504.
31. Paine, M.F.; Khalighi, M.; Fisher, J.M.; Shen, D.D.; Kunze, K.L.; Marsh, C.L.; Perkins, J.D.; Thummel, K.E. Characterization of interintestinal and intraintestinal variations in human CYP3A-dependent metabolism. *J. Pharmacol. Exp. Ther.* **1997**, *283*, 1552–1562.
32. Hlavica, P.; Schulze, J.; Lewis, D.F. Functional interaction of cytochrome P450 with its redox partners: A critical assessment and update of the topology of predicted contact regions. *J. Inorg. Biochem*. **2003**, *96*, 279–297.
33. Kandel, S.E.; Lampe, J.N. Role of protein-protein interactions in cytochrome P450-mediated drug metabolism and toxicity. *Chem. Res. Toxicol.* **2014**, *27*, 1474–1486, doi:10.1021/tx500203s.
34. Zanger, U.M.; Schwab, M. Cytochrome P450 enzymes in drug metabolism: Regulation of gene expression, enzyme activities, and impact of genetic variation. *Pharmacol. Ther.* **2013**, *138*, 103–141, doi:10.1016/j.pharmthera.2012.12.007.

35. Yun, C.H.; Ahn, T.; Guengerich, F.P. Conformational change and activation of cytochrome P450 2B1 induced by salt and phospholipid. *Arch. Biochem. Biophys.* **1998**, *356*, 229–238, doi:10.1006/abbi.1998.0759.
36. Yun, C.H.; Song, M.; Ahn, T.; Kim, H. Conformational change of cytochrome P450 1A2 induced by sodium chloride. *J. Biol. Chem*. **1996**, *271*, 31312–31316.
37. Voznesensky, A.I.; Schenkman, J.B. The cytochrome P450 2B4-NADPH cytochrome P450 reductase electron transfer complex is not formed by charge-pairing. *J. Biol. Chem.* **1992**, *267*, 14669–14676.
38. Voznesensky, A.I.; Schenkman, J.B. Quantitative analyses of electrostatic interactions between NADPH-cytochrome P450 reductase and cytochrome P450 enzymes. *J. Biol. Chem.* **1994**, *269*, 15724–15731.
39. Waskell, L.; Kim, J.J.P. Electron Transfer Partners of Cytochrome P450. In *Cytochrome P450: Structure, Mechanism, and Biochemistry*, 4th ed.; De Montellano, P.R.O., Ed.; Springer International Publishing: Basel, Switzerland, 2015, pp. 33–68.
40. Im, S.C.; Waskell, L. The interaction of microsomal cytochrome P450 2B4 with its redox partners, cytochrome P450 reductase and cytochrome b(5). *Arch. Biochem. Biophys*. **2011**, *507*, 144–153, doi:10.1016/j.abb.2010.10.023.
41. Zhang, M.; Huang, R.; Im, S.C.; Waskell, L.; Ramamoorthy, A. Effects of membrane mimetics on cytochrome P450-cytochrome b5 interactions characterized by NMR spectroscopy. *J. Biol. Chem.* **2015**, *290*, 12705–12718, doi:10.1074/jbc.M114. 597096.
42. Zhang, M.; Le Clair, S.V.; Huang, R.; Ahuja, S.; Im, S.C.; Waskell, L.; Ramamoorthy, A. Insights into the role of substrates on the interaction between cytochrome b5 and cytochrome P450 2B4 by NMR. *Sci. Rep.* **2015**, *5*, 8392, doi:10.1038/srep08392.
43. Pikuleva, I.A.; Cao, C.; Waterman, M.R. An additional electrostatic interaction between adrenodoxin and P450c27 (CYP27A1) results in tighter binding than between adrenodoxin and P450scc (CYP11A1). *J. Biol. Chem.* **1999**, *274*, 2045–2052, doi:10.1074/jbc.274.4.2045.
44. Nunez, M.; Guittet, E.; Pompon, D.; van Heijenoort, C.;Truan, G. NMR structure note: Oxidized microsomal human cytochrome b5. *J. Biomol. NMR.* **2010**, *47*, 289–295, doi:10.1007/s10858-010-9428-6.

45. Kranendonk, M.; Carreira, F.; Theisen, P.; Laires, A., Fisher, C.W.; Rueff, J.; Estabrook, R.W.; Vermeulen, N.P. *Escherichia coli* MTC, a human NADPH P450 reductase competent mutagenicity tester strain for the expression of human cytochrome P450 isoforms 1A1, 1A2, 2A6, 3A4, or 3A5: Catalytic activities and mutagenicity studies. *Mutat. Res.* **1999**, *441*, 73–83.
46. Bauer, S., Shiloach, J. Maximal exponential growth rate and yield of *E. coli* obtainable in a bench-scale fermentor. *Biotechnol. Bioeng*. **1974**, *16*, 933–941, doi:10.1002/bit.260160707.
47. Palma, B.B.; Silva, E.S.M.; Vosmeer, C.R.; Lastdrager, J.; Rueff, J.; Vermeulen, N.P.; Kranendonk, M. Functional characterization of eight human cytochrome P450 1A2 gene variants by recombinant protein expression. *Pharmacogenom. J*. **2010**, *10*, 478–488, doi:10.1038/tpj.2010.2.
48. Kranendonk, M.; Mesquita, P.; Laires, A.; Vermeulen, N.P.; Rueff, J. Expression of human cytochrome P450 1A2 in Escherichia coli: A system for biotransformation and genotoxicity studies of chemical carcinogens. *Mutagenesis* **1998**, *13*, 263–269.
49. Maron, D.M., Ames, B.N. Revised methods for the Salmonella mutagenicity test. *Mutat. Res*. **1983**, *113*, 173–215.

3. DISCUSSION

CONTENT

3.1 DISCUSSION AND CONCLUSIONS

Despite the large number of microsomal CYP genes present in the human genome there is only one gene encoding CPR. The total CYP content of the human liver is estimated to be between 5- and 25-fold higher than that of CPR, suggesting competition and differential expression (Reed *et al.*, 2011; Peterson *et al.*, 1976; Estabrook *et al.*, 1971). The fact that CPR and CYP interact "one on one" raises an important challenge: from a structural perspective, all the different CYP isoforms must share a "common" functional CPR binding surface. Indeed, several studies have proposed that the binding interaction between CYP and CPR takes place between the positively charged proximal surface near the CYP heme and the negatively charged FMN and FAD/NADPH domains of CPR, suggesting that CPR:CYP interaction is primarily driven by electrostatics (Bridges *et al.*, 1998; Shen and Strobel, 1993; Shimizu *et al*., 1991). Although mitochondrial CYPs seem to have a signature of key basic amino acids on the proximal side for their interaction with the iron–sulfur protein adrenodoxin, such signature sequences do not to exist for microsomal CYPs in their interaction with CPR (Pikuleva *et al*., 1999). Studies from more than two decades ago, demonstrated the strong dependence of CPR/CYP mediated catalysis on ionic strength conditions (Tamburini and Schenkman, 1986; Voznesensky and Schenkman, 1992; Schenkman *et al*., 1994; Sem and Kasper, 1995). The salt effect over CPR's ET function was attributed to CPR:CYP interactions, as described two decades ago by Yun *et al* (Yun *et* al. 1996, 1998). Still other authors have suggested that hydrophobic interactions are more predominant (Voznesensky and Schenkman, 1992; Kenaan *et al*., 2011).

More recently, CPR was demonstrated to exist both in a compact structure, allowing internal ET but unable to reduce external acceptors (Wang *et al*., 1997; Xia *et al*., 2011a; Vincent *et al*., 2012), and an assembly ensemble of open conformers that allow ET to redox partners (Hamdane *et al*., 2009; Aigrain *et al*., 2009; Ellis *et al*., 2009). In 2015, the study from Gilles Truan's group provided a new paradigm for CPR functioning and domain dynamics (Frances *et al.*, 2015). Their SAXS experiments showed a shift from locked (closed) to unlocked (open) CPR states as a function of salt concentration. Additionally, their NMR analyses showed the co-existence of these two CPR states, interchangeable with a rapid switch (600 s^{-1}). Results of both these SAXS and NMR

experiments lead them to conclude that the ionic strength dependency of cytochrome *c* reduction by soluble CPR can be partly considered as a direct measure of the proportion of the locked *vs*. unlocked states (Frances *et al.*, 2015).

It was still not fully clear what factors may control CPR's function and dynamics, particularly in relevant physiological conditions and with natural redox partners. The role of the competition between CYP isoforms for CPR and its relation to CPR's conformational transitions is complex. CPR:CYP interactions were suggested to be influenced by many factors including CPR genetic variants, CYP isoform, availability of substrates, membrane anchoring, ionic strength and redox status of the flavin cofactors (Hlavica *et al*., 2003; Kranendonk *et al*., 2008; Marohnic *et al*., 2010; Moutinho *et al*., 2012; Subramanian *et al*., 2012; Pandey and Fluck, 2013).

The hinge segment of CPR, inserted in the LD between FAD and FMN domains, had already been considered of importance for conformational transitions that occur through a rapid swinging and rotational movement (Frances *et al*., 2015; Sündermann and Oostenbrink, 2013). Specifically, hinge residues G240 and S243 were seemingly involved in the large conformational changes of the protein (Aigrain *et al*., 2009) while residues I245 and R246 were considered, by an *in silico* molecular dynamics study, to form a pivot where the opening and rotational movement of the domain takes place (Sündermann and Oostenbrink, 2013). However, besides the suggestions of the putative function of these residues, little is known about the role of the hinge segment of CPR in the ET mechanism and in the interaction between CPR and its redox partners. Hence, the aim of this PhD study was to understand the role of specific residues of the hinge segment in the conformational equilibrium of human CPR, their role in the ionic strength effect in the open-closed dynamics and interaction with structural diverse redox partners, such as CYPs.

The four hinge residues previously mentioned were tested for their role in the flexibility and ionic interactions of CPR dynamics, as described in **Section 2.1**. For this purpose, the four amino acids were substituted by alanine or proline, with the aim of modifying either the flexibility and/or the potential ionic interactions of the hinge segment of CPR. The effect of each these hinge mutations were studied both when CPR was soluble (i.e. lacking the N-terminal membrane anchoring section) or membrane-bound (full-length), to obtain

clues on the interaction with its redox-partners. Work described in this section focused on the effect of reduction of the frequently used, although soluble, surrogate substrate cytochrome *c* (Campelo *et al.*, 2017).

Reduction of cytochrome *c* by these CPR hinge mutants and WT form was measured at different salt concentrations, to assess the role of ionic strength in CPR's dynamics and its ET function. Introduced mutations had pronounced effects either on the conformational equilibrium or the ET efficiency. Yet, all the mutants remained active: i.e. all mutants were found capable of reducing cytochrome *c*, although with different efficiencies. Maximal rates of cytochrome *c* reduction were shifted to lower salt concentration, in comparison to WT CPR, which means that generated mutants had greater tendency to favor the unlocked state, regardless of the presence or absence of the membrane. Data seem to indicate that the targeted positions are part of a larger network of structural determinants controlling the conformational exchange between the locked and unlocked state of CPR. Based on the research outcome described in this section a salt bridge network at the interface of the hinge and the connecting domain was hypothesized with a central role of residue R246.

The studies with CPR hinge mutants sustaining cytochrome *c* reduction showed that the effects of CPR mutations, although similar for some, were specifically different when present in the soluble or membrane-bound context. In particular, data of mutations of residues S243 and I245 seemed to indicate that these two residues are of importance for the open/closed dynamics of membrane anchored CPR. The N-terminal hydrophobic anchoring sequence of CPR had previously been suggested to establish hydrophobic interactions with the membrane domains of CYPs, of importance for a productive alignment of CPR with its redox-partners to support a successful ET (Hlavica *et al.*, 2003; Kandel and Lampe, 2014). The rate limiting steps might not be equivalent between the soluble and membrane bound form, which suggested a role of the membrane anchoring and hydrophobicity in the activity and dynamics of CPR (Campelo *et al*., 2017).

In the interaction with cytochrome *c*, the velocity data of the CPR hinge mutants confirmed that the electrostatic and flexibility properties of the hinge segment are important conformational factors in CPR's function (Campelo *et al.*, 2017). However, cytochrome *c*, although frequently used as surrogate substrate, is a soluble and non-

physiological redox partner of CPR. Although informative, the use of cytochrome c might have obscured important clues for CPR's ET with membrane-bound natural redox partners as CYPs, which is thought to be of importance as described above.

Drug-metabolizing CYPs have a promiscuous nature (Davydov and Helpert, 2008; Atkins *et al*., 2006) and can be susceptible to functional variation due to CPR mutations (Fluck *et al*., 2010; Agrawal *et al*., 2010; Chen *et al*., 2012). Some polymorphic CPR variants as well as several rare variants found in patients with *POR* deficiency (Antley Bixler Syndrome), were previously shown to express themselves in the form of alterations in the isoform dependent CYP-mediated metabolism of certain substrates (Huang *et al*., 2005; Huang *et al*., 2008; Kranendonk *et al*., 2008; Xia *et al*., 2011b; Moutinho *et al*., 2012; Pandey and Fluck, 2013; McCammon *et al*., 2016). Small structural changes, such as a single amino acid substitution, could have dramatic functional consequences on the ability of CPR to efficiently deliver its electrons to a particular CYP isoform. In a study examining the effect of the 35 most common (polymorphic) CPR mutations, Miller and colleagues could show that while most mutations either decreased CYP activity or eliminated activity all together, other mutations enhanced CYP activity (Agrawal *et al*., 2010). It is clear that there are important functional consequences for subtle alterations in the interactions between CPR and CYP isoforms (Kandel and Lampe, 2014), although the mechanisms behind these consequences are still unknown.

Research described in **Section 2.2** addresses this issue specifically. A selection of the former described CPR hinge mutants of **Section 2.1**, were tested with three CYPs isoforms (1A2, 2A6 and 3A4), representative for three major human drug-metabolizing CYP enzyme families. Three membrane-bound CPR hinge mutants were used, namely mutant R246A, for its role in H-bond network, and mutants S243P and I245P for presenting augmented cytochrome *c* reduction when compared to WT CPR. The role of these hinge residues in CPR interaction with different CYP were probed using different approaches (Campelo *et al.*, 2018). Most interestingly, the three CPR hinge mutants demonstrated differential effects which were CYP-isoform and seemingly substrate dependent. The results clearly demonstrated, that each CYP interacts with CPR in a unique manner, according to specific structural requisites that allow CPR:CYP interactions and the formation of specific and productive ET complexes. It is shown that

the “salt” effect observed in CPR:CYP interaction and CPR’s ET function, is mainly determined by its effect on the conformational equilibrium of CPR and only in a minor manner by electrostatic interactions between the FMN domain and the CPR’s redox partner (Campelo *et al.*, 2018). More importantly, the obtained data suggests that the highly flexible hinge of CPR is responsible for the existence of a conformational aggregate of different open CPR conformers, suggesting an underlying mechanism enabling ET-interaction with structural varied redox partners. This can additionally explain that subtle structural deviations in CPR as found in the human population, might have CYP isoform specific effects, as described above.

The precise way by which CPR interacts with all structural different microsomal CYPs for ET, and how each of these redox partners probes the ensemble of CPR’s open conformers and also what mechanisms guide the protein-protein interactions that are at play within CYP enzyme complex are still matters to be further clarified. It has been shown that basic residues in CYP form a positive electrostatic ring that steers the docking site near the heme to a negatively charged patch on CPR at the FMN domain (Rwere *et al.*, 2016). The degenerated signature of CYP-surface amino acids at the CPR-binding interface suggests that CPR interacts with microsomal CYPs in an isoform dependent manner, which was shown with our studies on the hinge segment of CPR, as described in **Section 2.2** (Campelo *et al.*, 2018). Differential affinity parameters of microsomal CYPs for CPR may be a key element in the assembling of CPR with specific CYP-isoforms. In our laboratory, studies are currently being conducted with the aim of modifying CPR’s FMN-domain residues for increased activity of specific CYP-isoforms, i.e. to specialize CPR for interaction with a specific redox partner. This will allow the identification of structural requisites of the FMN domain of CPR, responsible for “degenerated” interactions with its structural diverse redox partners.

CPR has other natural redox partners besides CYPs, such as HO, that were not subject of this PhD research. CPR’s structural requisites with different redox partners might not be equivalent to those with CYPs’ (Higashimoto *et al.*, 2005). To complete a cycle of the HO reaction, HO consumes seven electrons provided by CPR whereas CYPs consume only two electrons (Sugishima *et al.*, 2014). Sugishima and colleagues showed that the open-closed mechanism proposed for ET from CPR to CYP also occurs

with HO (Sugishima *et al*., 2014), reinforcing the notion that the open-closed dynamics is an integral part of CPR's capacity in sustaining activity of structural diverse redox partners. However, unlike CYPs, electrons are proposed to be supplied by CPR through interaction with HO, involving the binding of the phosphate moiety of $NADP^+$/NADPH, bound to CPR (Wang and de Montellano, 2003; Pandey *et al*., 2010). Studies by Pandey and colleagues have shown that mutations in CPR identified from patients with *POR* deficiency lead to reduced HO activities. Further analysis of additional genetic variants of CPR may also lead to the identification of specific target proteins, including CYPs and HO that are affected by CPR variants (Pandey *et al*., 2010).

Finally, CPR may function as a model for diflavin protein reductase and for other multidomain redox systems such as nitric-oxide synthase, methionine synthase reductase, dihydropyrimidine dehydrogenase, NADPH-dependent diflavin oxidoreductase 1 (Lienhart *et al.*, 2013). That is in particular the case for a novel human dual flavin reductase, that was found overexpressed in cancers and may play a role in the metabolic activation of bioreductive anticancer drugs and other chemicals activated by one-electron reduction (Paine *et al.*, 2000).

Results described in this thesis assisted in further clarifying the precise control of the catalytic cycle of CPR and other diflavin reductases, the coupling with their redox partners and its involvement in relevant human physiological pathways.

3.2 REFERENCES

Agrawal V, Choi JH, Giacomini KM, Miller WL. Substrate-specific modulation of CYP3A4 activity by genetic variants of cytochrome P450 oxidoreductase. Pharmacogenet Genomics. 2010; 20(10): 611-8. DOI: 10.1097/FPC.0b013e32833 e0cb5.

Aigrain L, Pompon D, Moréra S, Truan G. Structure of the open conformation of a functional chimeric NADPH cytochrome P450 reductase. EMBO Rep. 2009; 10(7): 742-7. DOI: 10.1038/embor.2009.82.

Atkins WM. Current views on the fundamental mechanisms of cytochrome P450 allosterism. Expert Opin Drug Metab Toxicol. 2006; 2(4): 573-9. DOI: 10.1517/ 17425255.2.4.573.

Bridges A, Gruenke L, Chang YT, Vakser IA, Loew G, Waskell L. Identification of the binding site on cytochrome P450 2B4 for cytochrome b5 and cytochrome P450 reductase. J Biol Chem. 1998; 273(27): 17036-49.

Campelo D, Esteves F, Brito Palma B, Costa Gomes B, Rueff J, Lautier T, Urban P, Truan G, Kranendonk M. Probing the Role of the Hinge Segment of Cytochrome P450 Oxidoreductase in the Interaction with Cytochrome P450. Int J Mol Sci. 2018; 19(12). DOI: 10.3390/ijms19123914.

Campelo D, Lautier T, Urban P, Esteves F, Bozonnet S, Truan G, Kranendonk M. The Hinge Segment of Human NADPH-Cytochrome P450 Reductase in Conformational Switching: The Critical Role of Ionic Strength. Front Pharmacol. 2017; 8: 755. DOI: 10.3389/fphar.2017.00755.

Chen X, Pan LQ, Naranmandura H, Zeng S, Chen SQ. Influence of various polymorphic variants of cytochrome P450 oxidoreductase (POR) on drug metabolic activity of CYP3A4 and CYP2B6. PLoS One. 2012; 7(6): e38495. DOI: 10.1371/ journal.pone.0038495.

Davydov DR, Halpert JR. Allosteric P450 mechanisms: multiple binding sites, multiple conformers or both? Expert Opin Drug Metab Toxicol. 2008; 4(12): 1523-35. DOI: 10.1517/17425250802500028.

Ellis J, Gutierrez A, Barsukov IL, Huang WC, Grossmann JG, Roberts GC. Domain motion in cytochrome P450 reductase: conformational equilibria revealed by NMR and small-angle x-ray scattering. J Biol Chem. 2009; 284(52): 36628-37. DOI: 10. 1074/jbc.M109.054304.

Estabrook RW, Hildebrandt AG, Baron J, Netter KJ, Leibman K. A new spectral intermediate associated with cytochrome P-450 function in liver microsomes. Biochem. Biophys. Res. Commun. 1971; 42: 132−139.

Flück CE, Mullis PE, Pandey AV. Reduction in hepatic drug metabolizing CYP3A4 activities caused by P450 oxidoreductase mutations identified in patients with disordered steroid metabolism. Biochem Biophys Res Commun. 2010; 401(1): 149-53. DOI: 10.1016/j.bbrc.2010.09.035.

Frances O, Fatemi F, Pompon D, Guittet E, Sizun C, Pérez J, Lescop E, Truan G. A well-balanced preexisting equilibrium governs electron flux efficiency of a multidomain diflavin reductase. Biophys J. 2015; 108(6): 1527-1536. DOI: 10.1016/ j.bpj.2015.01.032.

Hamdane D, Xia C, Im SC, Zhang H, Kim JJ, Waskell L. Structure and function of an NADPH-cytochrome P450 oxidoreductase in an open conformation capable of reducing cytochrome P450. J Biol Chem. 2009; 284(17): 11374-84. DOI: 10.1074/ jbc.M807868200.

Higashimoto Y, Sakamoto H, Hayashi S, Sugishima M, Fukuyama K, Palmer G, Noguchi M. Involvement of NADPH in the interaction between heme oxygenase-1 and cytochrome P450 reductase. J Biol Chem. 2005; 280(1): 729-37. DOI: 10.1074/ jbc.M406203200.

Hlavica P, Schulze J, Lewis DF. Functional interaction of cytochrome P450 with its redox partners: a critical assessment and update of the topology of predicted contact regions. J Inorg Biochem. 2003; 96(2-3): 279-97.

Huang N, Agrawal V, Giacomini KM, Miller WL. Genetics of P450 oxidoreductase: sequence variation in 842 individuals of four ethnicities and activities of 15 missense mutations. Proc Natl Acad Sci USA. 2008; 105(5): 1733-8.

Huang N, Pandey AV, Agrawal V, Reardon W, Lapunzina PD, Mowat D, Jabs EW, Van Vliet G, Sack J, Flück CE, Miller WL. Diversity and function of mutations in P450 oxidoreductase in patients with Antley-Bixler syndrome and disordered steroidogenesis. Am J Hum Genet. 2005; 76(5): 729-49. DOI: 10.1073/pnas. 0711621105.

Kandel SE, Lampe JN. Role of protein-protein interactions in cytochrome P450-mediated drug metabolism and toxicity. Chem Res Toxicol. 2014; 27(9): 1474-86. DOI: 10.1021/tx500203s.

Kenaan C, Zhang H, Shea EV, Hollenberg PF. Uncovering the role of hydrophobic residues in cytochrome P450- cytochrome P450 reductase interactions. Biochemistry 2011; 50(19): 3957−3967. DOI: 10.1021/bi1020748.

Kranendonk M, Marohnic CC, Panda SP, Duarte MP, Oliveira JS, Masters BS, Rueff J. Impairment of human CYP1A2-mediated xenobiotic metabolism by Antley-Bixler syndrome variants of cytochrome P450 oxidoreductase. Arch Biochem Biophys. 2008; 475(2): 93-9. DOI: 10.1016/j.abb.2008.04.014.

Lienhart WD, Gudipati V, Macheroux P. The human flavoproteome. Arch Biochem Biophys. 2013; 535(2): 150-62. DOI: 10.1016/j.abb.2013.02.015.

Marohnic CC, Panda SP, McCammon K, Rueff J, Masters BS, Kranendonk M. Human cytochrome P450 oxidoreductase deficiency caused by the Y181D mutation: molecular consequences and rescue of defect. Human Drug Metab Dispos. 2010; 38(2): 332-40. DOI: 10.1124/dmd.109.030445.

McCammon KM, Panda SP, Xia C, Kim JJ, Moutinho D, Kranendonk M, Auchus RJ, Lafer EM, Ghosh D, Martasek P, Kar R, Masters BS, Roman LJ. Instability of the Human Cytochrome P450 Reductase A287P Variant Is the Major Contributor to Its Antley-Bixler Syndrome-like Phenotype. J Biol Chem. 2016; 291(39): 20487-502. DOI: 10.1074/jbc.M116.716019.

Moutinho D, Marohnic CC, Panda SP, Rueff J, Masters BS, Kranendonk M. Altered human CYP3A4 activity caused by Antley-Bixler syndrome-related variants of NADPH-cytochrome P450 oxidoreductase measured in a robust *in vitro* system. Drug Metab Dispos. 2012; 40(4): 754-60. DOI: 10.1124/dmd.111.042820.

Murataliev MB, Feyereisen R, Walker FA. Electron transfer by diflavin reductases. Biochim Biophys Acta. 2004; 1698(1): 1-26. DOI: 10.1016/j.bbapap.2003.10.003.

Paine MJ, Garner AP, Powell D, Sibbald J, Sales M, Pratt N, Smith T, Tew DG, Wolf CR. Cloning and characterization of a novel human dual flavin reductase. J Biol Chem. 2000; 275(2): 1471-8.

Pandey AV, Flück CE, Mullis PE. Altered heme catabolism by heme oxygenase-1 caused by mutations in human NADPH cytochrome P450 reductase. Biochem Biophys Res Commun. 2010; 400(3): 374-8. DOI: 10.1016/j.bbrc.2010.08.072.

Pandey AV, Flück CE. NADPH P450 oxidoreductase: structure, function, and pathology of diseases. Pharmacol Ther. 2013; 138(2): 229-54. DOI: 10.1016/j. pharmthera.2013.01.010.

Peterson JA, Ebel RE, O'Keeffe DH, Matsubara T, Estabrook RW. Temperature dependence of cytochrome P-450 reduction. A model for NADPH-cytochrome P-450 reductase:cytochrome P-450 interaction. J Biol Chem. 1976; 251(13): 4010-6.

Pikuleva IA, Cao C, Waterman MR. An additional electrostatic interaction between adrenodoxin and P450c27 (CYP27A1) results in tighter binding than between adrenodoxin and P450scc (CYP11A1). J Biol Chem. 1999; 274(4): 2045-52.

Reed JR, Cawley GF, Backes WL. Inhibition of cytochrome P450 1A2-mediated metabolism and production of reactive oxygen species by heme oxygenase-1 in rat liver microsomes. Drug Metab Lett. 2011; 5(1): 6-16.

Rwere F, Xia C, Im S, Haque MM, Stuehr DJ, Waskell L, Kim JJ. Mutants of Cytochrome P450 Reductase Lacking Either Gly-141 or Gly-143 Destabilize Its FMN Semiquinone. J Biol Chem. 2016; 291(28): 14639-61. DOI: 10.1074/jbc. M116.724625.

Schenkman JB, Voznesensky AI, Jansson I. Influence of ionic strength on the P450 monooxygenase reaction and role of cytochrome b5 in the process. Arch Biochem Biophys. 1994; 314(1): 234-41. DOI: 10.1006/abbi.1994.1435

Sem DS, Kasper CB. Effect of ionic strength on the kinetic mechanism and relative rate limitation of steps in the model NADPH-cytochrome P450 oxidoreductase reaction with cytochrome *c*. Biochemistry. 1995; 34(39): 12768-74.

Shen S, Strobel HW. Role of lysine and arginine residues of cytochrome P450 in the interaction between cytochrome P4502B1 and NADPH-cytochrome P450 reductase. Arch Biochem Biophys. 1993; 304(1): 257-65.

Shimizu T, Tateishi T, Hatano M, Fujii-Kuriyama Y. Probing the role of lysines and arginines in the catalytic function of cytochrome P450d by site-directed mutagenesis. Interaction with NADPH-cytochrome P450 reductase. J Biol Chem. 1991; 266(6): 3372-5.

Subramanian M, Agrawal V, Sandee D, Tam HK, Miller WL, Tracy TS. Effect of P450 oxidoreductase variants on the metabolism of model substrates mediated by CYP2C9.1, CYP2C9.2, and CYP2C9.3. Pharmacogenet Genomics. 2012; 22(8): 590-7. DOI: 10.1097/FPC.0b013e3283544062.

Sugishima M, Sato H, Higashimoto Y, Harada J, Wada K, Fukuyama K, Noguchi M. Structural basis for the electron transfer from an open form of NADPH-cytochrome P450 oxidoreductase to heme oxygenase. Proc Natl Acad Sci U S A. 2014; 111(7): 2524-9. DOI: 10.1073/pnas.1322034111.

Sündermann A, Oostenbrink C. Molecular dynamics simulations give insight into the conformational change, complex formation, and electron transfer pathway for cytochrome P450 reductase. Protein Sci. 2013; 22(9): 1183-95. DOI: 10.1002/pro. 2307.

Tamburini PP, Schenkman JB. Differences in the mechanism of functional interaction between NADPH-cytochrome P-450 reductase and its redox partners. Mol Pharmacol. 1986; 30(2): 178-85.

Vincent B, Morellet N, Fatemi F, Aigrain L, Truan G, Guittet E, Lescop E. The closed and compact domain organization of the 70-kDa human cytochrome P450 reductase in its oxidized state as revealed by NMR. J Mol Biol. 2012; 420(4-5): 296-309. DOI: 10.1016/j.jmb.2012.03.022.

Voznesensky AI, Schenkman JB. The cytochrome P450 2B4-NADPH cytochrome P450 reductase electron transfer complex is not formed by charge-pairing. J Biol Chem. 1992; 267(21): 14669-76.

Wang J, de Montellano PR. The binding sites on human heme oxygenase-1 for cytochrome P450 reductase and biliverdin reductase. J Biol Chem. 2003; 278(22): 20069-76. DOI: 10.1074/jbc.M300989200.

Wang M, Roberts DL, Paschke R, Shea TM, Masters BS, Kim JJ. Three-dimensional structure of NADPH-cytochrome P450 reductase: prototype for FMN- and FAD-containing enzymes. Proc Natl Acad Sci U S A. 1997; 94(16): 8411-6.

Xia C, Hamdane D, Shen AL, Choi V, Kasper CB, Pearl NM, Zhang H, Im SC, Waskell L, Kim JJ. Conformational changes of NADPH-cytochrome P450 oxidoreductase are essential for catalysis and cofactor binding. J Biol Chem. 2011a; 286(18): 16246-60. DOI: 10.1074/jbc.M111.230532.

Xia C, Panda SP, Marohnic CC, Martásek P, Masters BS, Kim JJ. Structural basis for human NADPH-cytochrome P450 oxidoreductase deficiency. Proc Natl Acad Sci U S A. 2011b; 108(33): 13486-91. DOI: 10.1073/pnas.1106632108.

Yun, C. H.; Ahn, T.; Guengerich, F. P. Conformational change and activation of cytochrome P450 2B1 induced by salt and phospholipid. Arch Biochem Biophys. 1998; 356(2): 229-38, DOI: 10.1006/abbi.1998.0759.

Yun, C. H.; Song, M.; Ahn, T., Kim, H. Conformational change of cytochrome P450 1A2 induced by sodium chloride. J Biol Chem. 1996; 271(49): 31312-6.

4. ANNEXES

CONTENT

4.1 ANNEX 1: Experimental Procedures and optimization of protocols

4.1.1 Generation of CPR hinge domain mutants

CPR variants (alanine and proline substitutions) of hinge residues G240, S243, I245 and R246 were obtained using different approaches. The alanine substitution mutants, targeting residues I245 and R246, were obtained through standard site-directed mutagenesis (Phusion Site-Directed Mutagenesis Kit, Thermo Fisher Scientific) using specific PCR primers (Table 4.1), and the sub-cloning vector pUC_POR containing the initial section (1-1269 bp) of human *POR* cDNA encoding the FMN domain. The segment of the mutated human *POR* gene was then obtained through a *Eco*RI+*Aat*II preparative digestion, its purification (GeneJET Gel Extraction kit, Thermo Fisher Scientific) and cloning into the CPR expression vector pLCM_POR (Rapid DNA Ligation kit, Thermo Fisher Scientific), followed by transformation into DH5α competent *E. coli* cells, prepared in our laboratory by standard protocol. The proline substitution mutants, were generated in the laboratory of Gilles Truan by introduction of relevant mutations in the cDNA encoding a human soluble CPR form (i.e. contains a N-terminal deletion of amino acids 1-44), present in vector pET15b. The proline substitution mutations were sub-cloned in the pUC_POR, using Megaprimer PCR procedure of the whole pET15b_CPR plasmid (MEGAWHOP) (Miyazaki and Takenouchi, 2002) (for used primers, see Table 4.2). The DNA segment containing the mutated human *POR* cDNA was then obtained through a *Eco*81I+*Sac*I preparative digestion (GeneJET Gel Extraction Kit, Thermo Fisher Scientific) and cloned into the CPR expression vector pLCM_POR (Rapid DNA Ligation kit, Thermo Fisher Scientific), followed by transformation into DH5α competent *E. coli* cells as described above. All plasmidic DNA fragments of interest were extracted and purified (GeneJET plasmid Miniprep Kit, Thermo Fisher Scientific). The *POR* cDNA of all mutant pLCM_POR plasmids was confirmed by extensive direct Sanger sequencing (StabVida®) of the *POR* cDNA, for which four appropriate primers were used (see Table 4.3). The chromatograms were analysed using FinchTV v1.4.0 software (Geospiza Inc.® 2006) and sequences were aligned using dedicated software (Clustal Omega Multiple Sequence Alignment Tool, Analysis Tool Web Services from the EMBL-EBI 2013 and MultAlin Multiple sequence alignment by F. Corpet, 2000). After sequence confirmation,

large plasmidic DNA isolations were performed (ZymoPURE™ Plasmid Midiprep Kit, Zymo Research).

Table 4.1: Primers used for site-directed mutagenesis.

Primer [1]	CPR sequence 5' – 3'	Length (nt)	Tm (ºC)	Aminoacid Substitution
Fw 1	**GCG**CGCCAGTACGAGCTTGTGGTCC	25	72,2	I245A
Fw 2	**GCG**CAGTACGAGCTTGTGGTCCACACC	27	71,0	R246A
Fw 3	**GCGGCG**CAGTACGAGCTTGTGGTCCACACC	30	71,0	I245A – R246A
Fw 4	**CGCATT**CAGTACGAGCTTGTGGTC	24	70,9	I245R – R246I
Rev 1	gctggactcctcgccagtgg	20	72,1	
Rev 2	aatgctggactcctcgccagtg	22	72,0	

[1] Forward primer (Fw) 1, 3 and 4 were used with reverse primer Rev 1; Primer Fw 2 was used with Rev 2. Mutated nucleotides for amino acid change are highlighted in grey.

Table 4.2: Primers for MEGAWHOP.

Primer	Sequence 5'- 3'
Fw	CAGACATTGACCTCCTCTGTCAGAG
Rv	gacgagagcagagtcgttggctgg

Table 4.3: Primers used for sequencing.

Primer	Sequence 5'- 3'	Tm (ºC)
F1	CTGCCGCCAGGCAAATTCTG	56
F2	CGGCGGGTTGGTGATGTCCA	58
R1	AACCAGCTGGGCAAAATCCT	52
R2	AATTCTAATGGGAGACTCCC	50

4.1.2 Bacterial expression of membrane-bound forms of human CPR variants

CPR hinge variants were engineered and cloned in pLCM_POR, part of the bi-plasmid co-expression system of human CYP-competent bacterial cell model, *E. coli* BTC, previously developed for co-expression of human CPR and CYPs (Figure 1.6) (Duarte *et al.*, 2005). The different pLCM_POR expression vectors containing the cDNA of each of the CPR mutants were combined separately with one of the *E. coli* expression (pCWori) vectors (Kranendonk *et al.*, 1999). The pCWori vector, part of the bi-plasmid co-expression system has been used to co-express the different isoforms of representative human CYP involved in drug metabolism, namely CYP1A2 2A6, or 3A4. The mock-plasmid pCWΔ (i.e. not containing cDNA of any CYP) was used as control. The BTC bacteria were transfected simultaneously with each of the pLCM_POR and each of the pCW-vectors through electroporation (BioRad-gene pulser: 25 μF, 200 Ω, 1,35 kV) (Moutinho *et al.*, 2012). Plasmid maintenance and stability was verified by analysis of pDNA (extraction through GeneJET Plasmid Miniprep Kit, Thermo Fisher Scientific), after linearization with *Eco*RI (single-cut restriction enzyme) and confirmed by agarose gel electrophoresis. All BTC strains were verified for the correct phenotype, as described in Table 4.4.

Table 4.4: Phenotypic markers of BTC strain.

Trait	Test	Incubation (37ºC)	Description	References
Mutation *rfa*-	MacConkey agar plate	32 h	Mutation in the *rfa* operon originates a deficient lipopolysaccharide core (LPS^d), leading to an increased permeability of the cell wall and consequently penetration of voluminous compounds	Fralick and Burns-Keliher, 1994 Kranendonk *et al*., 2000
Mutation *ogt*-	LB antibiotic plate	16 h	DNA repair gene *ogt* is inactivated by transposon insertion to increase sensitivity to alkylating agents. The mutation confers resistance to chloramphenicol	Duarte *et al*., 2005
Auxotrophy for L-arginine	M9 Arg +/- plate	48 h	The genetic target of this *E. coli* strain is the auxotrophy of arginine. This can be reversed to prototrophy by base substitution (transitions/transversions) (DNA damage)	Kranendonk *et al*., 1996 Kranendonk *et al*., 1998 Duarte *et al*., 2005
Sensitivity for Mutagenicity detection	Mutagenicity test with 4NQO			
Plasmid maintainance	LB antibiotic plate	16 h	kanamycin and ampicillin resistance conveyed by plasmid pLCM and pCWhCYP, respectively	Kranendonk *et al*., 1998

4.1.3 Optimization of CYP expression

To obtain optimized CYP/CPR expression in the BTC cell model, multiple culture conditions were verified and optimized (Table 4.5).

Table 4.5: Tested parameters for culture growth/expression induction.

Parameter	Range tested
Molarity and pH of TB buffer of TB culture medium (CYP isoform dependent)	pH 6.4, 6.8, 7.0, 7.2, 7.4, 7.5, 7.6; Molarity 0.9, 1 M
Starter Culture/Inoculum/pre-culture (volume)	100, 150, 200, 250 µL/per 25 mL of induction culture
Induction level (IPTG)	0.05; 0.1; 0.2;0.25; 0.3 mM
Level of δ-Ala (heme percursor)	0, 10, 25, 50, 100 uM
Culture Temperature	27, 28 ºC
Container (Aeration/agitation)	Glass / polycarbonate; lid / no lid; 130, 150, 175 rpm
Culture growth time	12, 13, 14, 15, 16, 18, 20, 22, 24, 25, 40, 48 h

CYP expression was determined through CO difference spectrophotometry using both whole bacterial cells and corresponding membrane preparations (Moutinho *et al.*, 2012), with several modifications. Procedure was optimized to increase sensitivity and accuracy. Cultures were concentrated (3 x) leading to optical densities of OD $600_{nm} \approx 21$. Sodium dithionite was added (1 mg/mL, final concentration) prior to the initial scan. When using membrane preparations, improvement in quantification of the 450 nm absorption, was obtained by baseline adjustment (Amplitude of CYP peak = A_{450} - A_{436} - 0,412 x (A_{470} - A_{436})), based on spectral intercepts before (438 nm) and after (470 nm) the 450 nm peak (Figure 4.1) (Johnston *et al.*, 2008; Johnston and Gillam, 2013). This approach reduced variation between replicate measurements of samples by modeling the baseline distortion as linear in the spectral region directly under the 450 nm absorption peak.

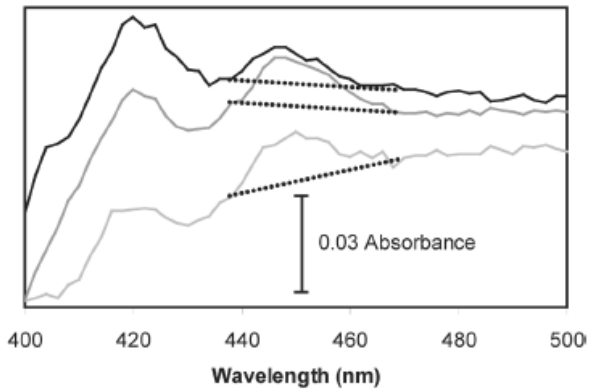

Figure 4.1: Baseline correction (at 436 and 470 nm) indicated by dotted lines (Johnston *et al.*, 2008).

4.1.4 Optimization of *E. coli* membrane isolation

Several parameters for isolation of bacterial membrane preparations were optimized, including sonication, centrifugation, precipitation and homogenization steps (Table 4.6). The formerly applied procedure, includes a relative long and high-speed centrifugation of the bacterial cell lysate (1h, 100k x g). This leads to a compact membrane pellet which is tedious to homogenize, using Potter homogenizer (Heidolph RZR-1). An alternative method was tested, used by collaborators of Dr. Gilles Truan in Toulouse for isolation of yeast microsomes. This protocol is based on an initial precipitation of the membrane fragments of whole cell lysate using NaCl (153 mM) and PEG-4000 (10%), with a subsequent shorter and relative low speed centrifugation (9k x g). Membrane pellets obtained with this procedure are less compact facilitating pellet homogenization. The new method and the former one were compared by assessing CYP- and CPR- contents and CYP activities. The CYP enzyme activity showed no interference by the use of NaCl and PEG-400 in kinetic parameters (k_{cat} and K_M). However, the total protein content (using the Bradford method with BSA as standard), showed consistently significant differences between the two methods. More importantly, semi-quantitative immune-detection of CPR in the membrane preparations of the new procedure showed considerable discrepancies with those obtained when CPR contents were determined based on cytochrome *c* reduction activity. This indicated an interference of a component of the new protocol, which could not be identified. Hence, the former method was maintained (Campelo *et al*., 2018).

Table 4.6: Tested methods for membrane preparation.

Method	Tested Parameters	Principal Step	Result	References
Bacteria	Sonication[1], centrifugation[2], precipitation and homogenization	Long (1 h) and high-speed (100 k x g) centrifugation of the whole cell lysate)	A compact membrane pellet difficult to homogenize	Palma *et al*., 2010 Campelo *et al*., 2018
Yeast		Precipitation with NaCl (153 mM) and PEG-4000 (10%) followed by a short (15 min) and low speed (9k x g) centrifugation	Less compact pellet, easily homogenized / Interference of a non-identified component	Urban *et al*., 1990 Cullin and Pompon, 1988 Pompon, 1988

[1] The following homogenizers were tested: Bullet Blender 50 DX (Integrated Scientific Solutions), Vibra-Cell VCX-500 Ultrasonic Processor (Sonics) and Sonopuls HD2070 (Bandelin). [2] For centrifugation step the following centrifuges were used: Beckman Optima L-100XP and Beckman L7-55.

4.1.5 Optimization of cytochrome *c* reduction assay

The cytochrome *c* reduction assay as used for the work described in **Section 2.1** (Campelo *et al*., 2017), was performed in microplate format. For this purpose, the standard cuvette procedure was adapted and optimized for microplate format. Electron-transfer activity of CPR is based on the measurement of the absorbance increase at 550 nm (Spec UV-2401PC, Shimadzu) when cytochrome *c* is reduced. Standardly, the reaction is followed in time (typically for 1 min) in a reaction mixture containing 50 µM cytochrome *c* and 200 µM NADPH (Shet *et al.*, 1993, Kranendonk *et al.*, 2008) in micro cuvette format (reaction volume: 1 mL). To increase through-put in cytochrome *c* reduction detection for application to test different ionic strength conditions, a micro-plate format of this method was established, together with colleagues from Toulouse (working with the soluble variants of the CPR hinge mutants). For this purpose, the reaction buffers used in Lisbon and Toulouse were checked and compared, still using the micro cuvette format, namely:

1) "Lisbon" buffer: 50 mM Tris HCl (pH 7.5), 10 mM $MgCl_2$, 150 mM KCl, 2 mM NaN_3, with or without the standardly used detergent (0,04% Triton X-100);

2) "Toulouse" buffer: 20 mM Tris-HCl, 2 mM NaN_3 with or without inclusion of 372 mM NaCl - optimum salt concentration for maximum activity of soluble CPR (Frances *et al*., 2015).

When downscaling to microplate format (i.e. 200 µL reaction volume), several optimizations and control experiments were subsequently conducted. Cytochrome *c* reduction was firstly followed for 30 min at both room temperature (21 ºC) and physiological temperature (37 ºC), using 5 and 50 uM cytochrome *c*, in the presence of a NADPH regeneration system (200 µM NADPH, 500 µM glucose 6-phosphate and 0,04 U/mL glucose 6-phosphate dehydrogenase, all final concentrations), to ensure constant and maximum reduced cofactor content during 30 min reaction time. The optimal dilution of samples containing CPR variants was verified by determining WT CPR activity measured at different CPR levels (0,5, 1, 2,5 nM) and compared with the results from the cuvette assay. Regarding the optimum cytochrome *c* concentration, a calibration curve was performed to ensure linearity of the reaction. After optimization of the parameters (i.e. temperature 37 ºC, WT CPR concentration 0,5 nM, cytochrome *c* concentration 100-200 µM, buffer 100 mM Tris-HCl pH 7.4), reactions were followed for 4 min (measurement every 23 s). Each sample was assayed at least in triplicate (Campelo *et al.*, 2017). Background activity was determined by control experiments with *E. coli* BTC membranes without CPR expression, which demonstrated no cytochrome *c* reduction upon dilution (Campelo *et al.*, 2017).

4.2 REFERENCES

Campelo D, Esteves F, Palma BB, Gomes BC, Rueff J, Lautier T, Urban P, Truan G, Kranendonk M. Probing the Role of the Hinge Segment of Cytochrome P450 Oxidoreductase in the Interaction with Cytochrome P450. Int. J. Mol. Sci. 2018; 19(12): 3914. DOI:10.3390/ijms19123914.

Campelo D, Lautier T, Urban P, Esteves F, Bozonnet S, Truan G, Kranendonk M. The Hinge Segment of Human NADPH-Cytochrome P450 Reductase in Conformational Switching: The Critical Role of Ionic Strength. Front Pharmacol. 2017; 8: 755. DOI: 10.3389/fphar.2017.00755.

Cullin C, Pompon D. Synthesis of functional mouse cytochromes P-450 P1 and chimeric P-450 P3-1 in the yeast Saccharomyces cerevisiae. Gene. 1988; 65(2): 203-17.

Duarte MP, Palma BB, Laires A, Oliveira JS, Rueff J, Kranendonk M. *Escherichia coli* BTC, a human cytochrome P450 competent tester strain with a high sensitivity towards alkylating agents: involvement of alkyltransferases in the repair of DNA damage induced by aromatic amines. Mutagenesis. 2005; 20(3): 199-208. DOI: 10.1093/ mutage/gei028.

Fralick JA, Burns-Keliher LL. Additive effect of tolC and rfa mutations on the hydrophobic barrier of the outer membrane of *Escherichia coli* K-12. J Bacteriol. 1994; 176(20): 6404–6406.

Frances O, Fatemi F, Pompon D, Guittet E, Sizun C, Pérez J, Lescop E, Truan G. A well-balanced preexisting equilibrium governs electron flux efficiency of a multidomain diflavin reductase. Biophys J. 2015; 108(6): 1527-1536. DOI: 10.1016/j.bpj. 2015.01.032.

Johnston WA, Gillam EM. Measurement of P450 difference spectra using intact cells. Methods Mol Biol. 2013; 987: 189-204. DOI: 10.1007/978-1-62703-321-3_17.

Johnston WA, Huang W, De Voss JJ, Hayes MA, Gillam EM. Quantitative whole-cell cytochrome P450 measurement suitable for high-throughput application. J Biomol Screen. 2008; 13(2): 135-41. DOI: 10.1177/1087057107312780.

Kranendonk M, Carreira F, Theisen P, Laires A, Fisher CW, Rueff J, Estabrook RW, Vermeulen NP. *Escherichia coli* MTC, a human NADPH P450 reductase competent mutagenicity tester strain for the expression of human cytochrome P450 isoforms 1A1, 1A2, 2A6, 3A4, or 3A5: catalytic activities and mutagenicity studies. Mutat Res. 1999; 441(1): 73-83.

Kranendonk M, Laires A, Rueff J, Estabrook WR, Vermeulen NP. Heterologous expression of xenobiotic mammalian-metabolizing enzymes in mutagenicity tester bacteria: an update and practical considerations. Crit Rev Toxicol. 2000; 30(3): 287-306. DOI: 10.1080/10408440091159211.

Kranendonk M, Marohnic CC, Panda SP, Duarte MP, Oliveira JS, Masters BS, Rueff J. Impairment of human CYP1A2-mediated xenobiotic metabolism by Antley-Bixler syndrome variants of cytochrome P450 oxidoreductase. Arch Biochem Biophys. 2008; 475(2): 93-9. DOI: 10.1016/j.abb.2008.04.014.

Kranendonk M, Mesquita P, Laires A, Vermeulen NP, Rueff J. Expression of human cytochrome P450 1A2 in Escherichia coli: a system for biotransformation and genotoxicity studies of chemical carcinogens. Mutagenesis. 1998; 13(3): 263-9.

Kranendonk M, Pintado F, Mesquita P, Laires A, Vermeulen NP, Rueff J. MX100, a new *Escherichia coli* tester strain for use in genotoxicity studies. Mutagenesis. 1996; 11(4): 327-33.

Miyazaki K, Takenouchi M. Biotechniques. Creating random mutagenesis libraries using megaprimer PCR of whole plasmid. Biotechniques. 2002; 33(5): 1033-4, 1036-8. DOI: 10.2144/02335st03.

Moutinho D, Marohnic CC, Panda SP, Rueff J, Masters BS, Kranendonk M. Altered human CYP3A4 activity caused by Antley-Bixler syndrome-related variants of NADPH-cytochrome P450 oxidoreductase measured in a robust *in vitro* system. Drug Metab Dispos. 2012; 40(4): 754-60. DOI: 10.1124/dmd.111.042820.

Palma BB, Silva E Sousa M, Vosmeer CR, Lastdrager J, Rueff J, Vermeulen NP, Kranendonk M. Functional characterization of eight human cytochrome P450 1A2 gene variants by recombinant protein expression. Pharmacogenomics J. 2010; 10(6): 478-88. DOI: 10.1038/tpj.2010.2.

Pompon D. cDNA cloning and functional expression in yeast Saccharomyces cerevisiae of beta-naphthoflavone-induced rabbit liver P-450 LM4 and LM6. Eur J Biochem. 1988; 177(2): 285-93.

Shet MS, Sathasivan K, Arlotto MA, Mehdy MC, Estabrook RW. Purification, characterization, and cDNA cloning of an NADPH-cytochrome P450 reductase from mung bean. Proc Natl Acad Sci U S A. 1993; 90(7): 2890-4.

Urban P, Cullin C, Pompon D. Maximizing the expression of mammalian cytochrome P-450 monooxygenase activities in yeast cells. Biochimie. 1990; 72(6-7): 463-72.